

This item was submitted to Loughborough University as a PhD thesis by the author and is made available in the Institutional Repository (<https://dspace.lboro.ac.uk/>) under the following Creative Commons Licence conditions.



For the full text of this licence, please go to:
<http://creativecommons.org/licenses/by-nc-nd/2.5/>

BLL No. D 14788/76

LOUGHBOROUGH
UNIVERSITY OF TECHNOLOGY
LIBRARY

AUTHOR

JACKSON, V.S.

COPY NO.

054321/01

VOL NO.

CLASS MARK

~~Due for return~~ LOAN COPY 1

29 APR 1996

16 MAY 1996

27 JUN 1997

005 4321 01



BLL No. - D 14788/76

LOUGHBOROUGH
UNIVERSITY OF TECHNOLOGY
LIBRARY

AUTHOR

JACKSON, V.S.

COPY NO.

054321/01

VOL NO.

CLASS MARK

Due for return 15 JUL 1974	LOAN COPY	- 5 JUL 1991
2 LOAN 1 LIB + 2 UNLESS RECEIVED	10. 76	11 OCT 1991
1 Due for return	1861 HP 1	30 JUN 1995
15. 06. 76	21. FEB 95	14 NOV 1995
- 4 JUL 1979	14. NOV 95	5 DEC 95
- 2 JUL 1980		20 FEB 1996
		22 MAR 1996

005 4321 01



MORPHOLOGY AND PROPERTIES OF NYLON 66
: EFFECTS OF INJECTION MOULDING ON
STRUCTURE AND PERFORMANCE

by

VICTOR S. JACKSON

A Doctoral Thesis Submitted in Partial Fulfilment of the
Requirements for the Award of
DOCTOR OF PHILOSOPHY
of the
LOUGHBOROUGH UNIVERSITY OF TECHNOLOGY

DECEMBER 1973

Supervisors : Dr R.R. Smith

Mr B.J. Hawthorne

© by Victor S. Jackson, 1973

Loughborough University of Technology Library	
Date	30 MAY 1974
Cl. s.	
Acc. No.	054321/01

ACKNOWLEDGEMENTS

I would like to thank my supervisors Dr R.R. Smith and Mr B.J. Hawthorne for their help and encouragement throughout this project. Thanks are also due to various members of the staff at the Railway Technical Centre, Derby for useful discussions and assistance in certain aspects of the work; to Mrs E. Adamson, who typed the thesis and to the British Railways Board for making available the facilities to carry out this study and granting permission to submit the results for a higher degree.

SUMMARY

Nylon 66 injection-moulded insulators are used by British Rail outdoors for track insulation. It has been suspected that the conditions of initial moulding and treatment before use represent a significant factor affecting properties over a period of time in this application. A laboratory study has already been reported on the influence of spherulite size on mechanical properties, using a nucleated grade of Nylon 66 to compare with typical unnucleated polymer, but this work throws little light on the problem of unnucleated polymer as such or on the influence of injection conditions and the effects of moisture present after moulding.

It was therefore decided to investigate these aspects using a standard unnucleated grade of Nylon 66. The effects of processing parameters on the following have been investigated :-

- a) the variation of spherulite size from the surface of the moulding into the interior, and
- b) the effects on typical mechanical properties such as tensile strength, impact strength, flexural modulus and important practical qualities such as resistance to surface wear and to attack by weather.

In the present study an attempt has been made to investigate the above properties as a function of different mould temperatures, and to correlate and interpret the results with reference to the morphological structure of the moulded polymer.

Nylon 66 has been moulded at temperatures of 15, 55, 75 and 95°C, the other conditions including barrel temperature, injection pressure, injection speed being kept constant. Various test piece samples were moulded and a proportion of these conditioned in water at 95°C for 3 hours. A proportion of both sets of test samples were subjected to accelerated weathering in a Climatest Weatherometer. Solution viscosity measurements at 25°C using 90% formic acid were used to obtain an idea of the reduction in molecular weight on accelerated weathering. Attenuated total reflectance spectroscopy was used to study the changes in the surface of the mouldings after accelerated weathering, and differential scanning calorimetry to obtain information on the melting behaviour of the different mouldings. The density of samples was obtained for different positions in the test discs using a density gradient column. Wide angle X-ray and hot wire techniques were used to examine the overall and surface orientation of the mouldings. Optical microscopy using polarised light has been used to build up an overall picture of the structure of the mouldings. The structure was examined in greater detail using transmission electron microscopy. Techniques used included replication techniques on etched and fractured surfaces, and direct examination of ultra thin sections. Direct observation on etched and fractured surfaces was carried out using scanning electron microscopy.

Examination of the physical properties (tensile and impact strength, flexural modulus, wear and water absorption) of moulded test pieces showed that the flexural modulus and impact strength varied with mould temperature, but in an unexpected manner.

Accelerated weathering caused a general decrease in flexural modulus, tensile strength and impact strength, but tensile test bars moulded at high temperatures had a greater tendency to fail in a brittle manner after weathering than did samples moulded at lower temperatures. Specimens which had been given the water conditioning treatment after moulding showed a tendency to fail in a ductile manner after accelerated weathering, whereas unconditional samples were prone to brittle failure even though the ageing process included spraying with water. Optical microscopy showed the existence of layers of spherulites within the mouldings, thought to be due to the varying shear treatment received by the molten polymer as the mould is filled. However optical microscopy did not detect any morphological changes with change in mould temperature or after accelerated weathering. The weathered samples were observed to develop cracks on the surface and these formed different patterns depending on the relation of the position examined to the gate of the moulding. Measurements were made on the depth of the cracks, which varied, some actually penetrating beyond the non-spherulitic skin and into the spherulites. Inherent viscosity values for the weathered surfaces showed a reduction of 25 to 35% when compared to the unweathered interior of the mouldings.

The coefficient of expansion as measured using thermal mechanical analysis showed an increase with decreasing mould temperature. Differences in attenuated total reflectance spectrographs on weathered and unweathered surfaces indicated a chemical change in the nylon. Differential scanning calorimetry results showed that the surface of the mouldings start melting at lower temperatures than the interior and also the peak widths are wider indicating a greater spread of crystallite size.

A coherent account is presented of the many results described in the thesis and recommendations for moulding conditions drawn up.

Important conclusions include :-

- a) Secondary crystallisation of the surface material can take place in the mouldings; the surface samples having much higher densities after accelerated weathering than before.
- b) The water conditioning treatment given to the mouldings changes the mode of failure after accelerated weathering, i.e. exposure to ultra violet light and water, conditioned mouldings fail in a ductile manner whereas unconditioned ones fail in a brittle manner.
- c) The embrittlement of the surface during accelerated weathering causes a catastrophic reduction in impact strength especially at the lowest mould temperature.
- d) The best all round properties are obtained using a high mould temperature. When using lower mould temperatures the consistency in the moulding is reduced especially around 75°C.
- e) The influence of mould temperature on mechanical properties and morphology is interestingly complex, not as simple as many have believed in the past.

CONTENTS

	Page
CHAPTER 1 INTRODUCTION	1
CHAPTER 2 LITERATURE REVIEW	4
2.1 Morphology	4
2.2 Microscopy studies of nylons	19
2.3 Effects of processing on structure	30
2.4 Degradation and Weathering	40
2.5 Wear	45
CHAPTER 3 EXPERIMENTAL TECHNIQUES	54
3.1 Plan of procedure	54
3.2 Injection Moulding	55
3.2.1 After treatment of mouldings	57
3.3 Mechanical Testing	58
3.3.1 Tensile strength and flexural modulus	58
3.3.2 Impact Strength	59
3.3.3 Wear	59
3.4 Physical Characterisation	60
3.4.1 Water Absorption	60
3.4.2 Inherent Viscosity	61
3.4.3 Density	62
3.4.4 Attenuated total reflection spectroscopy	62
3.5 Thermal Techniques	64
3.5.1 Differential Scanning Calorimetry	64
3.5.2 Thermogravimetric analysis	66
3.5.3 Thermal Mechanical analysis	66

	Page
3.6 Microscopy	67
3.6.1 Optical Microscopy	67
3.6.2 Transmission electron microscopy	68
3.7 X-ray diffraction	69
3.8 Hot wire technique	69
CHAPTER 4 EXPERIMENTAL RESULTS	70
4.1 Mechanical Tests	70
4.1.1 Tensile strength	70
4.1.2 Flexural modulus	72
4.1.3 Impact	73
4.1.4 Wear	75
4.2 Physical and Thermal properties.	78
4.2.1 Water Absorption	78
4.2.2 Inherent Viscosity	80
4.2.3 Density	82
4.2.4 Attenuated Total Reflectance	84
4.2.5 Differential Scanning Calorimetry	85
4.2.6 Thermogravimetric Analysis	85
4.2.7 Thermal Mechanical Analysis	86
4.3 Microscopy	88
4.3.1 Optical Microscopy	88
4.3.2 Transmission Electron Microscopy	90
4.3.3 Scanning Electron Microscopy	91
4.4 X-Ray Diffraction	95
CHAPTER 5 DISCUSSION OF PRACTICAL WORK AND EXPERIMENTAL RESULTS	97
5.1 Tensile yield strength, flexural modulus and Impact properties	97
5.2 Wear Properties	101

	Page
5.3 Water Absorption	104
5.4 Inherent Viscosity	105
5.6 Attenuated Total Reflectance	106
5.7 Morphology and Moulding	112
5.7.1 Influence of Moulding conditions	112
5.7.2 Additional Experimental Work to check orientation	116
5.7.3 Morphological Situations	117
5.7.4 Comparisons	119
5.8 Additional Note	119
CHAPTER 6 CONCLUSIONS	121
CHAPTER 7 RECOMMENDATIONS FOR FURTHER WORK	124
REFERENCES	126

CHAPTER 1INTRODUCTION

This work has been carried out at the Railway Technical Centre, Derby as part of a programme of work on nylon 66.

While British Rail are interested in engineering thermoplastics such as polyethylene terephthalate (and related polymers), polyacetals, polycarbonates and modified polyphenylene oxide, the work has initially been with nylon 66. The reason for looking at this polymer is that approximately 5 million nylon rail fastening insulators are used by B.R. per year for use in the track with concrete sleepers. This is just one of several injection moulded nylon components used in the track system, and many other examples of nylon mouldings exist throughout industry, being used or misused in respect of engineering properties.

There is a wide range of skills and standards in the injection moulding industry. The performance of the same moulding could vary if it was obtained from two moulders of widely different standards. This could be due to the different processing conditions being used. It is interesting to note that in the raw material manufactures literature on the processing of nylon 66 different processing conditions are given, for example one manufacturer uses an upward temperature gradient from the hopper to the nozzle in the injection barrel whereas another uses practically the same temperature along the barrel. From this one could infer that the wide range of conditions does not matter, but on the other hand it is known that different processing conditions can give products with different properties.

In extreme cases voids and high built in stresses can be obtained in mouldings, for example moulders to obtain a quicker cycle time use a chilled mould and eject the moulding when the majority of the moulding

is still molten. Some moulders also place ejected mouldings in buckets of water, which in thick sections will give voids and also built-in stresses.

Our aim was to try to obtain a knowledge of how these changes in processing affect the morphology and mechanical properties of mouldings, for example how much is it possible to vary the extent of the amorphous skin on the moulding? Differences in the degree of amorphous character should affect not only the weatherability of the moulding, but also other properties like wear resistance. In widely produced items like automobile speedometer gears, domestic appliance components as well as rail components the wear resistance is important. Also the effect of these variables on dimensional stability and water uptake could have important technological significance.

The purpose of this project was to try to obtain a better understanding of the properties of injection moulded items when moulded under different conditions. The aim of this project was to give some sort of perspective or scale to these factors. Not only could this information be of technological value but also it could have a considerable influence on buying and engineering specifications for components to be purchased from industry.

In order to investigate the problem, moulding of a new design of rail fastening insulator as well as a range of test piece mouldings have been made and studied in the laboratory using a variety of techniques. In the case of the rail fastening beside studying the mouldings in the laboratory, field trials have been carried out in an attempt to determine whether or not the features identified in the laboratory have any significance under conditions of practical usage. Before any mouldings were made the possibility of instrumenting the injection moulding machine with thermocouples and transducers was considered, but was rejected as it could

have caused variations in the flow and also possibly given trouble in the positioning of the ejector pins. Moreover in a normal moulding shop the possibility of using thermocouples and transducers is remote.

CHAPTER 2LITERATURE REVIEW2.1 MORPHOLOGY

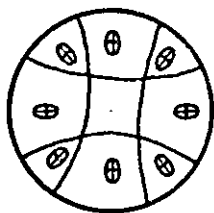
The morphology of crystalline polymers has been the subject of much speculation for the last 40 years. Work has intensified since the mid 50's and especially since 1957 when polymer single crystals were discovered^{6,7,8}. While our picture of polymer morphology has been widened there still remain conflicting views about several morphological situations, and there is inadequate information relating morphology with moulding and practical behaviour.

Polymer morphology has been studied using a variety of techniques with optical microscopy, electron microscopy and X-ray diffraction work being to the fore.

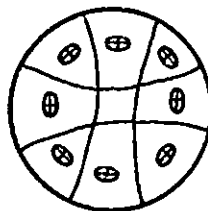
Several reviews have been written over the years on the morphology of crystalline polymers^{9,10,11,12,13,14}. Keller¹⁰ briefly discussed the fringe micelle model and showed how gradually new ideas have to be invoked to account for textured elements. Spherulites are described as having a characteristic fibrous morphology and may often consist of twisted crystalline elements. The fringe micelle concept¹⁵ assumes two phases, sub-microscopical bundled chain crystals embedded in an amorphous matrix. Every macromolecule passes alternatively through crystalline and amorphous regions, the long linear molecules being arranged randomly but in regions of sufficient chain alignment being able to form a crystal lattice.

The features of the diffraction pattern obtained for man-made fibres were attributed either to small crystal size or to defects within an extensive pattern. The measured broadening corresponded to crystal dimensions of about 200 Å. From the simultaneous appearance of diffuse

rings characteristic for amorphous materials, it was concluded that a partially crystallised polymer contains very small crystals embedded in an amorphous matrix. This concept ideally represented crystallisation with highly stretched rubber and also accounted for a number of experimental observations on bulk materials. However, this theory did not account for spherulites which were discovered in polymeric solids in 1929,¹⁶ and again brought to notice in 1945 by Bunn and Alcock.¹⁷ These structures were on a scale larger than that implied by the fringe micelle model and were gradually recognised as being typical products of crystallisation in polymers. Spherulites were recognised by their characteristic appearance under the polarising microscope. In ideal cases they are seen as circular birefringent areas possessing a dark Maltese cross with arms parallel and perpendicular to the direction of polarisation when viewed between crossed polaroids. This appearance can be accounted for by a spherically symmetrical arrangement of uniaxial index ellipsoids as shown.



positive



negative

If the larger refractive index is radial the spherulites are termed positive and if it is tangential it is termed negative. The black cross clearly arises from the vibration directions of the ellipsoids lying parallel or perpendicular to the plane of polarisation in those localities¹⁸.

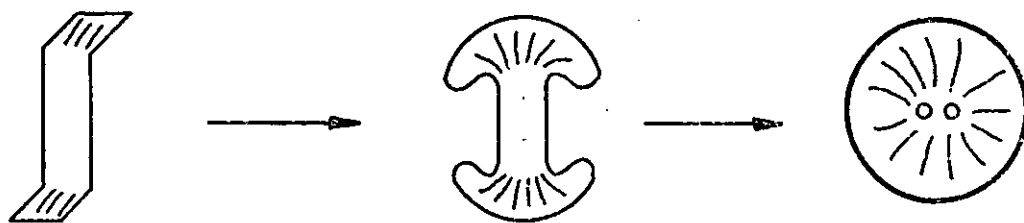
This birefringence effect in crystalline polymers is associated with a characteristic fibrous morphology leading to a radiating array of crystals. Only under favourable conditions when this morphology leads to regular enough structure and is on a large enough scale does it manifest the birefringence effect by which the spherulitic structure has been originally defined. It may be noted that spherulites can occur with paracrystalline material, i.e. the crystallinity need not be perfect even in the most highly ordered regions.

Electron microscope studies have demonstrated the existence of the spherulite morphology even on a scale where it could not be recognised optically^{19,20,21,22,23}. Micro-X-ray investigations of partially spherulitic polyethylene terephthalate revealed that the spherulities only were crystalline but not the spaces between them²⁴.

Even if the polymer consists entirely of spherulites, further crystallisation may occur on ageing which frequently manifests itself in recrystallisation of the spherulites²⁵. During this development spherulites which have been originally too small to be recognised as such, may become detectable with the optical microscope.

Already the first investigators recognised a radiating fibrous structure within the spherulites even if definite structural elements could not be clearly distinguished. In the earlier work the fibrous elements were not considered as definite entities but rather points of a continuous matrix. This type of picture implies that a polymer spherulite is a molecularly interlocked, spherically symmetrical assembly of fringe micelles and that the spherulite is a direct consequence of the long chain nature of the molecules. However, evidence accumulated to suggest genuine discontinuities along the spherulite radii^{26,27,28,29}. As this fact becomes gradually recognised, increasing attention has been given to

the possible relation between polymer spherulites and spherulites formed by non-polymeric substances. Spherulitic growth starts with the formation of crystal needles which continue to grow in the length direction by means of a fanning out mechanism.



In this way the spherical shape is gradually approached through the intermediate form of sheaves. There will remain however cavities in the centre which even if filled later may remain noticeable in the final spherulite. This theory was proposed by Bernauer³⁰ in 1929; a more involved mechanism being postulated by Keller and Waring²⁷. Spherulites grow from a well defined growth mechanism from a single nucleus which can lead to a remarkable degree of co-ordination with the final spherulite. Popoff³¹ considers such a spherulite as a rather complex single crystal. Besides these typical spherulites there are spherulitic aggregates of different, often accidental origin.

A typical spherulite is a surprisingly compact structure revealing only few details under the optical microscope. Electron microscopy requires special specimen preparation which makes the correlation with optical observations difficult. Studies revealed an intertwining fibrillar structure being about 100 Å wide^{20,27,21,32,33}. A tendency to form laminae or ribbons was also noticed by certain workers^{34,35}. It has been observed that a number of further extinction effects could appear in addition to or in place of the Maltese cross, these include a zig-zag line in place of the Maltese cross, and concentric dark ring extinction patterns which are associated with a twisting crystallisation^{35,36,37,38,39,40,41}

The orientation of the molecules was first assessed by the sign of birefringence of the spherulite. The direction of the largest refractive index is expected to be along the length of the molecular chain. Therefore, when the spherulites in polyethylene were found to be negative it was concluded that the molecules must be oriented tangentially with them. Sometimes the spherulite can be either positive or negative in the same material, depending on the crystallographic direction which lies along the spherulite radius, while the molecules could be tangential in both cases (e.g. the positive and negative polyamide spherulites)^{18,25,42,43,44} Keller^{24,37} revealed that in the most common positive spherulites, in addition to the tangential disposition of the molecules, the planes containing the H-bonds were parallel to the spherulite radius, while in the one case, where a rare negative spherulite was large enough for such an investigation, these planes were also tangential. With polyethylene the b crystallographic axis was found to lie along the radial direction^{24,25}. The orientation in polyamide spherulites as established by X-rays, has also been identified in individual sheaves by electron diffraction³³. These results confirm the "spherulitic" orientation even within sub-microscopic units.

Various models representing the structure of a spherulite have been proposed. Bryant et al visualised induced crystal growth along the length of the chain⁴⁶, this perhaps bears some relation to the concept of secondary nucleation⁴⁷.

"Spherulitic" orientations with the molecules perpendicular to the fibre axis can be found in filaments extruded without tension and were also observed in some slightly drawn polyamide films. This was interpreted by visualising the fibrous units which form spherulites, grown spontaneously in the extrusion direction, or aligned on stretching in the draw direction in the extruded and slightly drawn specimens⁴⁸.

The discovery of spherulites^{16,17} and polymer single crystals^{6,7,8} drastically changed the concepts of polymer crystallisation and of fine structure of crystalline polymer solids. The relatively thin single crystal lamellae with a thickness between 100 and 200 Å directly observed in electron microscopy or derived from small angle X-ray diffraction contain folded chains perpendicular to the lamellae surface. The folded chain model of lamellae grown from solution postulated a one phase system in which all the polymer material was included in the single crystals. The amorphous X-ray diffraction pattern and the density defect were due to crystal defects, particularly chain folds at the crystal surfaces. Later development has brought both models closer together. In spite of rather regular chain folds with immediate re-entry there are some chains folding back in a switchboard manner. In a sample crystallised from the melt there are still more chains incorporated in two different crystals so that the intervening portion is prevented from crystallisation. Together with uncrystallisable components such tied molecules constitute an amorphous phase of the very same type as assumed by the fringe micelle model. The basic improvement of this model is just the comprehension of the important role of chain folds in establishing a discontinuity between the crystals and the amorphous material. A particularly important problem in crystalline polymers is the plastic deformation and the resulting high orientation in drawn fibres and films. The basic mechanism of plastic deformation is associated with phase transformation, twinning, chain tilt and slip which finally leads to complete break up of original crystals into smaller blocks which are incorporated in the extended fibrils. The tied molecules in such highly oriented material are markedly strained and aligned which show up in a decrease of entropy and enthalpy as compared with a completely relaxed amorphous phase. The decrease in enthalpy quantitatively explains

the conspicuous depression of sorption, dyeability, diffusion and permeability of drawn fibres and films.

With regard to polymer single crystals Sauter⁴⁹ reported single polyoxymethylene crystals formed in the course of polymerisation. Crystals grow through formation of spiral terraces, centred on screw dislocations, thickening along the edges of the crystals⁵⁰. In polymer fibrils it was found that the molecules lie along the shortest extension of the crystalline units³³. As the molecules are expected to be many hundreds or thousands Angstroms long they cannot be perpendicular to layers say 100 Å thick and remain straight. Hence it was postulated⁷ that the molecules must be sharply folded at regular intervals. In the laminar crystals the fold period and the corresponding thickness of the layers could be identified also by means of low angle X-ray methods²³. In the case of polyamides the fold might well lie in the planes containing the hydrogen bonds. This could also account for the ease by which polycaproamide crystallises with the neighbouring chains in antiparallel orientation. Detailed texts have been written on polymer single crystals notably those by Geil,⁵¹ Keller^{52,53,54} and Blackadder⁵⁵.

Keller⁵³ discussed the problem of disorder in chain folded single crystals and gave the conclusion that sizeable disorder exists within the usual single crystals,^{93,94} which formerly were considered to be completely ordered. Fibrous crystals and crystallisation during flow are also considered. Long strings of platelets termed shish-kebabs after Lindenmeyer⁵⁶ have been observed in studies of solution grown crystals. It has become apparent that they are the result of crystals originating along lines of nuclei.^{56,57} Pennings^{58,59} found that the shish-kebabs are readily produced when a rotary stirrer is immersed in a supercooled solution.

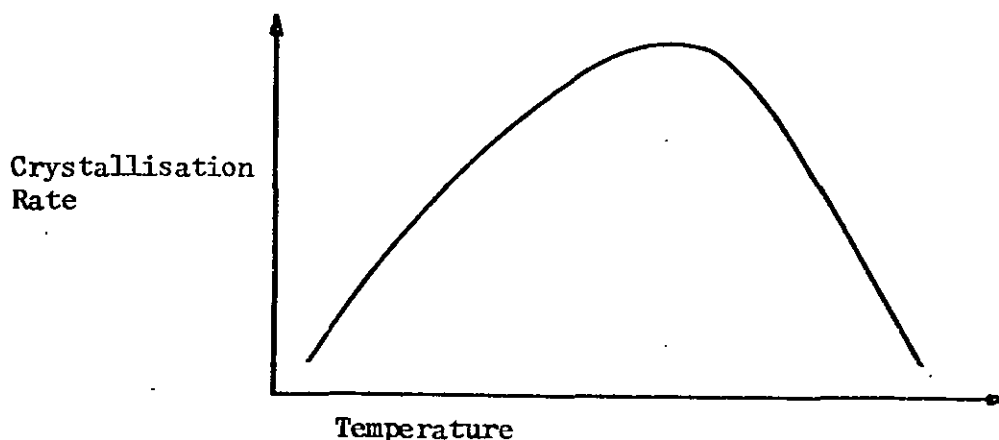
A paper by Keller and Machin⁶⁰ deals with crystallisation leading to oriented textures. The paper attempts to clarify the problem of extruded polyethylene sheet, which leads to the more general problem of crystallisation under stress. Keller and Machin found that the alignment and twisting of the lamellae and the density of the nucleating lines are the principal stress-dependent variables. The structures formed are shish-kebabs as described earlier. Keller and Machin state that row nucleation is the basic process of crystallisation under stress or during flow. The proximity of the nuclei along the rows confines crystal growth to the plane at right angles to the direction of the stress. If the stress is small, then the crystals will grow as they do in spherulites. If the stress is higher, the chains will be aligned in the draw direction, giving a c-orientation fibre pattern. Here the plane of the ribbons will be roughly perpendicular to the draw direction. Intermediate stresses will lead to an incomplete twisting of the ribbons. It has been found that films crystallised in a more highly stretched state, are comparatively weaker at right angles to the draw direction. With regard to the nucleation of the row structure any inhomogeneity within the material could be drawn out into the stress direction and used as a nucleus, (e.g. remnants of the original crystalline material). Keller and Machin sum up by saying that there are at least indications of central threads underlying row-nucleated crystallisation from stressed melts, and of their extended chain character. A further paper by Hill and Keller⁶¹ details definitive evidence for the nucleating crystals proposed earlier.⁶⁰ X-ray diffraction patterns recorded while the samples crystallised under stress, at the appropriate elevated temperature, conclusively demonstrated the two-stage nature of the crystallisation. First a small number of crystals form which are highly c-axis oriented, followed by a second group of crystals having a more complex stress

dependence of texture patterns. This is in complete agreement with the model that c-axis oriented fibres induce transversely growing lamellar crystals.

Crystallisation of polymers from the melt and the structure of bulk semi-crystalline polymers was the subject of a paper by Keith⁶². Two stages in crystallisation can be recognised, the first unmistakably gives rise to spherulites composed of chain folded lamellar crystals⁶³, the second probably to a diversity of morphological forms including both chain-folded and extended chain crystals⁶⁴ which grow in interstices within the spherulites. Crystals of these various kinds are connected both by tie molecules and by more substantial intercrystalline links,^{65,66,67} and between them are disordered regions arising both from irregular folds at crystal surfaces and from polymer whose crystallisation has been impeded by entanglements.

The solidification and overall crystallisation rate of melted polymer can be described by the Avrami equation⁶⁸.

$$\text{overall crystallisation rate} \propto 1 - e^{-Kt^n}$$



n = Avrami coefficient associated with nucleation and mode of crystallisation

t = time

The growth constant K depending on nucleation and crystal growth, first very rapidly increases with increasing supercooling, reaches a maximum and afterwards decreases again. This behaviour is the consequence of the different temperature dependence of single factors affecting the nucleation and growth rate. Nucleation generally increases with decreasing temperature, growth is a product of the tendency of crystallisation increasing with supercooling and of chain mobility rapidly decreasing with lowering the temperature. At sufficiently low temperatures the crystallisation may be practically prohibited, e.g. for polypropylene or polyoxymethylene. With polyethylene however K reaches such high values during cooling that even drastic quenching in liquid nitrogen yields a rather high degree of crystallinity. The spherulite starts from a single crystal which through low angle non crystallographic branching first grows into bundle like structures. This gradually approaches the typical spherulitic structure with radially arranged more or less helically twisted, ribbon like lamellae. As a rule spherulites are birefringent and hence good light scatterers. Thus the solid polymer is rather opaque. The larger they are the more they reduce the elongation, ultimate and impact strength of the material. Far smaller or even no spherulites are obtained by rapid quenching which therefore yields more transparent and less brittle material.

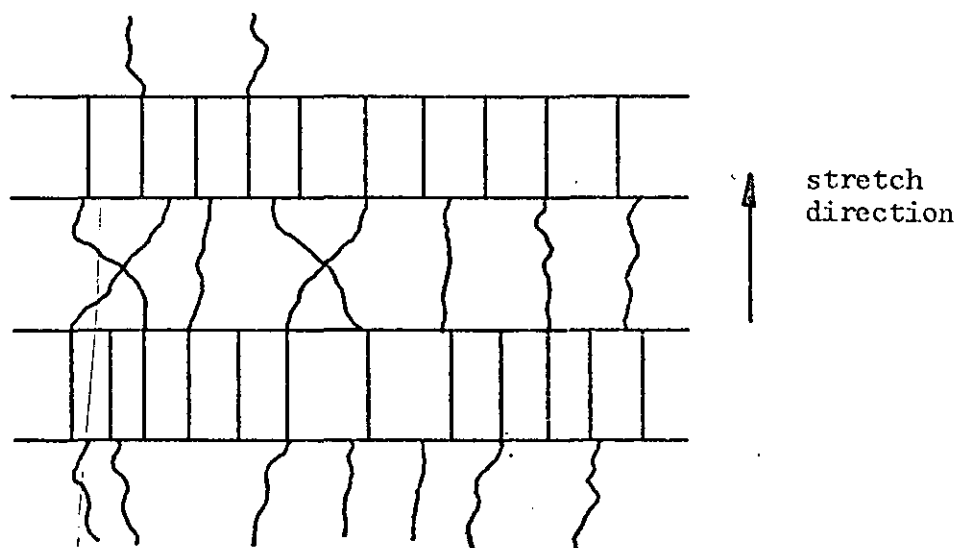
With high molecular weight polymers, higher concentration, very viscous solvent and particularly in the melt, the crystallisation is severely restricted by diffusion processes by which the rejected impurities accumulating in front of the advancing faces of a growing crystal are transported out of the way of the incoming solid front. To a large extent they are pushed to the sides compelling the crystals to grow in the form of ribbon-like lamellae characteristic for spherulite formation^{69,70,71}.

Two concepts have been advanced to explain chain folding, one based on the kinetics of crystallisation^{72,73,74,75} and the other on the thermodynamic stability of folded chains containing crystals⁷⁶. Both predict an increase of crystal thickness with temperature of crystallisation and surface energy. The theory of thermodynamic stability assumes that every newly deposited layer of folded chains adjusts in such a way that the free energy density becomes minimum.

A particular case is extended chain crystals. Crystallisation experiments⁷⁷ show first a linear increase of crystal thickness with chain length, and later a nearly constant thickness independent on chain length. The former crystals contain extended and the latter folded chains.

Peterlin¹² states that due to the reduced surface to volume ratio, extended chain crystals correspond to an absolute minimum of free energy density and hence agree with the thermodynamic theory. Extended chain crystal formation is enhanced by low molecular weight and high crystallisation temperature⁶⁴. With bulk samples on annealing the density first drops to a minimum in a distinctive manner and then very slowly increases, suggesting an increase of the crystalline core at the expense of density -- deficient surface layers.

The mechanism of orientation by Kobayashi⁷⁸ proposed the drawing out of folded chains to give extended chain crystals. Peterlin¹² proposed that lamellae are broken into clumps which are then arranged in the fully oriented structure as stacks of lamellae, retaining the folded chain structure. Samuels⁸⁰ proposes the oriented interlamellar amorphous model as shown overleaf.



However Takayanagi and co workers⁷⁹ indicated that this structure is present only upon annealing. Cold drawing by itself causes a break up of the lamellae into blocks, fibrils being formed 100 to 400 Å wide. Upon annealing these fibrils disappear as the crystal blocks reform lamellae.

A simple chain refolding scheme has been proposed for the annealing behaviour of polymer crystals by Dreyfus and Keller.⁸¹ Fold-length increase has been invoked to account for secondary crystallisation phenomena from the melt in the form of lamella thickening following the primary formation of crystal lamellae^{82,83}. This thickening occurs by discontinuous jumps involving factors of two (e.g. a spacing of 115 Å going to 230 Å after annealing for 5 minutes).

Blackadder and Lewell⁸⁴ have recently compared polyethylene crystal aggregates with bulk crystallised polyethylene. In this work single crystals obtained from dilute solution were aggregated together to form macroscopic samples large enough for mechanical and physical testing. Conclusions obtained included the fact that in low strain regions the tensile properties of an aggregate of polyethylene crystals are very

similar to those of bulk crystallised polymer with the same density as individual single crystals. This concordance lends support to the view that lamellar crystalline regions are indeed the fundamental building blocks in the structure of bulk crystallised polymer though they are disguised to such an extent that the resemblance to an aggregate of single crystals is not manifest under all conditions. Further work by Blackadder and Lewell⁸⁵ on annealing behaviour of bulk and aggregates can provide a key to the understanding of bulk - crystallised polymer in terms of microstructure.

+ / A paper by Morgan and Stern¹³ discusses a helical theory of the morphology of crystalline polymers with particular reference to fibres. The fundamental problem of the physics of crystalline polymers is to relate the polymerisation conditions, through fabrication methods and the resulting morphology, to the physical properties. There is a considerable literature with many conflicting interpretations. Controversy especially centres around the morphology and the mechanism whereby the long chain molecules arrange themselves while crystallising into the hypothetical models proposed to explain the properties of the fabricated samples. According to Morgan and Stern current hypotheses based on crystallites and chain folding have limited interpretative values as they can only be applied to narrow facets of the overall problem and are known to be unsatisfactory because of this lack of general applicability. The basic facts of our knowledge of the mechanism and kinetics of crystallisation from molten polymer are outlined and the most probable affect of orienting and relaxing the resulting semi-helical structure considered. This leads to morphologies which unify the interpretation of the data obtained by the many disciplines that have been brought to bear in this field.

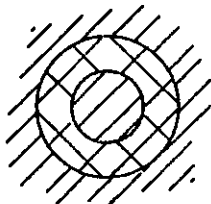
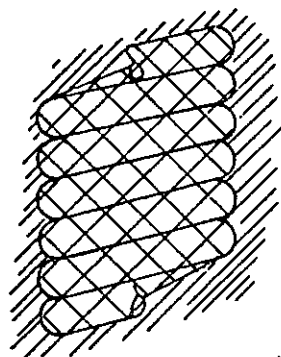
Meibohm and Smith⁸⁶ reported that a comparison of the low angle X-ray diffractions and the orientations as indicated by wide angle X-ray diffraction showed no good correlation between the orientation of the polymer regions responsible for the two classes of diffraction.

Stern and Morgan limited their considerations to polymers crystallised from the melt under the normal conditions of technical interest and certainly without the influence of surfaces such as would be pertaining if the crystallisation occurred in thin films, say between tightly pressed microscope slides or very slow crystallisations at temperatures just below the melting point.

Information on low angle X-ray diffraction of unoriented crystalline polymers is scant. Meibohm and Smith⁸⁶ however reported that unoriented crystalline polyethylene terephthalate gives a ring indicating a periodicity of 87 Å and Statton⁸⁷ has reported similarly on polyhexymethylene sebacamide (nylon 610). In both cases the differences in the electron density between the amorphous and crystalline regions had to be augmented by annealing to be detectable by the techniques used.

Morgan and Stern state that postulated models largely disregard the polymer chain movements necessary for their formation and do not adequately explain the changes in the low angle reflections and all the data available from other disciplines.

With polyamides the chains can align themselves almost perpendicularly to the drawing direction during the early stages of the drawing performance⁴⁸. The basic coiled fibril unit of structure proposed by Morgan and Stern is shown below along with an oriented unit of extended coiled crystal.

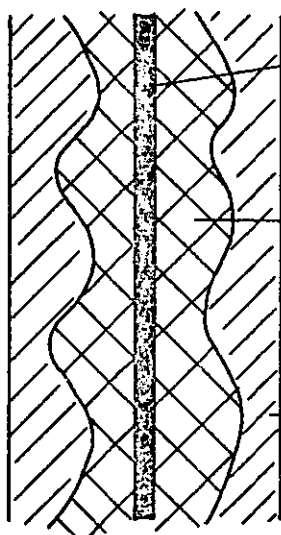


Imperfect strained
crystalline region



Boundary amorphous

Oriented
unit of
extended
coiled
crystal
Schematic
representation
Regions
A, B, & C
merge
continuously
into each
other



A - Imperfect crystalline region
polymer chains mainly oriented
in draw direction

B - Less perfect crystalline
region polymer chains
helically disposed

C - Boundary amorphous layer
polymer chains oriented in
drawn direction

The orientation in the interconnecting segments of polymer chains in the boundary - amorphous matrix will vary according to the mode of fabrication.

In a recent review Rees and Bassett¹⁴ consider the texture of crystalline polymers under two subsidiary headings, chain folding and morphology.

Chain folding has come to be accepted by the majority of workers in the field as a basic and general mechanism of polymer crystallisation.

In the review items such as lamellar thickening, theories of crystallisation, solution as well as melt grown materials and fold surface structure are considered. It is stated that the study of the morphology of semi-crystalline bulk polymers is more difficult than that of solution grown crystals. It is difficult to say if the area studied is representative of the whole of the bulk polymer.

Consideration is also given to extended chain polymers produced by crystallisation either at high pressures or under conditions of flow or stress. Extended chain crystals contain few or no chain folds. Hence in these crystals the crystal thickness in the chain direction is equivalent to the molecular length. Flow-induced crystallisation from the melt is known. Fast extrusion of molten polymer gives rise to anomalies in viscosity which can occur tens of degrees above the extended-chain melting point. At temperatures below it, however the same phenomenon can involve polymer solidifying spontaneously in the die giving a product which is highly oriented and has marked chain extension^{88,89}.

Polyethylene crystallised at pressures above 4 K bar revealed crystals up to 3 μ m thick, which is in the range expected for fully extended chain crystals,⁹⁰ the samples showing striated morphology. Rees and Bassett^{91,92} discovered that by annealing 100 Å thick lamellae at between 5 and 10 K bar pressure, it was possible to convert them continuously with maintained molecular orientation to higher melting layers some thousands of Å thick.

2.2 MICROSCOPY STUDIES ON NYLONS

The formation of spherulites in nylons has been studied by several workers. It had been observed during early work on filaments of polyhexamethylene adipamide (nylon 66) that when the polymer was cooled slowly from the melt the solid polymer was opaque and contained spherulites of the type later observed in polythene^{17,106}.

Langkammer and Catlin¹⁰⁷ describe the occurrence of spherulites in polyhexamethylene adipamide and the factors which appeared to be responsible for their formation in various physical modifications of the polymer. These authors stated that the most important factor in spherulite formation is usually the rate of cooling from the melt. Examination of a ribbon formed by extruding molten polymer into water showed 3 regions :

- (i) Optically clear
- (ii) A hazy band probably containing many small spherulites
- (iii) The centre of the ribbon containing large spherulites.

Langkammer and Catlin obtained a transparent, non spherulitic polymer by spinning the polymer into acetone at -80°C . They found that heat treatment or ageing of this polymer increases the lateral order (X-ray data) without the formation of microscopically visible spherulites. Spherulites were found to reduce tensile strength, increase opacity and decrease workability. There seemed no growth of spherulites after melting and holding the polymer at $240 - 245^{\circ}\text{C}$ for 30 minutes.

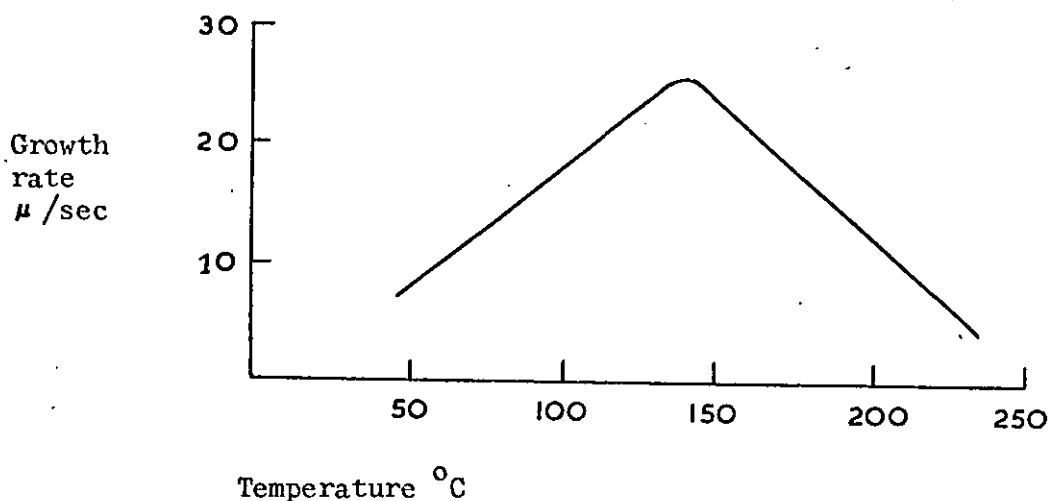
Barriault and Gronholz¹⁰⁸ considered the structure and optical properties of spherulites at room temperature. Bunn and Garner¹⁰⁹ reported spherulites in nylon 66 and stated that these spherulites possessed a radially positive birefringence in contrast to polyethylene spherulites which are negatively birefringent (that is having a larger refractive index in the vibration direction perpendicular to the radius). Brenschede¹⁸ and Herbst¹¹⁰ also observed spherulites in nylon 66. Herbst made an X-ray diffraction study of the chain orientation in nylon 66 spherulites and stated that the hydrogen bonds are in a plane perpendicular to the spherulite radius. Keller³⁷ however stated that in nylon 610 the polymer chains are perpendicular to the radius and the hydrogen bonds parallel to the radius and the work of Barriault and Gronholtz supported this. These workers found nylon 66 spherulites to be positively birefringent and also state that the basic crystallites shift from a pseudohexagonal to a triclinic lattice without destroying the spherulite structure below 160°C . Hence the crystal structure one studies at room temperature is usually not exactly the one that was present when the spherulites were originally formed. Herbst found that in polyamides the regions between the spherulites were as crystalline as the spherulites themselves. (However Keith and Padden, and Chappell et al¹¹⁴ agree with this finding).

In nylon 610 both positive and negative spherulites were formed, the majority being positive. Crystallisation above 160°C produced closely spaced extinction rings making the spherulites appear to consist of two alternating types of rings. Nylon 66 crystallises from 250°C to about -30°C and consequently it is always crystalline at room temperature. When fused above 275°C and crystallised above 100°C it gave well developed spherulites which were always positive. Keller suggested that the arrangement of the crystallites is one of closely coiled helices with the molecules lying along the winding direction. Keller stated that spherulites were built of distinct fibrillar units. Based on direct observations and on earlier work on non-polymeric spherulites a regular periodic branching mechanism of the fibrillar units was proposed, where in the case of maximum regularity the position of each branch with respect to the preceding one is defined by one constant branching period and two constant angles, and a constant direction of rotation in the 3 dimensional case. Keller and Waring²⁷ showed that this mechanism can lead to helices which produce the previously observed zig zag extinction effects. Investigations of the fine structure of the fibrils indicated a closely coiled rope-like arrangement in samples grown from solution. These are about 400 \AA and upwards, sometimes reaching the limit of the optical microscopic resolution dependent on the preparation. These units appear to be built of and connected by much smaller fibrils which themselves possess a periodicity of $100 - 200 \text{ \AA}$ or less. It is suggested that branching could be a possible consequence of the coiling structure. The conclusion was reached that, as far as the morphology is concerned, crystallisation in polymers represents a special case of the formation of crystalline aggregates in viscous media.

Boasson and Woestenenk⁴² found that under special conditions negative spherulites could be obtained in nylon 66. These conditions were :-

- (i) that the fusion temperature should be between 258 and 265°C and
 - (ii) that the crystallisation temperature, subsequent to fusion should be between 250 and 255°C.
- Khoury⁴⁴ has also studied the formation of negatively birefringent spherulites in nylon 66. He observed that although the formation of these spherulites was associated with the temperature range 250 - 265°C, the phenomenon was not necessarily one which was dependent on initially fusing the polymer and then allowing it to crystallise at a specific, lower temperature. Khoury's work indicated that the formation of negative spherulites in nylon 66 is a crystallisation phenomenon which occurs when the polymer is heated at constant temperature above its optical melting point within a restricted temperature range (250 - 265°C). No negative spherulites are formed when the polymer is initially fused above 265 - 266°C. Khoury²⁹ has investigated the fibrillar structure of spherulites of nylon 66 using a formic acid etching technique. These spherulites were in films crystallised from the melt at temperatures between 240 and 255°C.

Spherulites in nylon 610 and nylon 66 have been studied by Lindegren.¹¹¹ He found that samples of nylon 610 with a lower inherent viscosity had a higher growth rate. Lindegren showed that there are two types of positive spherulites characterised by differences in growth rate and level of birefringence as well as melting point. He stated that the large positive and highly birefringent spherulites as well as negative spherulites have the same melting point 273 - 274°C whereas the small positive spherulites with low birefringence melt between 269.5 and 270°C. Other observers quote different values for the melting point of these spherulites. Simultaneous growth of all three types of spherulites were observed only between 250 and 255°C. In contrast to the two other types small positive spherulites were formed in an extended temperature range. The growth rate curve for the positive spherulites has a maximum at about 140°C as is shown overleaf.



The course of the primary crystallisations in nylon 66 has been discussed by Hartley, Lord and Morgan²⁵. From the experimental data it was possible to infer that at low temperatures around -30°C , the primary crystallisation was from sporadically formed nuclei followed by fibrillar growth. In the temperature range between -20°C and 230°C the crystallisations were too fast to follow by the density balance method. The authors state that coarser spherulitic structures are produced at high temperatures in contrast to finer grain structures formed at low temperatures. It was stated that secondary crystallisation is much more pronounced in the case of nylon than polyethylene terephthalate. At some temperatures the primary and secondary crystallisation processes merge together and cannot easily be distinguished. Furthermore, since nylon 66 crystallises at an appreciable rate at low temperatures the so called second order transition must be in the region of -40 to -50°C and not at $+47^{\circ}\text{C}$ which is quoted in the literature. It was noted that the lower the fusion temperature the higher the rate of crystallisation. As molecular weight increases the crystallisation rate decreases. At $M_n = 12,600$ the primary and secondary crystallisations merge when crystallised at 247°C . The authors state that in secondary crystallisation small spherulites grow together to form larger spherulites and also give a brighter picture, indicating some rearrangement within the spherulites during the secondary crystallisation.

Symons¹¹³ studied the morphology of crystalline polymers with especial reference to single crystals grown from the molten state. He refers to work on nylons by Magill and Harris using very thin films. Electron diffraction patterns indicated that the molecular chain direction was essentially normal to the plane of the film. As the film was only about 1,000 Å thick it appears that chain folding probably takes place.

Chappel, Culpin, Gosden and Tranter¹¹⁴ studied some crystallisation phenomena in rapidly quenched nylon 66 as produced in melt spinning. Owing to the geometrical form of the nylon, cooling from the melt was extremely rapid. The structure in the solidified polymer is stable at room temperature for long periods in the absence of moisture. However, on exposure to moisture changes may occur in the crystalline character. In their work Chappell and co-workers had the advantage in that the conditions of rapid quenching enabled them to study crystallisation following cooling to 160°C or lower. This type of study cannot be undertaken using a hot stage microscope because below 230°C the nylon crystallises too rapidly. Spun filaments were observed at various points between the spinning head and the wind up point. The temperature of the filaments was obtained using the method of Culpin and Madoc Jones¹¹⁵ and the structure examined using a polarising microscope. It was found that the structure altered depending at what temperature the filaments were converged. Examination of chopped filaments using phase contrast illumination showed a crystalline skin to grow inwards in the presence of moisture. Examination of the filaments by X-ray showed a single halo which very slowly (about 100 hours) changed to the characteristic double ring. Samples put immediately into a desiccator after chopping showed only a single diffuse ring. Chappell et al disagree with Lord et al²⁵ over the question of the second order transition temperature. Chappell et al suggest that the effects observed at -34°C are due to the influence of moisture in relieving strain in the material, rather than to

crystallisation in the usual sense. It is stated by Chappell et al that unless the polymer is melted under pressure, the solid obtained by cooling it contains minute bubbles of water, even though the original chip is well dried. They also suggest a relaxation on the initial uptake of water (up to about 2% by weight), and that the material between spherulites may in the presence of moisture become both as crystalline and have as high a refractive index as the spherulites.

Fitchmun and Newman¹¹⁶ state that the polymer surface morphology varies with thermal conditions such as melting temperature, crystallisation temperature and cooling rate. They say that transcrystallisation is favoured by rapid cooling and high crystallisation temperatures. The rate of nucleation is known to have a negative temperature coefficient and to reach a maximum at some temperature below the melting point. Hence in thin films a temperature gradient occurs favouring a higher nucleation rate at the surface than in the bulk. Fitchmun and Newman state that transcrystallinity is a general morphological feature of many semi-crystalline polymers which can be induced by certain moulding conditions and is not necessarily controlled by the specific nature of the mould surface as described by Schonhorn¹¹⁷.

It is stated that because of secondary crystallisation the crystallinity in the surface regions must be about as high if not higher than that found in the bulk¹¹⁸. Collier¹¹⁹ in a paper on polymer crystallisation and resultant properties brought out the following points. The morphology formed during normal crystallisation from the melt is generally of a spherulitic nature. Electron microscopy shows spherulites to have lamellar fine structure the lamellae being 100 Å thick and 10^3 to 10^5 Å wide. The lamellar ribbons length is approximately equal to the radius of the spherulite. At lower crystallisation temperatures small spherulites are formed due to higher nucleation. (The fine structure changes, although

lamellar thickness is slightly decreased, the major effect is the decreasing lamellar ribbon width). Finer textured spherulites are obtained at lower crystallisation temperatures.

Magill has investigated the formation of spherulites in mainly non-commercial nylons, these have included, "odd-even" polyamides¹²⁰, "even - odd" polyamides,¹²¹ "odd - odd" polyamides¹²² and "even - even" polyamides¹²³.

The study on even-even polyamides showed striking similarities in spherulitic morphology. The observed variations in textural features of spherulites in nylon 210, nylon 66, nylon 106 and nylon 1010 showed parallel changes during growth conditions and conformed to a definite sequence of behaviour. At least four different types of spherulites were found to exist in each polymer. Crystalline platelets possessing single-crystal properties were grown in thin films of these polymers near their respective melting points. Farmer and Little¹²⁴ have described the preparation of sections of polymers for examination under the electron microscope. They are of the opinion that ultra thin sections will always be liable to create more problems than they solve. These authors state that the knife angle is the most important point when sectioning ultra-thin sections. In their studies the authors used a diamond knife and a butyl-isobutyl methacrylate embedding agent at room temperature.

Scott²¹ has examined selected areas on thin films of nylon 66 by electron diffraction. Bright field micrographs were obtained on spherulitic films. In the samples examined it was shown that the molecules were arranged in sheets with the hydrogen bonds in the plane of the film. In dark field electron microscopy the radial growth and branching of discrete crystalline regions was seen. Bright field electron microscopy showed the surface morphology of these structures.

Rusnock and Hansen¹²⁵ have made observations on both bulk and filament forms of nylon 66 using transmission electron microscopy on thin polymer sections. The nylon specimens embedded in an epoxy-phenolic resin alloy were sectioned to below 500 Å in thickness on an ultra-microtome with a 48° diamond knife. Contrast was obtained by staining the nylon sections with phosphotungstic acid. Observations of nylon 66 moulding pellets resolved the fibrillar structure of spherulites at the 100 Å level. Replication techniques have been used to examine fractured surfaces by transmission electron microscopy. Reding and Walter⁴⁵ used a replication technique on etched samples of polyethylene.

A 15% polyvinyl alcohol solution in water was used for replication. Then a film of carbon was evaporated onto the polyvinyl alcohol film which was removed by floating in hot water. The carbon films were shadowed to give better contrast in the electron microscope. It was found that a low density polyethylene crystallised in spherulites which tended towards a spherical shape, the associated fine structure being small and broken up. The high density polyethylene crystallises in a more perfect laminated fine structure, the spherulites themselves being less distinct. It was stated by these authors that spherulites formed by moulding contain a relatively low amount of internal order.

Bezruk et al¹²⁶ have used active oxygen as an etching agent. They noted a globular form which they say is normally associated with the amorphous part of the polymer. A polyamide 68 (probably 610) was examined and electron microscopy revealed the co-existence of single crystals and spherulites and spherulites and globules.

Crystal and Hansen¹²⁷ have examined the morphology of cold-drawn nylon 66. The nylon 66 was composed of uniformly sized spherulites approximately 50 μ in diameter and was examined before and after cold drawing using

light and electron microscopy on thin sections and by low angle X-ray diffraction. The thin section electron micrographs indicated that the spherulites were composed of radiating lamellae approximately 95 \AA thick. Low angle X-ray diffraction patterns confirmed this. Ultra thin sections were cut on an ultra microtome using a 45° diamond knife. The sections were collected in a 10% acetone in water solution.

Harris¹²⁸ examined thin films of steam annealed nylon 66 filaments using dark field electron microscopy. Spit¹²⁹ examined thin cast films of nylon 6 after staining with phosphotungstic acid and showed lamellae structure to be present. Anderson⁶⁴ has examined the internal morphology of bulk crystallised polyethylene using fractured surfaces. The samples were isothermally crystallised and fractured after cooling to liquid nitrogen temperatures. Lamellae structure was shown to be present.

Keller³³ has investigated the crystalline texture of polyamides using electron microscopy and electron diffraction. All the specimens examined were prepared from solutions. It was found that the electrons destroyed the diffracting ability of the crystals without affecting their shape. In some films a spherulitic morphology was observed which consisted of a flat layer structure within the film plane. In general however the spherulites developed through a fibrous texture which appeared to arise through the curling up of flat sheets. These sheets possessed a fibrous morphology.

Dlugosz and Keller¹³⁰ have discussed the beam-induced contrast in the electron microscope images of polymers as observed in ultra thin sections. It is suggested that selective etching and material rearrangement are thought to be responsible for changes induced in the polymeric specimens by the electron beam. In this work polyethylene was used, concentric ring structures being formed under the influence of the electron beam.

Grubb and Groves¹³¹ have studied the rate of damage of polymer crystals in the electron microscope with reference to temperature and beam voltage. It was found that the effect of temperature varied with the polymer examined but the damage rate was proportional to (electron velocity)⁻². The orientation in nylon 66 spherulites was a study by Mann and Roldan - Gonzalz¹³² using X-ray diffraction. It was concluded that in positively birefringent spherulites the crystallographic a axis is parallel to the spherulite radius. The zig-zag extinction pattern shown by such spherulites in a polarising microscope can be understood in terms of this orientation. The results on negatively birefringent spherulites was not in agreement with earlier results of Keller. Evidence was cited which showed that non-birefringent spherulites have random orientation. The spheruloidal aggregates which grow at the same time as negatively birefringent spherulites are found to have well defined optical properties when grown in thin films and confused optical properties when grown in thick films. This difference is reflected in differences in X-ray diagrams. In thin films a unique orientation exist in which a direction close to the crystallographic b axis lies parallel to the radius while the (002) plane lies near the surface of the film. This orientation provides an explanation of the observed optical properties. In thick films the (002) plane again tends to lie near the surface of film, but orientation relative to the radius varies from place to place, thus causing confused optical properties.

Chain folding in oriented nylon 66 fibres has been studied by Dismore and Statton¹³³ using wide and small angle X-ray diffraction and broad and narrow line NMR techniques. Using these and other techniques it was shown that some molecules in oriented nylon 66 fibres when heated to high temperatures under zero tension change from the elongated to the folded conformation, with no change in crystal orientation. The tensile strength was reduced by the introduction of these folded chains.

Dumbleton, Buchanan and Bowles¹³⁶ have used X-ray diffraction to characterise nylon 66 structure. The work was carried out on fibres using wide and small angle X-ray diffraction. The results indicated that the drawing process is one of crystal slip. While these methods gave a great deal of information about structure along the fibre axis, little information was obtained perpendicular to the fibre axis.

Campbell¹³⁴ demonstrated that water sorption does, in fact, cause changes in both amorphous and ordered regions of nylon 6. X-ray diffraction indicated that when water is added to the nylon matrix the two peaks in the diffraction curves representing order in the nylon change anisotropically. This would suggest that water plays a dual role in the modification of ordered regions of nylon 6. The order represented by the larger d value is increased while the order indicated by the smaller d value is decreased as water is sorbed by the nylon.

2.3 EFFECTS OF PROCESSING ON STRUCTURE

The structure of moulded polyamides has been investigated by several workers one of whom Kessler⁹⁵ has paid particular reference to nylon 6 and suggests that the composition of the structural pattern in the object is mainly determined by the following effects :-

- (i) Thermal effect due to the way of heating and cooling the poorly heat conducting polymer mass during the shaping process.
- (ii) The mechanical effect due to the mixing action exerted by the processing apparatus on the rather highly viscous polymer melt.

It is stated that palisades (row nucleated spherulites) are usually present because of poor mixing, little counter pressure and too low a melt temperature. Mechanical treatment during processing alters the

structural picture of the moulded article. When a piece of polymer chip is heated above its melting point and allowed to cool a normal spherulitic structural picture is obtained i.e. polyhedral spherulites and palisades. However, when the polymer is mixed in the molten state deviating structural pictures arise and disturbed spherulites are formed. Kessler is of the opinion that the mixing of the polymer in an injection moulding machine is often inadequate and can lead to flow - lines in the moulded product. (However Kessler used a plunger machine and not a screw type machine which has better mixing properties). It was found that by changing the cylinder temperature from 225°C to 215°C structural differences could be obtained. The effect of the mould temperature on the structure of the injection moulding mainly finds expression in the structural picture immediately on the surface of the object over a depth of about 0.5 to 1 mm. The result of the bad heat conduction of the polymer is that towards the core of a rather thick moulding the structural picture is only little influenced by the mould temperature. In respect of mechanical properties the mould temperature was found to play a greater part in the case of thin products than thick ones.

When a cold mould is used, phenomena may sometimes occur in the structure on the surface of the object which exert such an important influence on its quality that they are worth mentioning. Feeding may proceed irregularly due to a frozen skin of the moulding. The following molten polymer must burst this skin to fill the mould. This can produce pieces of this skin embedded in the moulding surface. Low melt temperatures or low injection speeds of the polymer may also cause this phenomenon.

Kessler in discussing the influence of properties on structure considers the properties of an amorphous, spherulite - free condition, and a completely crystallised spherulite-filled condition and postulates that :-

- (a) The moisture absorption of the spherulite-free material is about 1% higher than that of spherulite-filled material.
- (b) The dimensional change in spherulite-free material occurring as the result of water absorption is about twice as great as in spherulite-filled material.
- (c) The yield stress in spherulite-free material is about half that of spherulite-filled material.
- (d) The hardness and modulus of elasticity of spherulite-free material are half the values for spherulite-filled material.
- (e) The impact-resistance of spherulite-free material is extremely high, whereas that of spherulite-filled material is relatively low.

Vinogradskaya and Ozolin⁹⁶ believe that the supramolecular structure changes during ageing, affecting the physico-mechanical properties. The change in supramolecular structure seems due to relaxation of the internal residual stresses and secondary crystallisation. For nylon 6 an increase in density was produced by increasing the melt temperature, or applying a slower cooling rate. A high injection pressure slightly increased the density, while on ageing the density first dropped before increasing. On ageing larger spherulites were observed. The spherulite size decreased with higher melt temperature, while injection pressure had little effect on the spherulitic structure. With a slower rate of cooling a more structural specimen was obtained. The specimens were test rods 15 mm diameter and 30 mm long which were moulded in a special press mould. Using polyethylene in this work a hold-on time of 10 minutes was quoted but no figure was given for nylon 6. Surprising results for nylon 6 were that the microhardness decreased and the density increased as the moulding temperature was increased.

Muller and Pflunger⁹⁷ have examined the properties, chemical constitution and crystallinity of polyamides. They consider the difference in melting points in polyamides and associate this with the number of hydrogen bond linkages which are made. In nylon 6 not all the available H-linkages are used. Muller and Pfluger stated that of the general mechanical properties only the elongation at break depends on the molecular weight to any extent. As regards water absorption the capacity decreases with increasing crystallinity. If a polyamide is exposed to high humidity or immersed in water, the saturation value is hardly affected by the temperature of test.

In a further paper Muller and Pfluger⁹⁸ consider the influence of the crystalline and morphological structures of polyamides on moulded and extruded products. They state that a lower molecular weight material has a greater tendency for the formation of morphological structures than a higher molecular weight material. The speed with which the melts are cooled is important, the first step in the transition from liquid to solid being decisive. With slow cooling as is the case with casting, the long chain molecules have enough time to arrange themselves at least as far as the coiling and molecular obstacles permit. The slow solidification gives extensive morphological structures. As a result of limited heat conductivity adequate cooling is only possible in thin wall mouldings. Consequently the edges of injection mouldings are changed by the rate of cooling. The temperature to which the melt is raised before solidification has no direct influence on the crystallinity of the solid polyamide but it does affect the morphological structures. Most mouldings tend to recrystallise even at room temperature. No changes in the morphological structures detectable by optical polarisation have been observed alongside recrystallisation. With increasing temperature the rate of crystallisation rises and the equilibrium is displaced towards a greater crystallinity up

to a limiting temperature, which lies below the melting point. Every polyamide passes through a maximum crystallinity as the temperature rises. Two opposing mechanisms operate, on the one hand there is the increasing mobility of the polymer chains and the related increasing probability of the formation of regions of order, and on the other the growing tendency towards the dissolution of the lattice structure with rising temperature. At higher temperatures than room temperature, water causes a very fast recrystallisation. Steam has the greatest effect on crystallinity but should not be hotter than 140°C because of the danger of hydrolysis.

Overall, Muller and Pfluger state that as crystallinity increases, then yield point, tensile strength, modulus of elasticity, abrasion resistance, hardness increase but impact strength decreases. They also say that a high crystallinity product should be used for optimum heat stability, resistance to atmospheric oxidation and chemical attack. With dielectric properties higher crystallinity gives a lower temperature for the loss maxima. "Transcrystallisation" is said to occur due to oriented cooling in one direction (cooling front). Spherulites are formed in layers which tend to grow at right angles to the cooling front so orientating the chain molecules parallel with this front.

Mouldings which contain a variety of morphological forms e.g. the larger polyhedral aggregations in one part and fine granular forms in others, or even regions completely free of spherulites, must be considered as of inferior quality owing to their anisotropy and a greater tendency to produce internal stresses.

Steinbuch⁹⁹ has considered the effect of crystallinity on the properties of nylon 6. He agrees with other workers in the field that after boiling crystallisation has only a limited effect on spherulitic structure.

Probably the molecules will also fit into spherulite-like units during

after-crystallisation but these units are very small and need hardly be considered. He referred to a paper by Jacobi¹³⁵ who said that wear and abrasion resistance increased with crystallinity. Steinbuch believes that crystallinity only effects friction at a low level of crystallinity. He agrees with other workers that the influence of the mould temperature is greatest at the surface of the moulding and increases with decreasing thickness. Steinbuch is of the opinion that test mouldings should be treated in the same way as the production moulding will be. This may comprise annealing in oil or gas followed by a moisture conditioning and homogenising treatment. He believes that testing of "as moulded" specimens may always introduce a large spread in test results. Moreover it gives very little information about behaviour in actual practice, where the product will always contain some moisture. The choice of mould temperature and method of after treatment for injection moulded nylon 6 has been considered by Kessler¹⁰⁰. The conclusion arrived at was that the influence of the mould temperature on the final properties is just the reverse of what is usually assumed and that neither the microscopic structural picture nor the opacity is a correct indication of the ^{balance of properties of the} moulded article. For a 1 mm thick moulding a change of mould temperature from 20 to 80°C produced a density change of 1.094 to 1.120 g/cc. Therefore it was suggested that a mould temperature between 40 and 80°C should be avoided due to the large changes in density. The density can be varied even more by after treatment, e.g. cold water to boiling water, than by the mould temperature. According to the author a product moulded at a 'high' mould temperature obtains the highest impact strength but the lowest yield and modulus of elasticity. As regards the impact strength, stabilisation in hot water which increases the density to a smaller extent is more favourable than steam treatment, which increases the density to a higher extent (assuming that a treatment in hot water gives a product stable enough with respect to crystallisation under the

circumstances of end use). From these experiments it seems that the skin of a thick moulding will tend to continue crystallising to a higher density than the core. It is clear that after injection moulding an after treatment is required to obtain a stable crystallisation level.

The effect of crystallinity on the properties of nylons has been studied by Starkweather et al²⁶. They stated that samples with low degrees of crystallinity can be made only by very rapid cooling from the melt at low moisture content and only in the form of thin films (ideally 0.010") because of limited thermal conductivity. Water is rapidly absorbed from normal laboratory atmospheres by these thin films and catalyses the crystallisation at room temperatures. Starkweather and co-workers did their original work using compression moulded nylon 610 films. In injection moulding of nylon 66, one observes less variation in the crystallinity content with various moulding conditions than with the compression moulded thin films. This is due to the poor heat transfer through the thicker sections of the plastic resin usually encountered in injection mouldings. Thus a fabricator using conventional equipment cannot appreciably alter the fine structure of his mouldings. The surface of the cold mould quenches the surface of the moulding so that no visible spherulites can be observed microscopically.

In 1/8" test bars evaluated in Starkweather's study it was observed that the interior contained spherulites ranging from 30 μ to 50 μ diameter. Changing the mould temperature from 50 to 100°C did not affect the size of the spherulites. The following injection moulding conditions were used on a 6 oz machine for a 4-cavity test-bar mould :-

Cylinder temperature	275°C
	275°C
	290°C
Mould temperature	50 and 100°C
Cycle time	40 seconds
Cylinder pressure	21,000 psi

Annealing the samples in dry nitrogen at 175 and 240°C increased the crystallinity without altering the spherulite size. The crystallinity of the skin increased by 6% due to increasing the mould temperature while the centre of the moulding gave a 4% increase. A difference between the gate end and the extreme position from the gate gave a difference of about 1% crystallinity. It was found that flexural modulus, yield stress and tensile strength increased with crystallinity and are independent of molecular weight within the limits tested (M_n 17,200 to 24,200 for nylon films). The impact strength was increased by increasing the molecular weight.

Starkweather and Brooks¹⁰¹ have considered the effect of spherulite size on the mechanical properties of nylon 66. It had been reported in an earlier paper that spherulites did not adversely affect the toughness of nylon unless their diameter is an appreciable fraction of the thickness of the specimen. The authors moulded test piece samples using the following conditions :-

Cylinder temperature	275°C
Mould temperature	45°C
Cylinder pressure	11,200 psi

Treatment of the specimens at 175°C in an annealing wax for 30 minutes did not alter the spherulitic structure. Nucleated and unnucleated grades

of nylon were used giving spherulite sizes of about $2\ \mu$ and $25 - 30\ \mu$ respectively. The nucleated material had a higher density than the unnucleated grade corresponding to a 4% difference in crystallinity. The authors state that almost any finely divided material may act as a nucleating agent for nylon 66. Additional nuclei may be introduced by remoulding, e.g. once moulded samples had a maximum spherulite diameter of $30\ \mu$ whereas 4 times moulded samples had a maximum spherulite diameter of $5\ \mu$. It was found that a higher flexural modulus was obtained with smaller spherulites and a higher crystallinity, however this difference disappeared as the water content increased. It was also observed that at 23°C dry samples with small spherulites did not neck. These effects diminished with increasing temperature and water content. The yield point was found to increase as the spherulite diameter decreased, also for visible spherulites no change was observed in the yield stress as the crystallinity increased from 40 to 55% for constant spherulite size. Summarising the authors state that the presence of spherulites in nylon 66 increase the yield stress and reduces the effect of variations in % crystallinity. Decreasing the size of the spherulites through increased nucleation results in a higher flexural modulus and yield stress, a lower elongation and a loss of ductility. These effects are markedly reduced by raising the temperature or water content. It must be noted that some of this work was undertaken using thin film samples.

Maxwell¹⁰² suggests that by means of controlling the pressure, temperature and flow history of the polymer during fabrication processing, morphologies can be produced which result in desired properties. He considered the flow in the mould to be comprised of three regions :-

- (a) A stick-slip region near the cavity wall where there is an interaction between the polymer and the wall. Here oscillatory elastic distortion and recovery take place and there is no true rotational flow.

- (b) A region near the centre between the cavity walls which does not receive shear deformation associated with the flow.
- (c) A high velocity gradient region between (a) and (b) where true rotational flow is observed and the orientation is high.

Maxwell also considers the effect of remelting large spherulites which on cooling may form many nucleation sites within the old spherulites. He also states that if pressure is applied rapidly, a glassy state response at a much lower change in specific volume occurs which affects the density and morphology. With crystalline polymers as pressure is increased at elevated temperature, the pressure induces crystallisation in the polymer well above the normal atmospheric melting temperature. If crystallisation can be induced at elevated temperatures then it gives the opportunity of changing morphology. Pressure is in fact acting as a nucleating agent and a smaller spherulite size is given with a higher pressure¹⁰³. Shear also gives an increased number of nuclei and hence changes the spherulite size. Maxwell considers three points for mechanical strength :-

- (i) Small crystalline texture to make possible greater interaction by chain cohesion.
- (ii) Imperfect spherulitic structure to make possible greater interaction by chain cohesion.
- (iii) Non strained boundary conditions around the crystalline structure.

A paper by Sogolova¹⁰⁴ discusses the supramolecular structure of polymers and its effect on their mechanical properties. This work was mainly concerned with nucleation of polymer systems to control the non-uniformity and instability of the structure. The studies were concentrated on gutta percha, isotactic polypropylene and isotactic polystyrene, mainly in film form, formed either from the melt or from solution. It was found with

isotactic polypropylene that heating the melt for different times at 180°C produced films with different stress-strain properties. It was also found that heating the melt for 5 seconds at 180°C gave a ductile polymer while heating the melt for the same time at 170°C gave a brittle polymer. It has been found that when nylon 6 is rolled or subjected to repeated impacts appreciable changes occur in its supramolecular structure¹⁰⁵. It was stated that on remelting films of polyamide three times the elements of supramolecular structure of the initial specimen increased while those of specimens containing nucleating agents remained unchanged. This first statement disagrees with the work of Starkweather²⁶ who found that the size of spherulites decreased on reprocessing.

2.4 DEGRADATION AND WEATHERING

The U.V. degradation of plastics has been studied by a number of workers in particular contexts. Amongst these Stephenson and co-workers^{137,138,139,140} studied the relative efficiencies of different wavelengths of U.V. light in producing photolytic reactions in polymers in an inert atmosphere. The studies were carried out on thin films, nylon 66 being one of the polymers studied. The tensile strength and elongation at break were measured after irradiation with U.V. light of wavelength 253.7 mμ.

It was found that the tensile strength decreased with irradiation and the elongation at break decreased after an initial increase. The reduction in properties was more severe on specimens in nitrogen than in a vacuum. The U.V. radiation caused a darkening of the nylon and also a gumminess of the surface. Shorter wavelengths produced the greater changes in physical properties. The molecular weight (M_n) was found to decrease and then eventually increase with irradiation time; the specimens irradiated in a vacuum showing the greater effects. Gel formation was also observed on

irradiation more crosslinking taking place in vacuum conditions, the scission to crosslinking ratio in nitrogen being almost twice as great as it is for nylon irradiated in vacuum. Decomposition products of ultra violet - irradiated nylon include all of the primary amines from methyl through to hexyl. Nylon degraded more rapidly during U.V. irradiation in oxygen than in nitrogen.

Kamal¹⁴¹ considered the cause and effect in the weathering of plastics and proposed some new techniques for more reliable predictions of long-term outdoor weatherability on the basis of laboratory studies. The features of the weather that are generally responsible for degradation of plastics are heat, light, moisture and oxygen. It was stated that chain cleavage during the early stages of oxidation of crystalline polymers such as polyethylene permits smaller chains to crystallise. Therefore, oxidative degradation is usually accompanied by an increase in density. It has been shown that there is good correlation between oxygen uptake and the impact index (ultimate strength x ultimate elongation)¹⁴². Generally oxygen diffuses more slowly when the crystallinity of the sample increases. Branching and crosslinking, both of which tend to retard or inhibit crystallisation, lead to higher rates of oxygen uptake and embrittlement. Hydrolytic degradation usually leads to the deterioration of tensile properties by chain scission.

Kamal has proposed an exposure parameter approach which assumes an exponential relationship between the extent of degradation and exposure time :-

$$y = A \exp B (t - C)$$

y is the property under consideration

t is the time of outdoor exposure

ABC are constant and they may be estimated from laboratory studies or exposure in artificial weathering devices.

In an earlier paper Kamal¹⁴³ examined the effect of variables in artificial weathering on the degradation of selected plastics. The need for obtaining the right exposure conditions was stressed; ambient temperature, wetness fraction and time of water spray per cycle being important.

Dagaev¹⁴⁴ states that in the thermal ageing of polymers the two basic factors are temperature and atmospheric oxygen, and assumes that the values of impact and cross-breaking strength can serve as a criterion of the degree of ageing of plastics, the implication being that surface action is most important. Dagaev observed that the mechanical indices of polyamide 68 fall sharply at 100°C and 135°C after the first 30 days of ageing, quoted impact strengths being approximately 30% of the original after ageing at 100°C and approximately 20% of the original after ageing at 135°C.

The thermal degradation of some polyamides has been studied by Kamerbeck and co-workers¹⁴⁵. These workers examined the degradation products formed on heating nylon 66 and nylon 6 and a reaction scheme was drawn up. However this degradation was carried out at 305°C and relates to actual processing degradation rather than degradation in service. The reactions proposed are a primary reaction according to which an $\text{-NH-CH}_2\text{-}$ bond is subject to scission, the main products being a polyamide chain with a nitrile end-group, a polyamide chain stabilised by hexanoic acid, and a molecule of water. The latter may hydrolyse an amide linkage, and amine end-groups thus formed may react with formation of a secondary amine-group; carboxylic end groups will give a keto-group.

Hardy and MacNulty¹⁴⁶ have shown that the embrittlement of polyamide mouldings in air and in water includes a major surface effect due to rapid degradation. Removal of the surface essentially restored the original properties of the material. The change in elongation at break was used

as the criterion for brittleness. The deterioration of nylon 66 mouldings in dry air and air saturated with water vapour at elevated temperatures was analysed. The experiments were carried out as far as possible in the dark to avoid photochemical effects. Various test temperatures were used. Dry nylon became embrittled after 2 years at 70°C. When nylon was aged wet (7-8% water), embrittlement was rapid taking about 8 weeks at 70°C. The molecular weight of the wet nylon decreased both on the surface and in the interior of the mouldings after ageing at 70°C.

Zhurkov and Tomashevskii¹⁴⁷ have shown that a correlation exists between the rate of radical formation in uniaxially stressed nylon fibres and the lifetime of the material (i.e. the time between the application of stress and rupture). Campbell and Peterlin¹⁴⁸ studied commercial fibres and compression moulded rods. With the rods necking occurred. In spite of large deformations no radicals were detected, from which one may conclude that during the necking process when spherulites are destroyed and the crystal lamellae break into small blocks, the chains do not fracture or if they do the number is so small that the few free radicals formed cannot be detected. It was suggested that it is the tie molecules between lamellae which break and not the chains in the crystal lattice.

Electron spin resonance (E.S.R.) has also been used to study the initial reaction of the photo-degradation of nylon 6¹⁴⁹. The spectrum obtained indicated the formation of $-\text{CH}_2-\dot{\text{C}}\text{H}-\text{CH}_2-$ and $-\text{CH}_2-\dot{\text{C}}=\text{O}$ radicals. This supports the idea that the first step in photodegradation is the breaking of the amide bond. Evidence strongly suggests that low - energy radiation is capable of breaking bonds only in the unoriented amorphous regions. It was found that the energy of radiation from 2,500 to 3,500 Å was high enough to break bonds and form radicals but no radicals were produced by radiation with wavelengths above 3,500 Å. Taylor, Tincher and Hammer¹⁵⁰ investigated the photodegradation of nylon 66 containing titanium dioxide and showed

that titanium dioxide makes nylon 66 more susceptible to photodegradation due to absorption of light by the titanium dioxide and subsequent degradation of nylon.

Achhammer, Reinhart and Kline²⁰⁰ carried out a general investigation on the degradation of polyamides. Films of polyamides were exposed to heat, ultra-violet radiant energy, and different atmospheric conditions. The degradation products were collected in some cases and analysed by mass spectrometric techniques. The unexposed and exposed specimens were examined by the following techniques to obtain information concerning the changes in chemical and physical structure of the polymer: infra-red absorption, ultra-violet absorption, solution viscosity, measurement of dielectric constant and dissipation factor, photomicrography, X-ray diffraction, electron microscopy and effect of organic liquids. In addition pyrolysis studies were made and some physical properties were determined. The results of the investigation showed clearly that no single method gives a complete picture but that the results from several of the methods give an insight into the degradation mechanism. The general course of degradation of polyamides was described as follows :-

- (i) Splitting of the polymer chain at the C-N linkages.
- (ii) Changes in degree of crystallinity or local order.
- (iii) Loss of dipole - associated plasticisers.

The polyamides used in this investigation were copolymers of nylon salts with E-caprolactam in the form of thin films (0.002 to 0.004 in. thickness).

Summarising it appears that upon exposure to U.V. light, heat and water nylons degrade due to the cleavage of the polymer chain at the amide linkages. In certain instances gel formation can occur giving an increase in inherent viscosity figures but chain scission is common-place when oxygen is present. Reduction in certain mechanical properties such as

cross breaking strength occurs due to degradation, presumably taking place especially on outer surfaces.

2.5 WEAR

Several workers have investigated the wear of polymers notably the Russian workers Ratner and Lure. These workers¹⁵¹ demonstrated that main chain scission does in fact occur during abrasion. Abrasion in polymers usually occurs through repeated deformation of the surface by asperities of abradent (fatigue wear). When the number of such acts is very small the wear process is called abrasive. Intrinsic viscosity determinations showed a reduction in molecular weight of the surface, after abrasion for polyamide 68.

The abrasion resistance of nylon 6 has been shown to increase with increasing molecular weight¹⁶². Ratner and Lure stated that mechanochemical degradation always takes place during the abrasion of polymers. The analysis of abrasion as a fatigue process indicates the possibility of simultaneously improving fatigue and abrasion resistance of polymers by increasing their chemical stability.

Giltrow¹⁵² related the wear properties of several thermoplastics to their chemical constitution. The cohesion between portions of polymers chains is greater in crystalline regions than in amorphous regions. Failure during abrasion may involve not only overcoming dispersion forces, but also scission of inter-chain crosslinking hydrogen bonds such as occur in nylons. The wear rates of metals are usually inversely proportional to hardness, but for polymers the concept of indentation hardness is ill-defined and the controlling material parameters become more complex. Giltrow used a 5 mm diameter cylindrical pin of the thermoplastic bearing the plane end against a rotating disc of abrasive paper. Of the twelve polymers studied nylon 66 and nylon 6 had the lowest rate of wear, (measured by loss in weight).

These polymers have the highest cohesive energy of the polymers tested. Cohesive energy is the energy required to overcome all intermolecular contacts within one mole of material, it thus refers to dispersion, ionic forces and hydrogen bonding between polymer chains and may be equated to the latent heat of vapourisation less the mechanical work necessary to expand the chains beyond their spheres of influence. Although cohesive energies of polymers are not directly measurable, they may be estimated in several ways including calculations from sets of additive constants, derived from solubility and latent heat data, for each constituent atom or group of atoms within the molecule¹⁵³. The specific wear rates were the mean of between two and five determinations. Errors in repeatabilities of wear rates did not exceed 7%. Changing the abrasive paper from a surface roughness of $37\text{ }\mu\text{m}$ to one of $6\text{ }\mu\text{m}$ does not give the correlation between rate of wear and cohesive energy. (Lancaster¹⁵⁴ has shown that plastic deformation only becomes predominant during wear processes when the surface roughness of the counterface is of the order of $25\text{ }\mu\text{m}$). Giltrow concluded that the rate of abrasive wear of thermoplastics is inversely proportional to the square root of the cohesive energies.

Lancaster¹⁶⁹ determined the influence of some mechanical properties of a number of polymers on the wear rates against a rotating metal counterface at various temperatures. Many polymers exhibited a minimum wear rate at a particular temperature. The product of the breaking strength and the elongation to break is a very significant factor in changes in wear rate. Summarising Lancaster found that during sliding against steel, a number of polymers exhibit minimum wear rates at characteristic temperatures. The dependence of wear rate on temperature for any one polymer cannot be explained in terms of temperature variations of the relative proportion of plastic to elastic deformation, the ratio hardness/modulus remains almost independent of temperature until near the softening point of the polymer.

The product of the elongation to break and the breaking strength (S_e) is an important parameter in the wear of polymers. The inverse of this product varies with temperature in the same way as the wear rate. In conditions similar to those of abrasive wear (single traversals), the wear rates of a large number of polymers show an approximate linear correlation with the inverse of the ratio. The magnitude of the elongation to break affects the dependence of wear rate on the surface roughness of the counterface. Polymers with low elongation are very sensitive to counterface roughness. In conditions of repetitive sliding, steady-state wear rates do not correlate with $1/S_e$ because of transfer to the counter-face.

Jacobi¹³⁵ examined the friction/wear characteristics of polyamides.

No definite correlation was found between coefficient of friction and molecular weight. Jacobi found that crystallinity improved the wear and abrasion resistance. This part of the work was carried out exclusively on nylon 6 and it was found that the higher the monomer content the lower the friction but the greater the wear. Jacobi also showed the importance of using nucleated nylon 6 for better wear properties.

Watanabe et al¹⁵⁵ have examined the frictional properties of nylon 6.

They found that at a comparatively high speed, the coefficient of friction reaches a maximum of 1.0 to 2.0. The value of the maximum and the load at which it is reached vary with the sliding speed, the roughness of the surfaces, the ambient temperature and the contacting materials. The variation of the coefficient of friction with temperature was examined at low sliding speeds when little frictional heat is generated; and a maximum friction is observed. It is suggested that the dependence of the friction of nylon on the load can be ascribed to temperature effects caused by frictional heating and that the mechanism of this temperature effect of friction about an appropriate transition temperature is similar to that found in respect of the T_g of a rubber. Since in nylons the amorphous

content is $>50\%$ it is suggested that the rubber like behaviour of the amorphous areas may play a more important role on friction above the glass transition temperature of nylon. (45°C according to Stuart¹⁷¹).

If the load is at a higher sliding speed, it is well known that the surfaces of polymers like nylon melt at a certain load because of frictional heating^{170,172,173}. It is very likely therefore that the sliding surfaces of polymers melt locally before complete melting and the friction decreases (NB the rubber like behaviour of the amorphous areas may override other factors). As the roughness of the surface of nylon 6 increases the peak of maximum coefficient of friction goes to higher load. If the steel roughness is increased then the coefficient of friction decreases.

Lewis¹⁵⁶ states that sliding elements such as bearings, piston rings and seals can be designed with accurate prediction of the wear rate if certain factors are known. The wear rate of a plastic surface sliding without lubrication against another surface is predicable if :-

- (i) The temperature rise due to frictional heating added to the ambient temperature results in a surface temperature below the critical value associated with the plastics PV (pressure x velocity) limit.
- (ii) The mating surface is defined in terms of material hardness and roughness.
- (iii) The environment is defined and free of contaminants

Since temperature affects compressive strain and extrusion under load the maximum surface temperature at which a plastic will operate satisfactorily at high pressure and low velocity is not necessarily the same for low pressure and high velocity. For wear Lewis gives the equation :-

$$v = KFVt$$

v = volume of wear particles removed (cu ins)

F = load supported (lb)

V = sliding velocity (fpm)

t = time (hours)

K = wear factor (cu in min/ft lb hr).

Volume wear is rarely of specific interest to the designer so the given equation can be rewritten in terms of thickness terms for any specific geometry.

$$d = KPVt$$

d = wear (in)

P = pressure (psi)

The typical wear versus time curve for any unlubricated sliding application comprises of (a) break in wear and (b) steady state wear.

The wear factor K provides a direct comparison of the wear resistance of plastics at any PV value acceptable to the materials in question. It also can be used to predict wear rates of a plastic in applications such as bearings, seals, piston rings, and other components. (It is stated that wear can be measured with an accuracy of better than $\pm 10\%$).

Benedyk¹⁵⁷ has given a survey of plastic bearings and states that the performance of plastics in composites at high PV values is ultimately a function of thermal stability.

The wear testing of plastics has been the subject of a paper by Ratner and Farberova¹⁵⁸. They stated that wear of polymeric materials proceeds in two ways :- through cutting by the asperities of an abrasive surface (abrasive wear), and through elastic deformation and subsequent tearing by frictional force (frictional wear). Abrasive wear produces lengthwise lines, and frictional wear transverse lines or ridges. Both abrasive and frictional

components are present in the wear of polymeric materials their ratio being determined by the elasticity of the material; the blunter ~~the~~ asperities of the abrasive the greater is the frictional component. Mitrovich¹⁵⁹ investigated the friction and wear of certain polymers. The capacity of certain polymers for operating against steel lubricated with mineral oil was investigated under conditions approximating to those of bearings where heating of the friction part is possible.

With the polyamides tested the rate of wear did not increase as the temperature of the immersion oil was increased to 80°C. However above this temperature the wear rate increased sharply. It was found that the coefficient of friction increased with temperature at low loads (5 kgf/cm²) but did not at medium loads (38 kgf/cm²).

Ratner and Lure¹⁶⁰ studied the abrasion of flexible polymers as a kinetic thermo-activation process. According to the molecular-kinetic theory of failure proposed, abrasion is the failure of the chemical bonds as a result of certain fluctuations in the thermal movements of molecules.

Farberova et al¹⁶¹ investigated the effect of composition and processing methods on the abrasion of plastics. The following conclusions were stated :- The abrasion -resistance of a material can be determined on abrasive paper or metal mesh, the latter being the more sensitive method.

There is a correlation between abrasion on paper and on a free abrasive, and on mesh and a smooth metal surface. Determinations on paper and mesh gives a comparative assessment of abrasion-resistance in the two extremes of use, showing the two tendencies: (a) abrasive and (b) frictional wear. The abrasion resistance of plastics is correlated with the product of the work of failure and hardness. When fillers are added to thermoplastics, wear first decreases and then increases, this being connected with the compatibility of the filler and polymer.

Abrasion-resistance in plastics is connected not only with the resistance of the material to the penetration of abrasive particles but also with the work of failure of the material, which may be characterised by impact strength. A linear graph is obtained for the product of notched impact strength and hardness against abrasion resistance (on paper). A similar picture is observed in abrasion on mesh, although the work of failure is here the product of strength and elongation at break.

A study has been made of the friction between various types of polymers at bulk temperatures ranging from below 0°C to 150°C and at speeds up to several hundred cm/sec. In general the friction increases with speed, reaches a maximum and then falls. At higher bulk temperatures the behaviour is similar but the rise in friction is shifted to a higher speed range. The results suggest that the shearing of interfacial adhesions involves time and temperature dependent properties which are closely connected with the viscoelastic properties of the polymer. With some polymers friction in moist air is greater than in a moderate vacuum. With other polymers the friction is reduced, suggesting that in some cases adsorbed films can act as partial lubricants¹⁶³. It is stated that the friction becomes less dependent on velocity and temperature as the polymer structure becomes more rigid. The wear resistance of plastic has been related to other mechanical properties¹⁶⁴. For nylon 6 heat treatment in oil shows little effect on the breaking strength and hardness, but gives maximum wear corresponding to a minimum breaking elongation.

It has been shown¹⁶⁴ that wear is connected with the simple mechanical properties of plastics in the following qualitative relationship :-

$$V \propto \frac{\mu}{H \sigma \epsilon}$$

V = wear = decrease in volume of the body per unit of the path of friction

μ = coefficient of friction, H = Hardness,

σ = breaking strength, ϵ = elongation at break.

Tests have shown that an increase in ϵ plays a fundamental part in increasing wear resistance. Analysis of the basic formula shows that an increase in temperature may lead not only to decrease in wear resistance due to a reduction in σ and H , but also to an increase as a result of a sharp increase in ϵ , these effects overall being greater than any increase or decrease in μ . The temperature at which changes in friction occur can serve as a method of determining the heat resistance of materials in conditions of wear.

A review of the chemical aspects of wear processes in polymers has been given by Richardson¹⁷⁵. It was concluded that the chemical processes and phenomena associated with plastics in "wearing" applications are important technologically although as yet they are little understood.

The effect of structure on polymer friction has been studied by Bely and co-workers¹⁶⁵. The mean friction characteristics were shown to be influenced by the type and size of supermolecular structures and by thin structures of spherulite formation.

Usually the larger the size and the less homogeneous the supermolecular structure in the cross section of the sample, the poorer are the mechanical properties¹⁶⁶. As the spherulite size increased the coefficient of friction increased. Minimum friction was obtained at the spherulite boundary while the maximum coefficient of friction was near the centre of the spherulite. Preorientation in polymers leads to a lower coefficient of friction.

A study of heavily loaded polymer to metal friction duties and of the wear of hardened steel in the presence of polymers has been made by Vinogradov, Mustafaev and Podolsky¹⁶⁷. Under heavy polymer-to metal friction duties, modification of the contacting surfaces is of great importance.

The first reason for this modification is transfer of the metal to the polymer surface and of the polymer onto the metal surface. The intensity of this process depends mainly on the relative hardness of the contacting materials. The second cause of modification of the metal and polymer surfaces are the thermal processes which in the case of thermosetting resins and high melting polymers, may be accompanied by thermal or thermo-oxidative degradation of the polymers with the formation of highly reactive low-molecular compounds. In the case of thermoplastics a surface film of the melt may form. This sets up conditions for fluid instead of dry friction and renders the friction force independent of the load at high values of the latter. Ratner¹⁶⁸ has compared the abrasion of rubbers and plastics. Ratner states that it is reasonable to assume that "high impact" plastics have the greatest resistance to abrasive wear.

In a paper on the abrasive wear of polymers, Lancaster¹⁵⁴ states that as the counterface topography becomes smoother and/or the surface asperities become less sharp, the wear process for any one polymer changes from cutting on an asperity scale to surface fatigue. Variations in the mechanical properties of polymers also affect the wear process for a given counterface topography, cutting being most important for the rigid polymers and fatigue (or sometimes tensile tearing) for the more elastic polymers. Modifications to a counterface surface during repeated sliding, either by transfer or wear, further influence the wear process.

CHAPTER 3. EXPERIMENTAL TECHNIQUES

3.1 PLAN OF PROCEDURE

Initially it was decided to injection mould several nylon 66 insulators using different mould temperatures. These would be examined by optical microscopy and then placed in service in the track with a view to subsequent removal, checking and physical examination.

Two test piece moulds would be made, one containing tensile and flexural test bars the other containing falling weight impact and water absorption discs. Test samples made under different mould temperatures would be tested "as moulded" and after water conditioning at 95°C.

Moulded test samples would also be subjected to accelerated weathering conditions in a Climatest weatherometer, after which the samples would be tested. Examination by optical microscopy would be undertaken on the test samples before and after their various treatments. The possibility of using electron microscopy techniques for more detailed structural examination was considered.

Analytical techniques such as A.T.R. spectroscopy, D.S.C. and possibly wide angle X-ray diffraction would be used to look for differences in the moulded items.

The mechanical tests for tensile and flexural modulus would be carried out using an Instron testing machine while a Davenport impact tester would be used for falling weight impact tests.

Solution viscosity and density measurements would further characterise the mouldings. Wear tests would be undertaken on specimens cut from the test samples in an attempt to determine if the results of this work could be related to other practical data being obtained in the B.R. Plastics

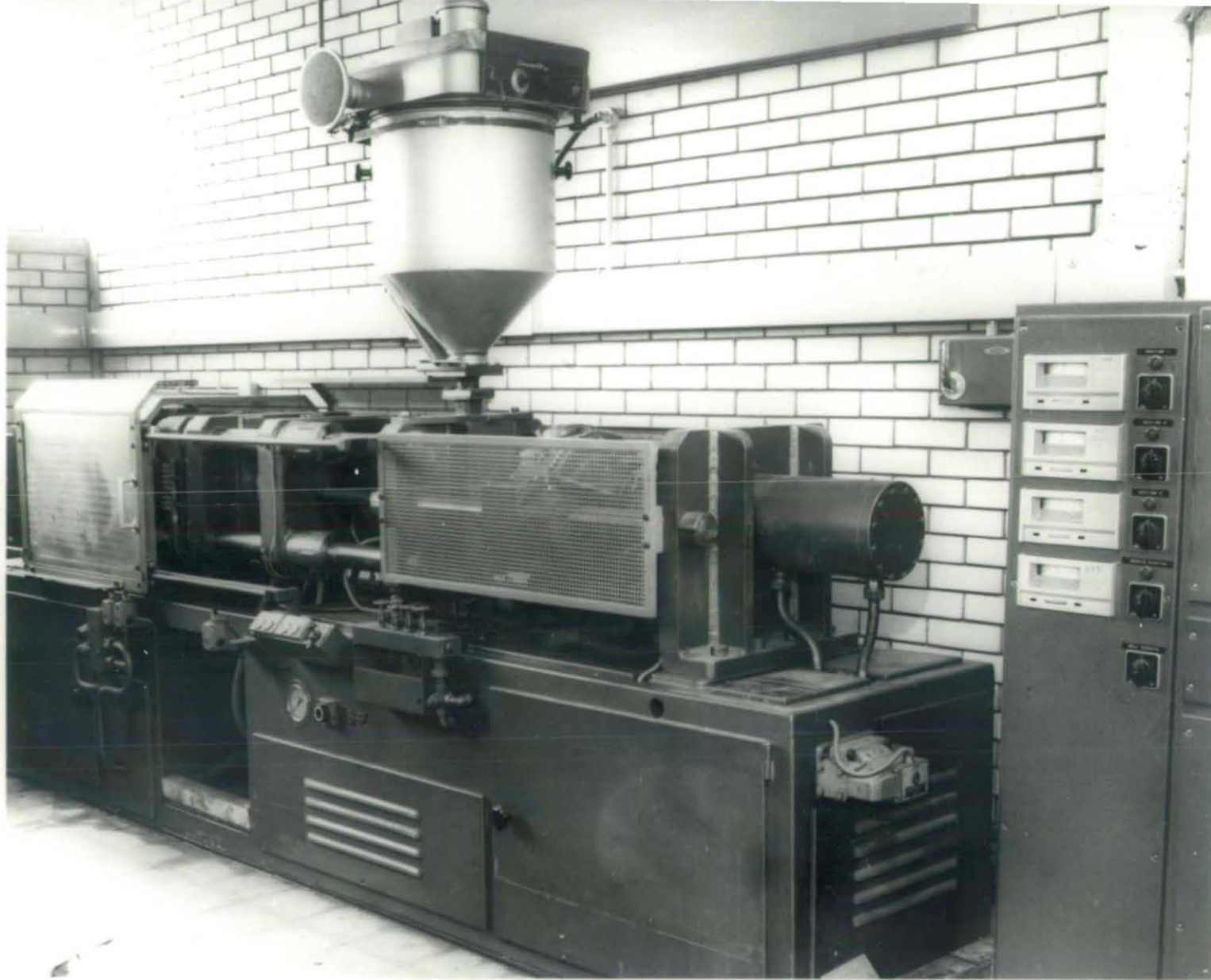


FIG. 1.

FIG. 1. ENGEL ES 100/200 SCREW INJECTION MOULDING MACHINE.

CENTRAL PHOTOGRAPHY UNIT
BRITISH RAILWAYS BOARD

NEG. No. D

7311/371 1

85 TRENT HOUSE
RAILWAY TECHNICAL CENTRE, DERBY
TEL. NO. 41442 EX. 3107

Development Unit where thermoplastic gears were being studied. It should be emphasised that the above plan was worked out to enable a comprehensive study to be made, but without foreknowledge of the relative importance attached to each particular technique of the investigation, in practice.

One of the aims of the study was to expose essentially important techniques.

3.2 INJECTION MOULDING

The polyhexamethylene adipamide (nylon 66) used in this work was "Maranyl" A100 a general purpose injection moulding grade supplied by I.C.I. Plastics Division. The injection moulding was undertaken using an Engel E S 100/200 screw injection moulding machine (Fig. 1). This machine consists of one locking and one injection unit and is driven hydraulically. The machine is controlled by electro-magnetically operated hydraulic solenoids. The electrical control impulses are given by contactors which are compiled in an automatic case together with other instruments (timers, relays, programme, switches etc). The sequence of programme is controlled either depending on stroke (by means of limit switches) or on time (by timers).

The locking unit is effected by means of a hydraulic cylinder over a strong toggle lever system. Closing and opening speeds are variable and independent of each other. The mould opening stroke can be adjusted and the mould height can be altered by means of an adjustment nut. The injection unit consists of a liquifying cylinder, injection cylinder, gear, hydraulic motor and limit switches for dosing. The liquifying cylinder is available in 3 different diameters, thus giving different injection volumes and maximum injection pressures. The maximum shot weight is $7\frac{3}{4}$ oz of polystyrene.

After injection is effected the screw starts to rotate and transports the raw materials through the cylinder to the end of the nozzle. During this movement the raw material is plasticised. The screw is backed to its initial position by the pressure of the raw material. Filling takes place at the same time, this process being called "dosing". A back pressure in the injection cylinder can be produced by means of a throttle valve. By this pressure a backward movement of the screw is made more difficult. The screw is made to move more slowly and the raw material is therefore better sheared.

The screw is driven by a hydraulic motor over a reducing gear. This motor is connected with the central hydraulic plant of the machine.

The screw rotation speed can be varied and during injection the screw acts as a plunger.

Irregularities of material feeding into the screw cylinder have no influence on the dosing volume as dosing is only finished when the required material volume is in the cylinder. The material cylinder and nozzle are heated by four resistance type bands which are individually controlled by thermostats.

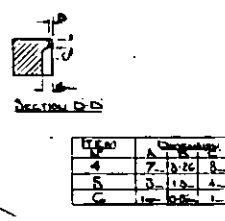
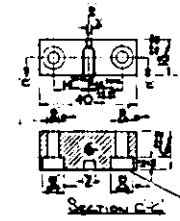
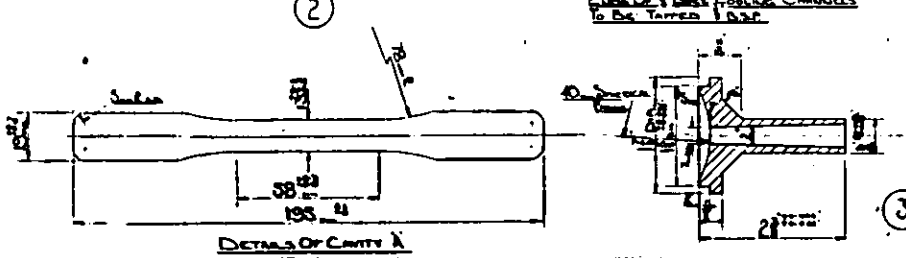
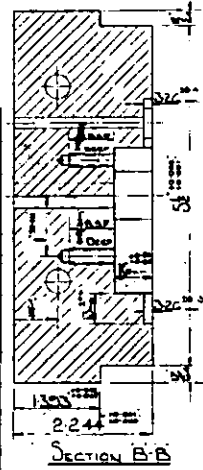
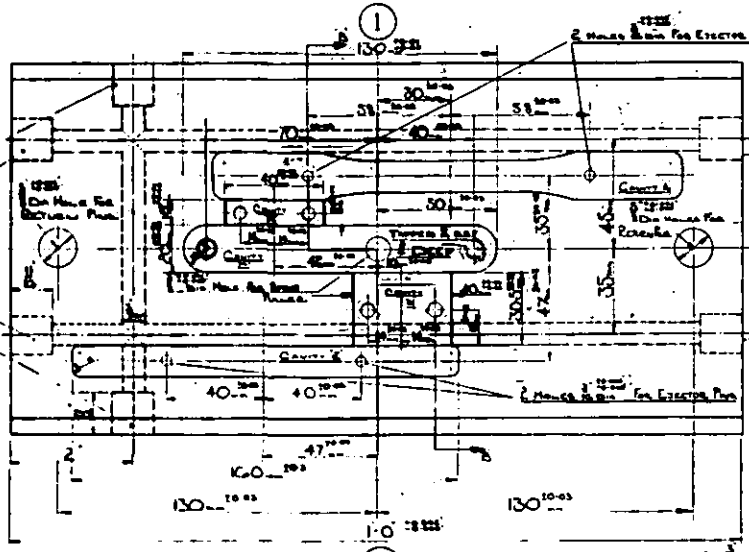
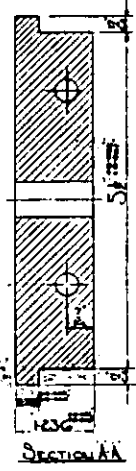
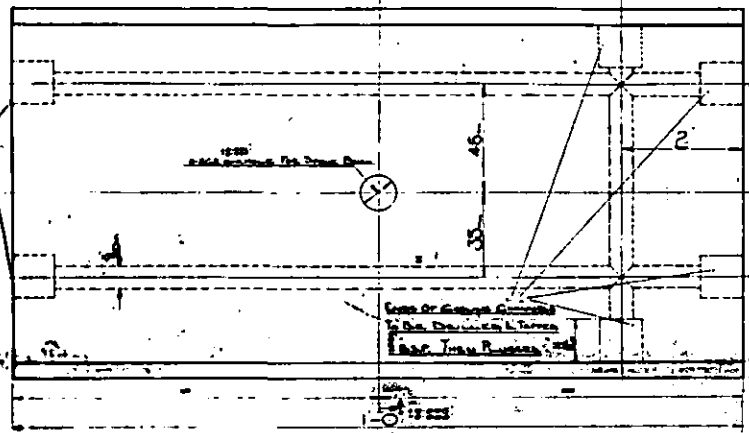
In this work a type C cylinder was used along with an open nozzle.

Control of the mould temperature was achieved using a Churchill oil heater for the three higher temperatures used, while the lowest mould temperature was obtained with a Churchill water circulating chiller unit using a water/glycol mixture. The machine was set up on "hand conditions" and then run under semi-automatic conditions. This involved starting the machine cycle each time after a moulding had been ejected by closing the mould safety screen. The machine was run for one hour to stabilise the conditions before any "lifts" were taken for examination. The moulding conditions used are given overleaf.

Fig. 2 Test piece tool drawing showing tensile and flexural bar
cavities.

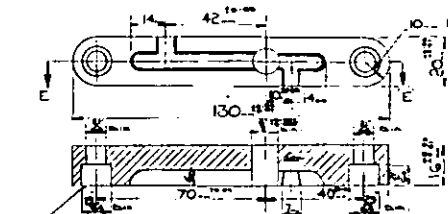
Line Of Contact Channel
To Be Drawn At 1/2" Scale

Line Of Contact Channel
To Be Drawn At 1/2" Scale



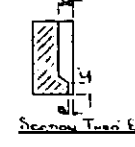
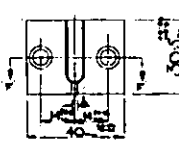
ITEM	DESCRIPTION
4	7-1/2" x 1/2"
5	3-1/2" x 1/2"
6	1-1/2" x 1/2"

DRILLED & COUNTERBORED FOR ITEM 5
TO FIT IN CAVITY D



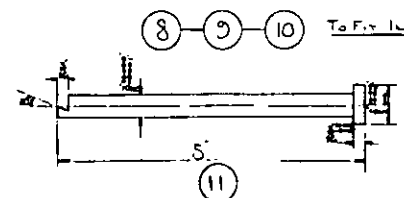
TO FIT IN CAVITY C

DRILLED & COUNTERBORED FOR ITEM 16



ITEM	DESCRIPTION
7	3-1/2" x 1/2"
8	3-1/2" x 1/2"
9	1-1/2" x 1/2"

DRILLED & COUNTERBORED FOR ITEM 14



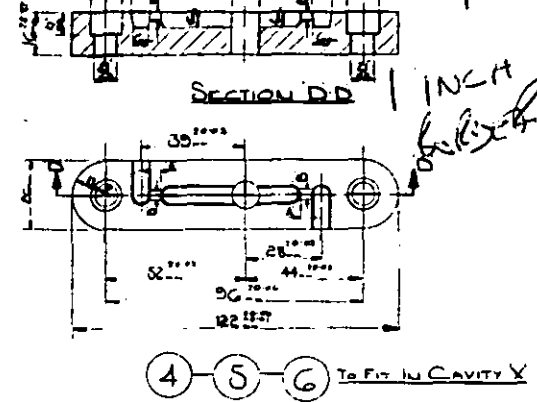
TO FIT IN CAVITY B

ITEM	DESCRIPTION	QTY	UNIT	REMARKS	ITEM	DESCRIPTION	QTY	UNIT	REMARKS
1	11
2	12
3	13
4	14
5	15
6	16
7	17
8	18
9	19
10	20

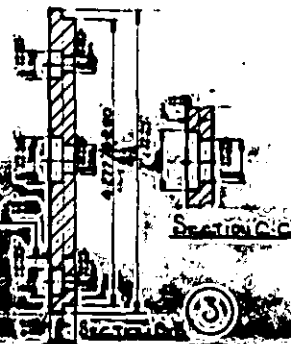
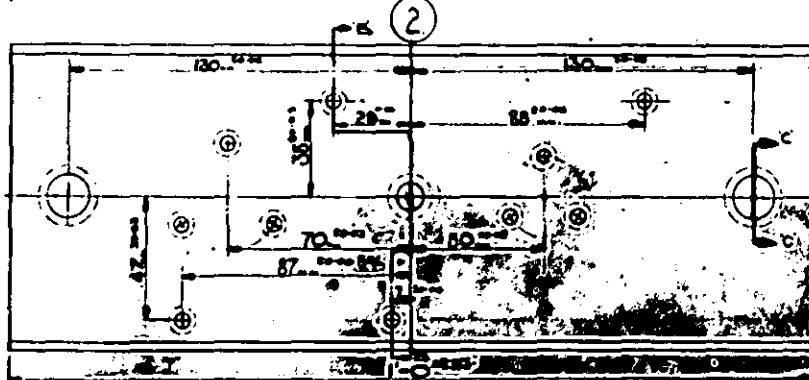
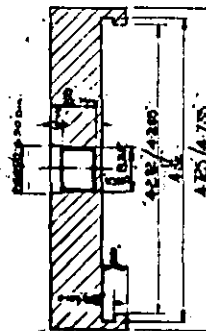
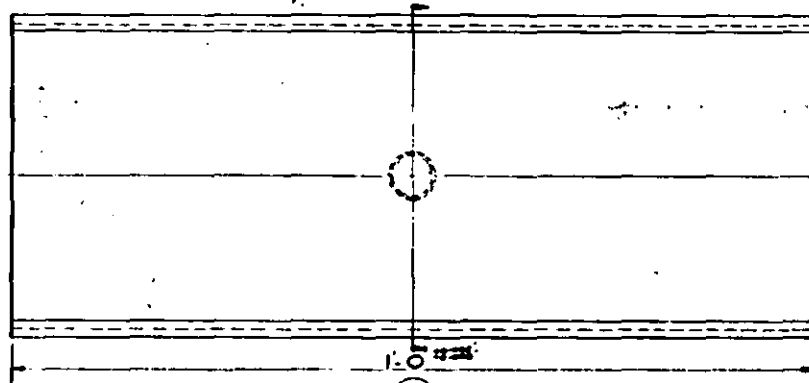
NOTES:
ITEMS 12-16 ARE NOT
DETAILED ON D.D.
SEE D.D. N° DD-PN-07
SHEET N° 3 FOR FURTHER
DETAILS.

PROJECT N° 4086	PROJECT TITLE Syst. Test Peas. Test
DRAWING TITLE DETAILS OF INTERCHANGEABLE CAVITIES.	
SHEET N° 2	N° OF SHEETS
BRITISH RAILWAYS BOARD CHIEF ENGINEER (T & RS) DIRECTOR OF DESIGN	
Scale Full Size	Drawn by DD-PN-07
Checked by L.M.	Checked by 12-1-00

Fig. 3. Test piece tool drawing showing impact and water absorption disc cavities.



ITEM N°	DIMENSION			
	A	B	C	D
4	2	2	1.54	2
5	4	3	1.0	1.3
6	1	1	0.5	0.5



NOTES. ITEMS 748 ARE NOT
DETAILED ON DEC.
SEE ALSO DEC
N° DD-P-N-97
SHEET N°2 FOR
FURTHER DETAILS

PROJECT N°	PROJECT TITLE:
4095	STD TEST PIECE Tm

DETAILS OF
INTERCHANGEABLE CAVITIES
SHEET N°: 3 OF SHEETS: 3

**UNITED STATES GOVERNMENT
COMP. NUMBER (7-2)
DIRECTOR OF BUREAU**

8	EXECUTE PAIR	6	STEEL	DMS. ENH TO 7" LONG CUT TO LENGTH
7	SOCKET HEAD CAP SCREWS	2		1 EAST FLOOR
6	RUNNER BR	1	PAINT	THAT REMAINS
5	RUNNER BR	1		
4	RUNNER BR	1		
3	RUNNER BR	1		
2	DECORATIVE	1		
1	CAVITY BR	1		THAT REMAINS
100	DECEPT	4	100	1 RUNNER

FULL SIZE.	
DD-P-AI-B7	
T.M.	1-1-60

Barrel temperatures	Zone 1	265°C	
	Zone 2	265°C	
	Zone 3	245°C	(Hopper end)
	Nozzle	270°C	
Injection Pressure	12,000 psi	(= 828	MN/m ²)
Hold-on pressure	7,000 psi	(= 483	MN/m ²)
Injection speed (time)	6 seconds		
Pre-injection time	7 seconds		
Post-injection time	6 seconds		
Screw-back time	.5 seconds		
Cooling time	10 seconds		
Total cycle time	33 seconds		
Mould temperatures	95, 75, 55 and 15°C		

The designed test piece tools consisted of one containing tensile and flexural bars while the other contained falling weight impact and water absorption discs. Details are shown in Fig. 2 and Fig. 3.

These moulds were made as interchangeable cavities for fitting into a Universal Bolster. The gating system was such as to reduce orientation in the cavities for the flexural and tensile test bars.

3.2.1 After-treatment of mouldings

After moulding, 50% of the samples were conditioned for 3 hours in water at 95°C. This is the normal conditioning treatment given to nylon 66 insulators used by B.R. It is used to decrease the time required for the nylon 66 to attain its equilibrium moisture content and to relieve moulded-in stresses.

Fifty per cent of the "as moulded" and 50% of the conditioned samples were submitted to accelerated weathering tests in a "Climatest" accelerated weathering machine. This is an environmental test cabinet designed specifically for the accelerated weathering of materials such as plastics. The conditions controlled within the main cabinet are air temperature, humidity and U.V. radiation.

The air temperature is controlled by various sets of air heaters. The humidity is controlled by using a spinning disc humidifier. The U.V. radiation is supplied by 32 fluorescent lamps arranged on the circumference of the lamp drum as 16 pairs of black and white (sun) lamps.

A water spray is fitted which can be programmed to give the required specimen spraying time. The outer specimen frame revolves around the lamps at 1 revolution per minute.

The samples were treated for 1,000 hours at 50°C and 65% RH using a water spray for 6 minutes in every 2 hours.

3.3 MECHANICAL TESTING

3.3.1 Tensile strength and flexural modulus

Tensile strength and flexural modulus values were determined using an Instron Universal testing machine. The tensile test bars were of the form and dimensions shown in Fig. 301. 11 in B.S. 2782 (1965).

Testing was carried out under constant temperature (20°C), and humidity (65% RH) conditions. The test bars were kept under these conditions for 24 hours before testing. The samples were tested at an elongation rate of 5 mm/min. The tensile strength at yield was determined for the unaged samples but after accelerated weathering most samples failed in a brittle manner and the tensile strength at break was obtained.

Threc-point bending tests were undertaken on specimens 6" (152 mm) long x $\frac{1}{2}$ " (12.7 mm) wide x $\frac{1}{8}$ " (3.2 mm) thick using a testing speed of 50 mm per minute. Tests were carried out at 20°C and 65% RH, samples being kept at these conditions for 24 hours before testing. Only flexural modulus figures were obtained from these tests; cross breaking strength figures were not determined since none of the samples failed during testing.

3.3.2 Impact Strength

Falling-weight impact strengths were obtained using a Davenport machine. This machine has the essential features as described in BS 2782 (1965) p. 154, however since the falling-weight impact strength of nylon 66 is quite high, the machine used has a dropping height of 6 feet (1,829 mm). Additional weights were also made to attach to the striker in order to obtain the impact strengths quoted. Tests were carried out at 20°C and 65% RH the specimens being kept at these conditions for 24 hours before test. The testing procedure used was that described in BS 2782 Method 306 B p.158 the specimens being unclamped during the test.

3.3.3 Wear

Wear measurements were obtained on two different rigs which were available at the Railway Technical Centre, Derby. The antifriction machine operates by a reciprocating motion, employing a specimen of surface dimensions 25.4 mm x 12.7 mm rubbing on a substrate of 300 Brinell hardness EN 44 steel with a .15 μ m CLA surface finish. The machine could be loaded up to 181 kg and operated at an average speed of approximately 10.06 m/min. The sliding block has the facility for water cooling to maintain the temperature at 23°C. The specimen is fitted into the holder which accepts the load plate and transmits the load onto the specimen. The sliding

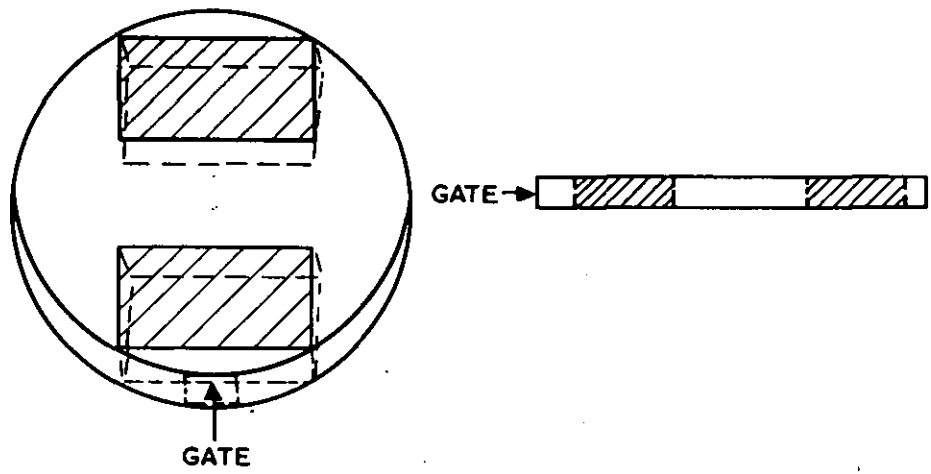


FIG 4 POSITION OF WEAR SAMPLES

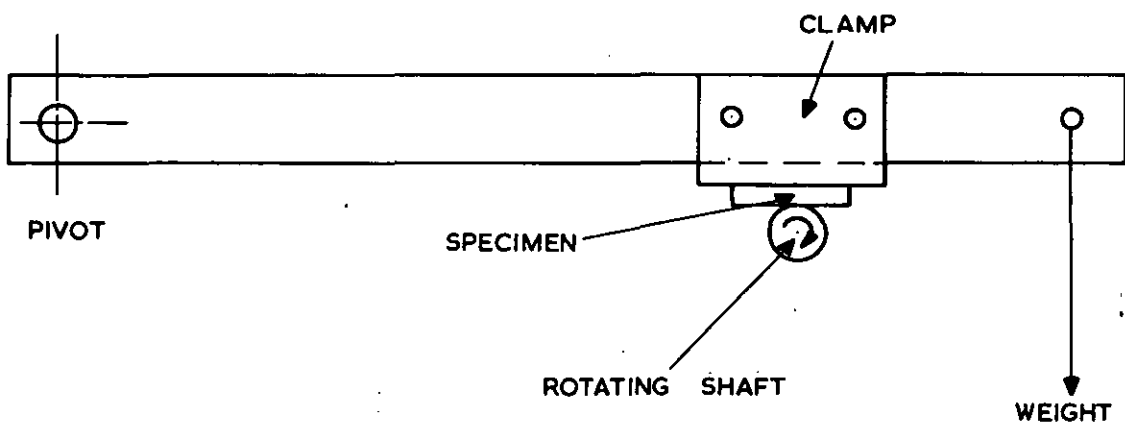


FIG 5 WEAR TEST RIG

action of the block is produced by connecting it with a wheel which is driven by a motor. The apparatus has the facility of measuring dynamic coefficient of friction. The bar preventing the holder to move with the sliding surface is calibrated against the signal it produced on the oscilloscope to read directly the horizontal force exerted on the specimen. The specimens tested were cut from water-absorption discs as shown in Fig. 4.

Wear measurements were also obtained on specimens in contact with a rotating metal bar (shaft). The rig used consists of weighted pivot bars onto which the specimens are clamped. The weights are applied as shown in Fig. 5, and hence the load on the specimen can be varied. The specimen bears on a 1" (25.4 mm) diameter EN 44 steel bar of 16 micro inch finish ($0.4\mu\text{m}$) which was rotated at 26 r.p.m. Wear tests were carried out on the surfaces of mouldings and also through the mouldings. Results were expressed as loss in weight and in some instances as wear scar width.

3.4 PHYSICAL CHARACTERISATION

3.4.1 Water Absorption

The 24 hour water absorption of moulded discs was determined using, basically, Method 502F from BS 2782 (1965). The specimen discs were dried in an oven for 24 hours at 50°C , cooled in a dessicator, and weighed to the nearest milligram (W_1). The specimens were then placed in a container of distilled water maintained at 20°C . Precautions were taken to prevent specimens from making contact with one another or with any substantial area of the container. After 24 hours the specimens were removed from the water dried with filter paper and weighed within 1 minute of removal from the water (W_2). The water absorption was expressed as a percentage

$$\frac{(W_2 - W_1)}{W_1} \times 100.$$

Three specimens were taken for each determination. The water absorption was also determined without the pre-drying treatment.

3.4.2 Inherent Viscosity

Inherent Viscosities were determined using solutions of nylon 66 in 90% formic acid. The nylon 66 was dried in a vacuum oven (29 mm Hg) at 95°C for 3 hours and allowed to cool in a dessicator before weighing out approximately 0.25 g. This was then transferred to a 50 ml volumetric flask after which 40 ml of 90% formic acid were added and the stopper inserted. The flask was shaken until the nylon had dissolved, placed in a water bath at 25°C and made up to the 50 ml mark with 90% formic acid. A U-tube viscometer type BS/U size B was used to determine flow times at 25°C for the solvent and solution. The nylon solution was filtered through a No. 1 sintered glass crucible before use. Two runs on both solvent and solution were made, corresponding flow times agreeing to ± 0.2 seconds.

The inherent viscosity was determined from :-

$$IV = \frac{\log e \ t_1/t_2}{C}$$

where t_1 = flow time in seconds of nylon solution

t_2 = flow time in seconds of 90% formic acid

C = solution concentration in g/100 mls.

Inherent viscosity readings were obtained for the surface and interior of accelerated weathered mouldings. Scrapings were obtained by using a coarse file on the weathered surfaces, a depth of up to 0.005" being removed.

3.4.3 Density

The density of various samples of nylon 66 cut from specimens was determined using a Davenport density gradient column apparatus at 23°C. Essentially two different miscible liquids whose densities are above and below that of the material to be determined are used. Two mixtures of these liquids are made of differing densities (the two extremes of the range required) and placed in separate conical flasks having an inter-connecting joint. To the flask containing the lower density mixture a long capillary tube is connected which extends almost to the bottom of a glass tube in which the density gradient column is prepared. The connecting tube between the two flasks is opened and the contents of the flask nearest the long capillary stirred using a magnetic stirrer. The liquids are allowed to flow down the capillary tube into the glass tube, the rate of flow being such that the column takes approximately two hours to fill. The column obtained is calibrated using glass marker floats of known density at 23°C. A graph of column height against density is plotted for the floats and a graph drawn. A satisfactory column is obtained if the graph is a straight line. For the nylon 66 samples toluene and carbon tetrachloride were the two liquids used to prepare the column, the column range being 1.11 to 1.17 g/cc. Samples for density determination were washed with acetone and then wetted with a toluene/carbon tetrachloride mixture before being lowered into the column. The density was obtained by measuring the height of the sample in the column after 2 hours and measuring the corresponding density of the calibration graph.

+ Crystallinity.

3.4.4 Attenuated total reflection spectroscopy (ATR)

When radiation passing through a medium of high refractive index strikes the interface between that medium and one of lower refractive index, it

is reflected with but little attenuation when the angle of incidence is greater than a certain critical angle. The attenuation is in fact dependent on the refractive index change. By placing a sample in optical contact with a material of high and constant refractive index, any change in its refractive index will give rise to a change in reflection at the interface. Since the refractive index of a material changes rapidly at those wavelengths where it absorbs, the plot of ATR will resemble the absorption spectrum.

To make measurements by ATR, sample materials are placed in contact with the high refractive index material, usually in the form of a prism or hemi-cylinder of silver chloride, KRS-5, or germanium. Successful operation depends to a great extent upon intimate contact between the sample and the crystal, but this was readily achieved in the present work, where direct measurement was made on various samples.

The angle of incidence is important and must be carefully chosen.

This angle determines the apparent depth of beam penetration into the sample, a steep angle (a small angle of incidence) produces a deeper penetration than a shallow angle. Optimum results are generally obtained between two and five degrees above the critical angle. As this angle depends on the relative values of refractive index of sample and crystal, the angle of incidence should be variable. A refractive index ratio of 0.65 is chosen because it is very close to the figure obtained for the interface between most organic materials and a KRS-5 prism (KRS-5 is a mixed crystal of thallium bromide and thallium iodide).

A Grubb Parsons infra-red grating spectrometer Model DB 1/GS 4 with a KRS-5 prism was used to obtain ATR spectra on impact discs before and after accelerated weathering. The samples were arranged so that 9 reflections were obtained, the reflections being at 45° .

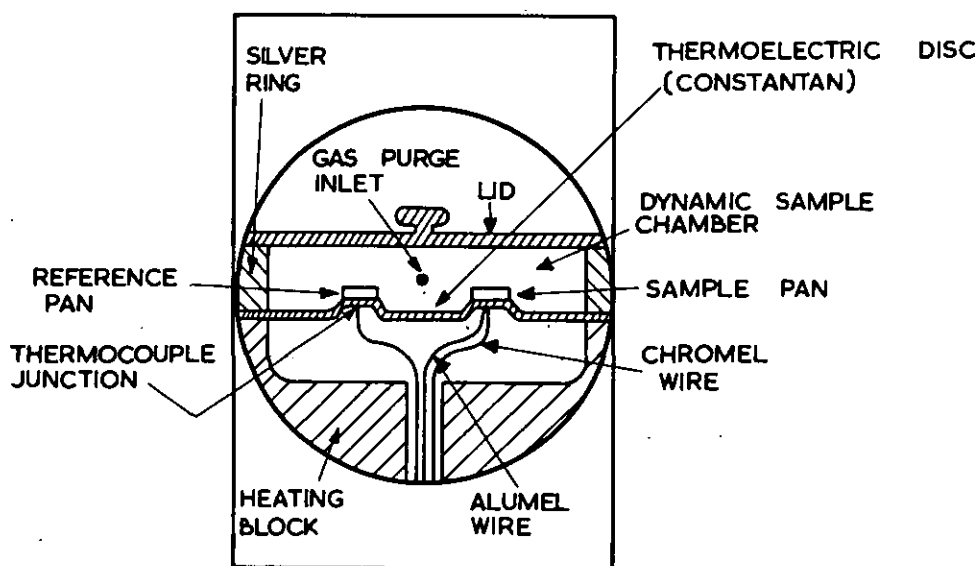
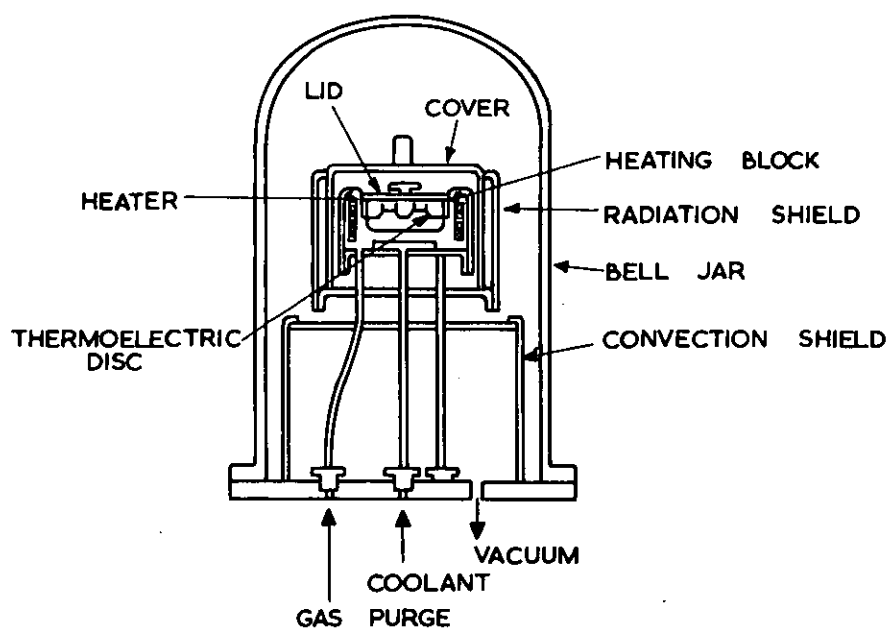


FIG . 6 DSC CELL

3.5 THERMAL TECHNIQUES

In this work the basic unit used was the Du Pont 900 Thermal Analyser. Into this unit are plugged a variety of modules and accessories. These include modules for DTA, DSC, TGA, TMA. The basic unit contains the amplifying, programming and recording capabilities common to the various measurements from a number of transducers. The various modules and transducers are given below :-

MODULE	TRANSDUCER
DTA	Differential Thermocouple
DSC	Thermoelectric disc
TGA	Electronic Balance
TMA	Linear Variable Differential Transformer (LVDT)

The heart of the 900 thermal analyser is the solid state electronic temperature programmer controller, which permits a wide range of temperature scanning conditions from -190°C to 1600°C . Heating, cooling, isothermal, hold and cyclic operations are selected by a "programme mode" switch. The heating or cooling rates and the starting temperature of the programme can be varied to suit individual needs.

The 900 X-Y Recorder plots chemical, physical and mechanical properties on the Y-axis as a function of sample temperature or time on the X-axis. Charts are printed to provide direct reading of sample temperature in degrees centigrade, corrected for inherent thermocouple non-linearity.

3.5.1 Differential Scanning Calorimetry (DSC)

A diagram of the DSC cell is shown in Fig. 6. Sample and reference pans made of aluminium are placed on the raised platforms of a thermoelectric disc, which is made of constantan. Chromel wire is welded at the centre

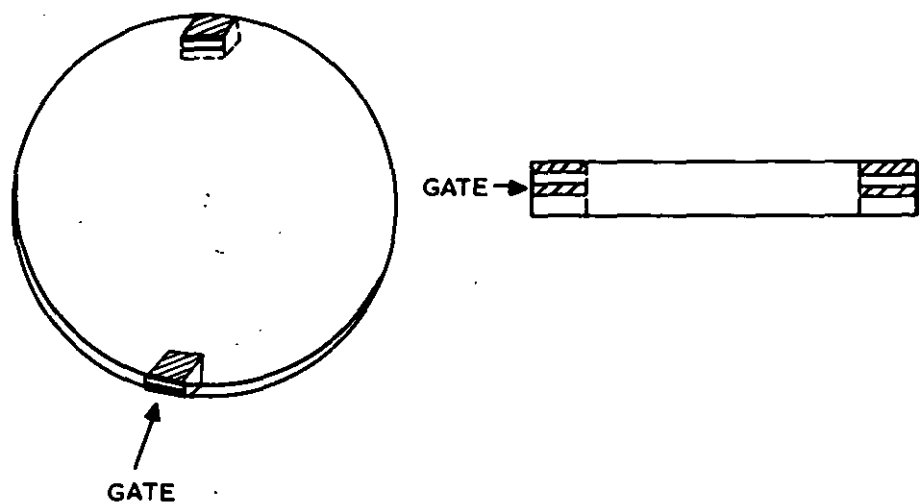


FIG 7. POSITION OF SAMPLES FOR DSC EXPERIMENTS

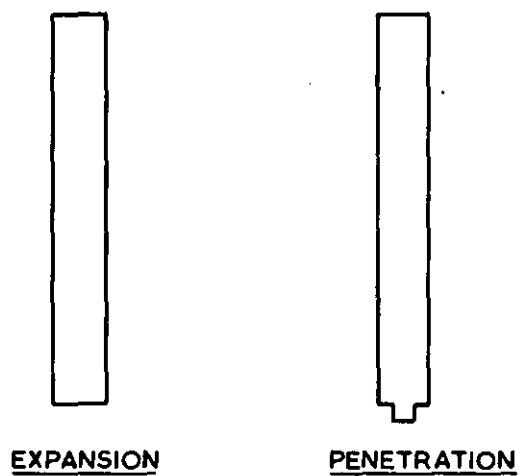


FIG 9. TMA QUARTZ PROBES

of the base of each platform. Thermocouple junctions thus formed are used for measuring the temperature difference between sample and reference. The signal between these two junctions is fed to the 900 amplifier and observed on the Y-axis of the recorder. An alumel wire is also welded to the centre of the front raised platforms, forming a chromel-alumel thermocouple, which is used to measure the temperature of that platform.

The corresponding cold junction of the thermocouple is placed in crushed ice at 0°C and the output observed on the X-axis of the recorder. The constantan disc also serves to transfer heat radially inwards from the heating block to the sample and reference which are otherwise thermally isolated. A chromel-alumel thermocouple situated close to the heater windings is used to operate the temperature programmer-controller via a feed back mechanism. The sample chamber is protected from external temperature changes by a series of shields and lids. The entire cell being covered with a glass bell jar.

y DSC is a technique in which a quantity of heat (calories) or a measurement of heat flow (calories/unit time) is obtained by dynamically heating or cooling a sample and an inert reference. Thermograms were run on samples cut from water absorption discs. Samples were cut from two different positions in the moulding namely, near the gate and extreme from the gate. Samples were taken from the surface as well as the interior of the mouldings as shown in Fig. 7. The heating rate used was $7.5^{\circ}\text{C}/\text{min}$ using a Y-axis scale of $0.1^{\circ}\text{C}/\text{inch}$. Samples were run in air since it had been shown that these thermograms did not differ from those run in nitrogen in the temperature range used.

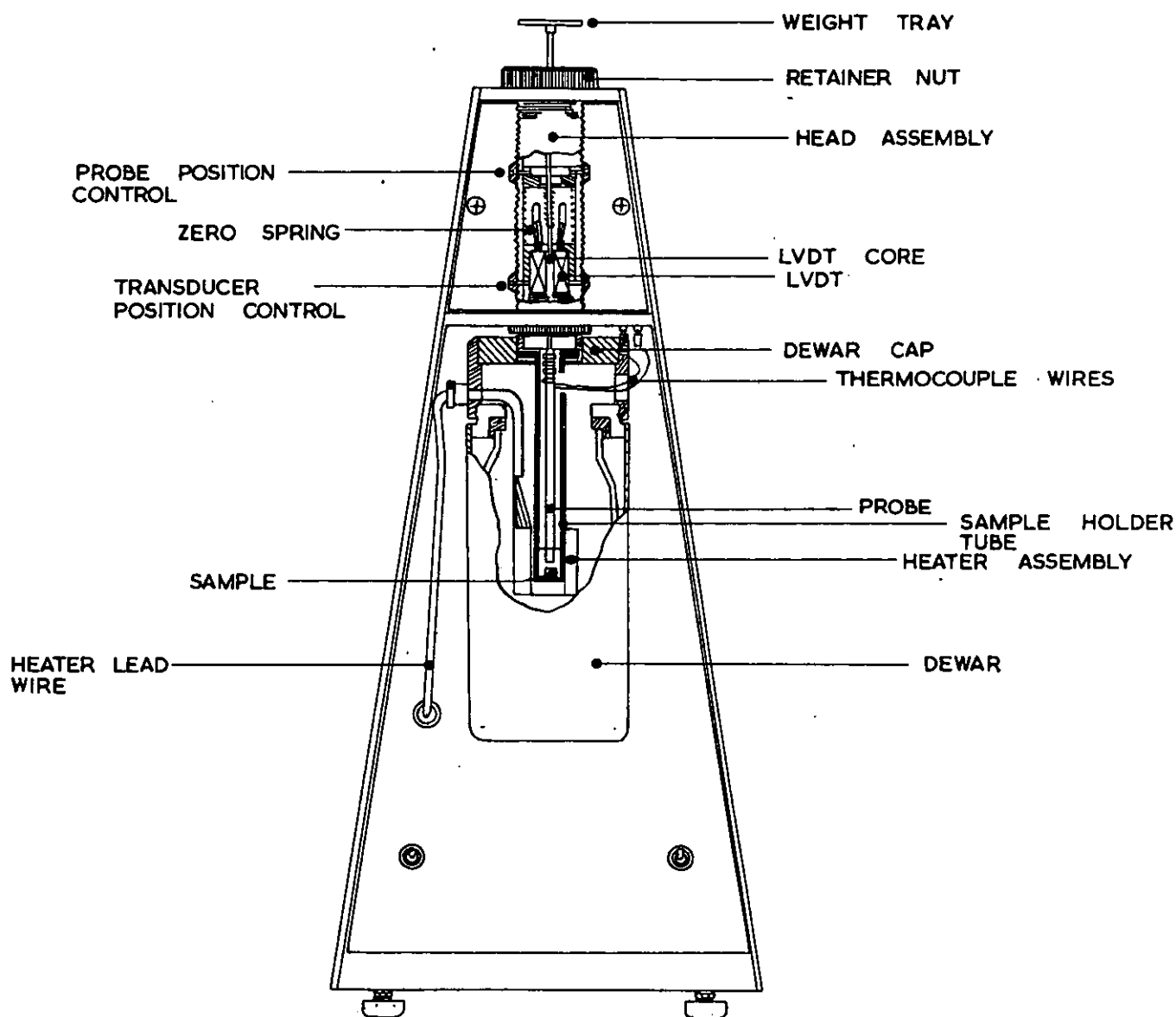


FIG 8 TMA APPARATUS

3.5.2 Thermogravimetric analysis (TGA)

The Du Pont 950 TGA module measures weight loss or gain of materials as a function of temperature or time. The sample weighing about 10 mg is placed in a aluminium or platinum boat suspended from a horizontal balance beam, and a movable sample thermocouple is positioned just above the sample, measuring the temperature directly on the X-axis.

Water content determinations were undertaken by measuring the weight loss at 175°C.^{19.4} These determinations were mainly on wear samples which were cut from water absorption discs as previously indicated (see Fig. 4). A heating rate of 7.5°C/min was used.

3.5.3 Thermal Mechanical Analysis (TMA)

The Du Pont 941 Thermo-mechanical analyser (see Fig. 8) measures vertical displacement as a function of temperature or time. This analyser comprises of a movable core differential transformer to which is coupled a quartz probe to sense displacement changes as small as 10^{-5} inches.

Movement of the core in the transformer results in a change in output of the transformer which is fed to the Y-axis of the recorder. A thermocouple attached to the sample holder tube contacts the sample and provides an output proportional to the sample temperature. The voltage, compensated with a suitable reference junction is applied to the X-axis of the recorder. The sample and probe head are surrounded by a cylindrical heater containing a control thermocouple. In penetration measurements the penetration probe which can be weighted or loaded, sinks into the sample when the sample "viscosity" is no longer capable of supporting the probe. When operated in the expansion mode, the TMA expansion probe rest on top of the sample with a loading sufficient to maintain contact. As the sample expands, the probe is pushed up and sample expansion is recorded.

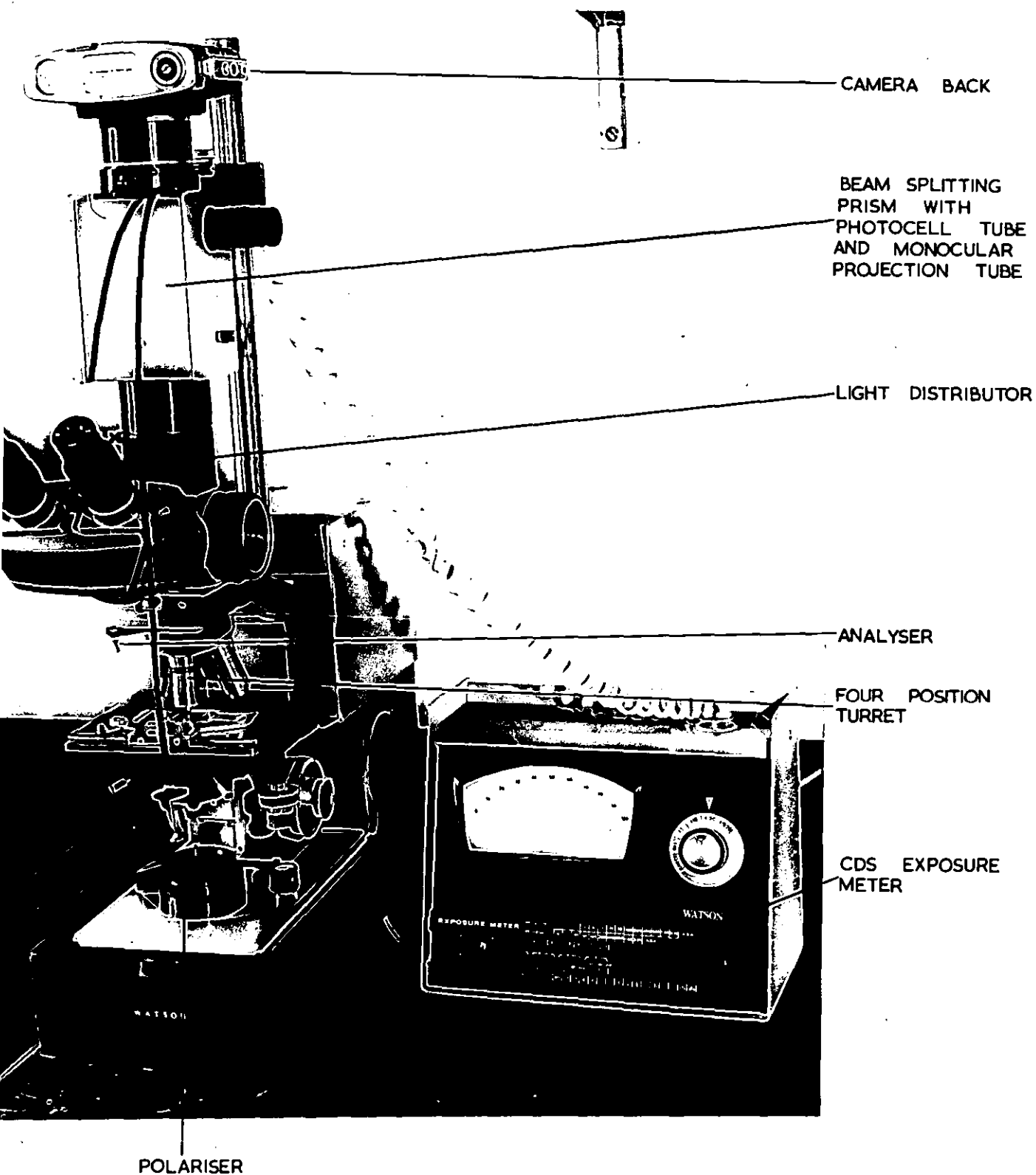


FIG 10 POLARISING MICROSCOPE

Both expansion and penetration thermograms were obtained using the respective quartz probes (see Fig. 9) on samples cut from water absorption discs. Various heating rates, namely 7.5, 10, 20°C/min with a tray load of 50 grams were used with the penetration probe, while with the expansion probe no load was applied, the heating rate being 20°C/min.

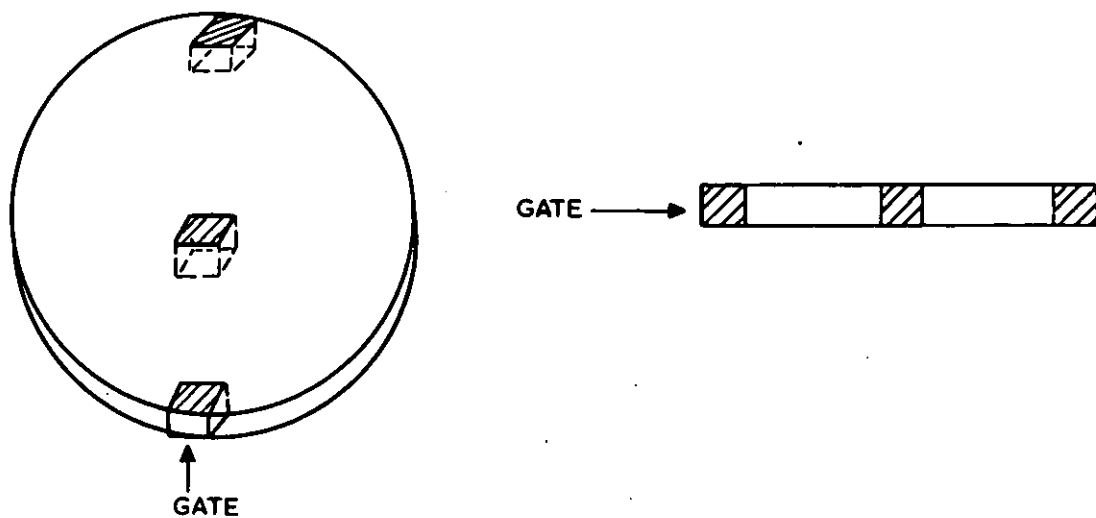
3.6 MICROSCOPY

3.6.1 Optical Microscopy

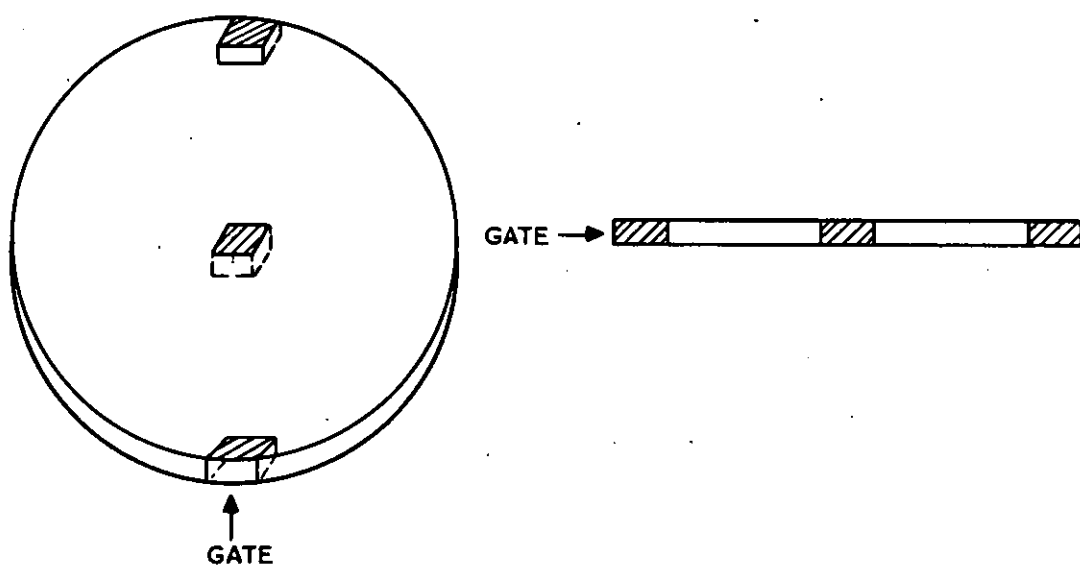
Optical microscopy was undertaken using a Watson Hilux - 70 microscope. This is a binocular microscope fitted with a four position turret, which contains a slideway to house a polaroid analyser; and a rotating polariser unit which fits over the condensing lens window.

The illumination is provided by a 12 V, 100 W quartz iodine bulb. The microscope is fitted with a light distributor which enables a 35 mm camera back to be permanently mounted on the microscope. A photo-binocular head is used in conjunction with the light distributor and a basic unit which incorporates a beam splitting prism allowing 80% of the light to go straight through to the camera back, and 20% of the light to a photocell tube for exposure readings to be made. A CdS integrating exposure meter measuring the total light over the field is used with the system. Fig. 10 shows the microscope with the different features labelled. Microscopy was usually undertaken using either a X10 or X40 parachromatic objective. Optical micrographs were obtained using Ilford FP4 film. Exposure settings were obtained after calibrating the exposure meter with a film using different exposure times.

Spherulite sizes were measured either from the micrographs or by direct observation using a micrometer eyepiece which was calibrated against a micrometer slide.

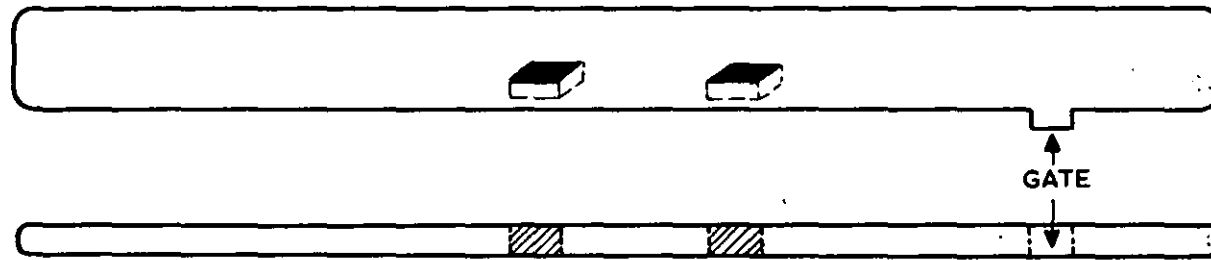


a) Water Absorption Disc

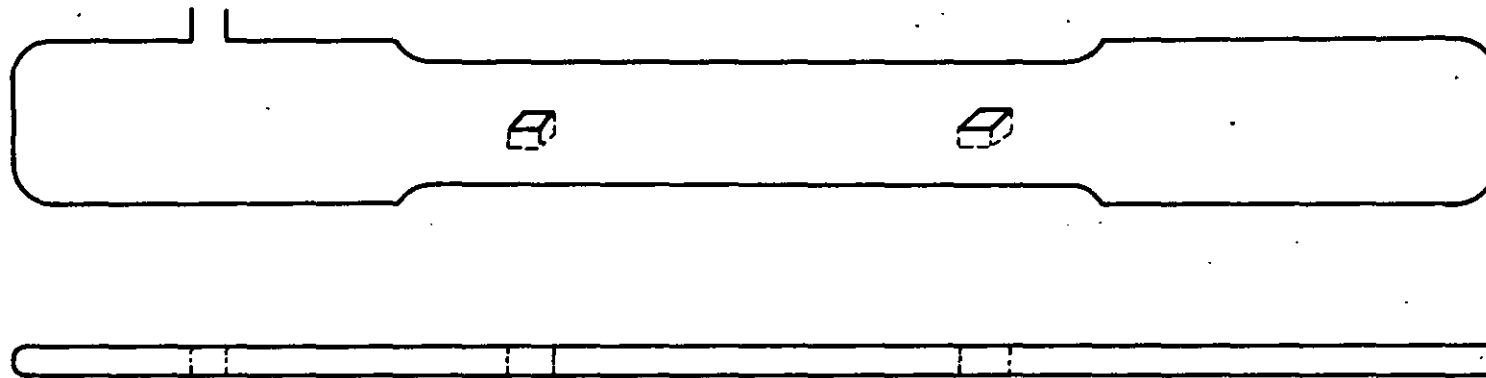


b) Impact Disc

FIG II a & b POSITION OF MICROSCOPY SAMPLES



c) Flexural Bar



d) Tensile Bar

FIG II c & d POSITION OF MICROSCOPY SAMPLES

Nylon 66 sections approximately $12\mu\text{m}$ thick were obtained on samples cut from mouldings using a MSE base sledge microtome fitted with a steel plano-concave knife. These sections were placed in silicone fluid on a glass slide and covered with a No. 1 glass cover slip.

Sections were cut from the surface and also through the mouldings as shown in Fig. 11. All the different types of moulded test samples were examined :- as moulded, conditioned, and after accelerated weathering.

3.6.2 Transmission electron microscopy

An AEI type EM 6 electron microscope was used in this work. A detailed description of this microscope is given in the instruction manual¹⁹⁵. In most instances an accelerating voltage of 75 kV was used with weak beam illumination.

Etched surfaces of mouldings were examined using a two stage replication technique. A small drop of a 5% polystyrene in benzene solution was placed on the etched sample and allowed to dry. After removal the polystyrene replica was coated with a thin film of carbon using an AEI vacuum coating unit. The polystyrene film was dissolved away by floating on benzene and the replica picked up on a copper grid before shadowing with gold/palladium to enhance contrast. The replicas were then examined in the electron microscope. Electron micrographs were obtained from plate exposures.

Ultra-thin sections were made for examination by transmission electron microscopy using a Porter-Blum microtome (MT2).

Glass knives were used for cutting sections of nylon 66 which were embedded in an epoxy resin using a cutting angle of 45° , the cut sections being floated onto an acetone/water mixture before being picked up on copper grids. Sections were stained using phosphotungstic acid vapour to enhance contrast before examination in the electron microscope.

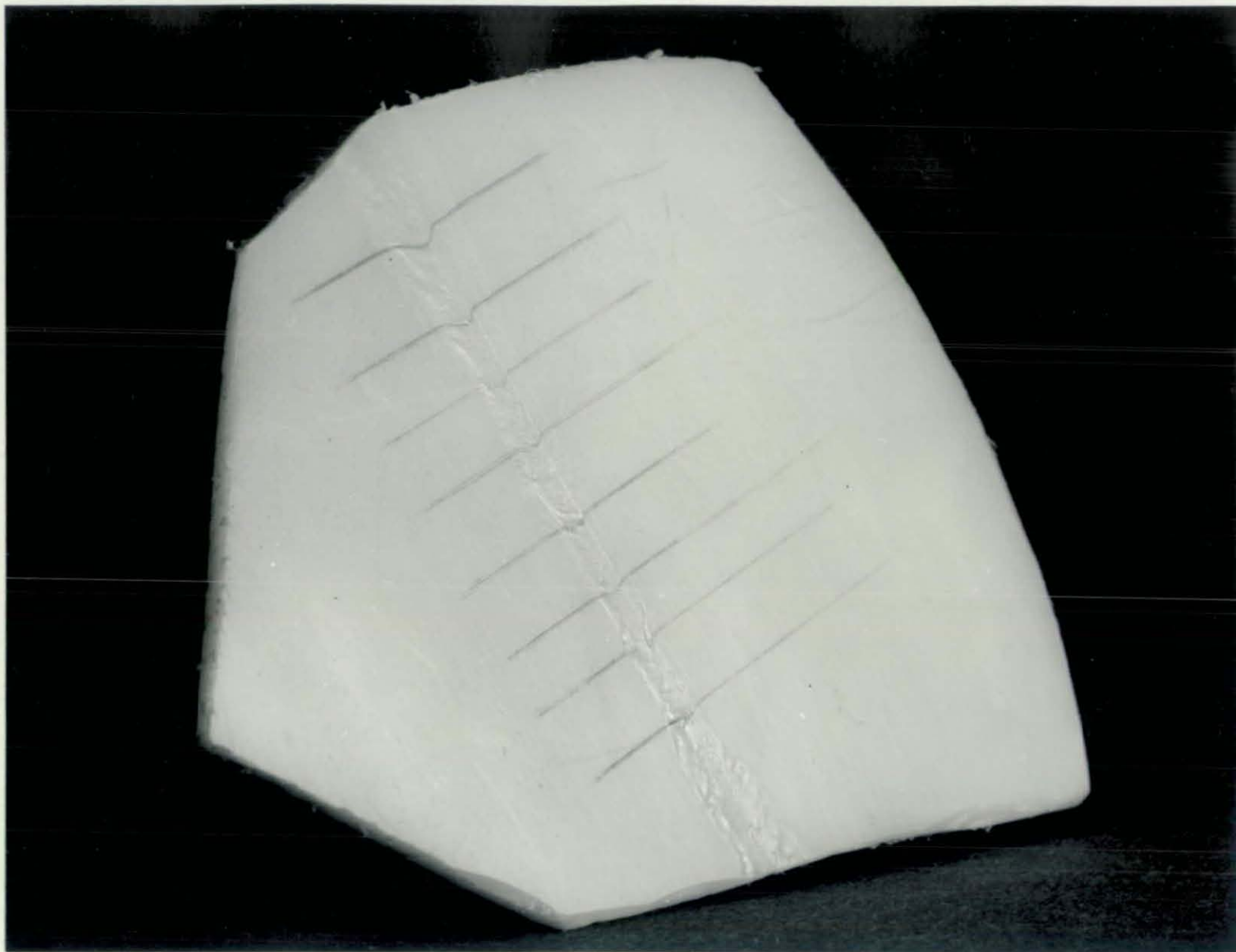


FIG.12.

FIG.12. HOT WIRE TEST ON A POLYPROPYLENE MOULDING.

3.7 X-RAY DIFFRACTION

Samples $1'' \times \frac{1}{2}'' \times \frac{1}{8}''$ (25.4 mm x 12.7 mm x 3.2 mm) were examined by X-ray diffraction for orientation. The sample was placed in a specimen holder of a Philips flat plate camera. Ni filtered CuK radiation was provided using a Philips 1010 X-ray generator with an accelerating voltage of 40 kV and a cathode current of 26 mA. The film used was Ilford G X-ray film. The exposure times initially used to obtain transmission photographs were 4 hours.

A double film was used, the first to pick up weak reflections, the second to give reasonable exposures of the higher intensity reflections. Later in the study only 1 hour exposure times were used with only a single film.

X-ray intensities were also obtained in some instances using a Geiger-Muller counter diffractometer.

3.8 HOT WIRE TECHNIQUE

This technique has been used by Atkinson and co-workers on ABS mouldings,¹⁹⁶ and is used to show surface orientation in polymer mouldings. A wire is placed about 1 mm above the surface of the specimen, and heated by passage of an electric current. This softens the surface layer of the moulding under the wire and the relaxation occurring during the test is shown by the shift of lines previously drawn on the moulding perpendicular to the presumed flow direction. Normal reversion tests apply to the whole moulding and not just to the surface. Fig. 12 shows this shift on a moulding of polypropylene.

CHAPTER 4. EXPERIMENTAL RESULTS

4.1 MECHANICAL TESTS

4.1.1 Tensile strength

Tensile strength for samples moulded at various mould temperatures are given in Table 1. Values are given for both "as moulded" and conditioned samples, the figures quoted being an average for nine specimens.

TABLE 1. TENSILE YIELD VALUES FOR DIFFERENT MOULD TEMPERATURES

MOULD TEMPERATURE °C	TENSILE YIELD AS MOULDED PSI (MN/m ²)	TENSILE YIELD CONDITIONED PSI (MN/m ²)
15	9,500 (65.5)	7,200 (49.6)
55	10,500 (72.4)	7,900 (54.5)
75	10,700 (73.8)	7,700 (53.1)
95	10,900 (75.2)	8,300 (57.2)

It can be seen that a higher mould temperature gives a sample with a higher yield strength the difference being greatest for "as moulded" samples moulded at 15°C. The conditioned samples again give the lowest figures for samples moulded at 15°C. The effect of water can be clearly seen when one compares the results obtained for "as moulded" and conditioned samples moulded at the same temperature, the water taken up during conditioning greatly reducing the tensile yield strength. Tensile values for specimens after accelerated weathering tests are shown in Table 2 (a).

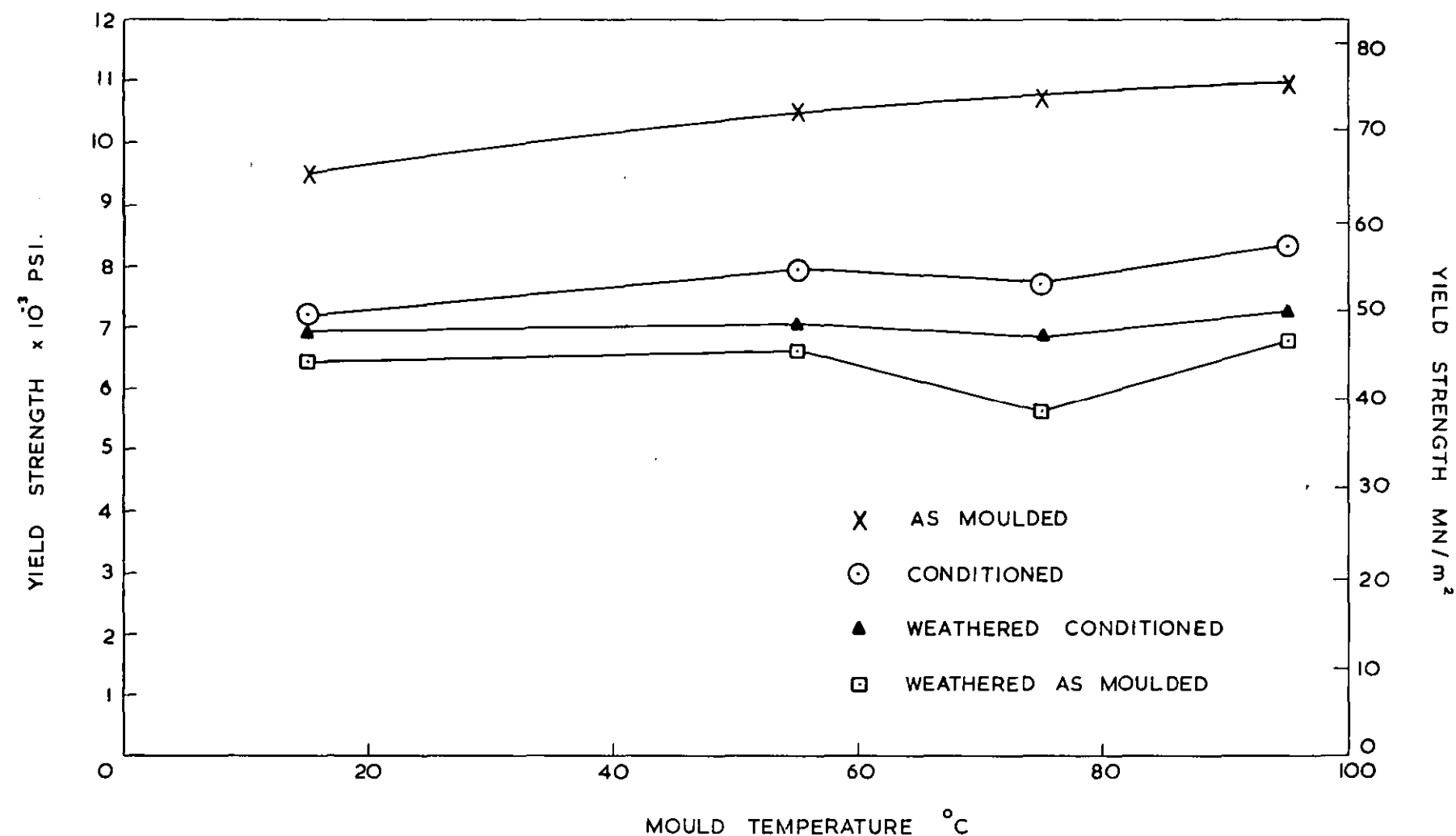
TABLE 2(a)YIELD STRENGTHS AFTER ACCELERATED WEATHERING,
EXCLUDING SAMPLES WHICH FAILED IN A BRITTLE MANNER

MOULD TEMPERATURE °C	TENSILE YIELD STRENGTH AS MOULDED PSI (MN/m ²)	CONDITIONED PSI (MN/m ²)
15	6,700 (46.2)	6,900 (47.6)
55	7,400 (51.0)	7,200 (49.7)
75	-	7,200 (49.7)
95	7,300 (50.3)	7,250 (50.0)

TABLE 2(b) TENSILE STRENGTH AT YIELD INCLUDING SAMPLES WHICH FAILED
BEFORE YIELDING, I.E. FAILED IN A BRITTLE FASHION

MOULD TEMPERATURE °C	AS MOULDED PSI (MN/m ²)	CONDITIONED PSI (MN/m ²)
15	6,400 (44.1)	6,900 (47.6)
55	6,600 (45.5)	7,050 (48.6)
75	5,600 (38.6)	6,850 (47.2)
95	6,750 (46.6)	7,250 (50.0)

Tables 2(a) and 2(b) show the drastic reduction in tensile yield strength for "as moulded" samples after accelerated weathering and also highlight the smaller reductions for the conditioned samples. Another interesting point is that very few brittle failures were obtained for conditioned samples whereas brittle failures were quite prominent for "as moulded" samples. A tendency towards brittle failure when moulded at a higher mould temperature is also indicated.



GRAPH. 1.

GRAPH. 1. TENSILE STRENGTH AT YIELD vs. MOULD TEMPERATURE.

The tensile yield strength figures obtained at various mould temperatures and after treatments are summarised in Graph 1.

4.1.2 Flexural Modulus

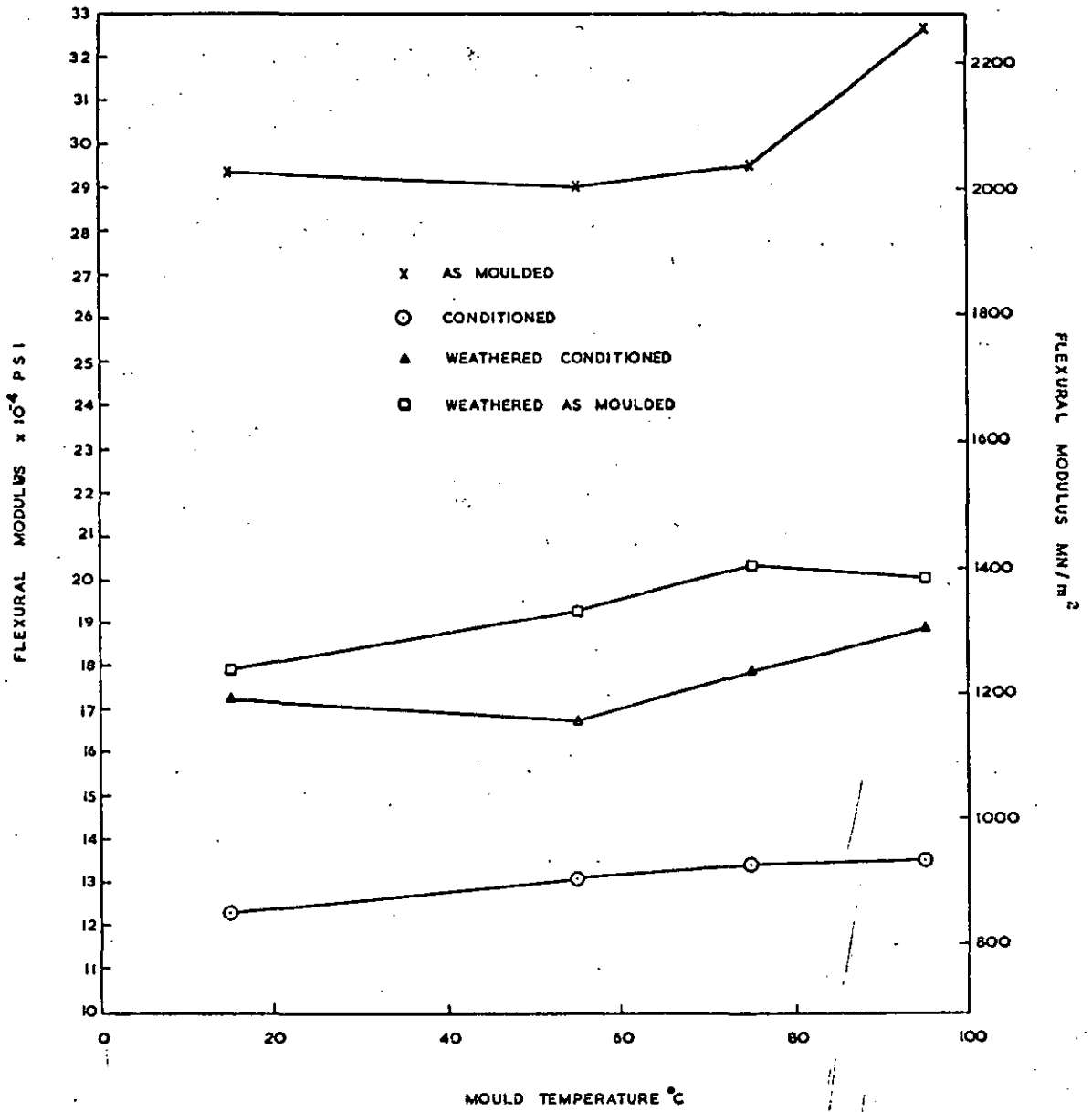
Table 3 gives the figures obtained for the flexural modulus of the "as moulded" and conditioned unweathered samples.

TABLE 3

MOULD TEMPERATURE °C	FLEXURAL MODULUS AS MOULDED PSI (MN/m ²)	CONDITIONED PSI (MN/m ²)
15	293,300 (2,022)	123,000 (848)
55	290,500 (2,003)	131,100 (904)
75	295,100 (2,034)	134,200 (925)
95	326,600 (2,252)	135,500 (934)

Table 3 shows a very great difference in the flexural modulus figures for "as moulded" and conditioned samples and to much lesser extent the difference between the values obtained at different mould temperatures. The only main difference for the "as moulded" samples being that the value obtained for a mould temperature of 95°C is significantly higher than for the other three mould temperatures, whereas for conditioned samples the flexural modulus obtained at a mould temperature of 15°C is significantly lower than the figures obtained at the other mould temperatures. The flexural modulus figures after accelerated weathering are given in Table 4.

GRAPH.2.



GRAPH.2. FLEXURAL MODULUS vs. MOULD TEMPERATURE.

TABLE 4. FLEXURAL MODULUS AFTER ACCELERATED WEATHERING

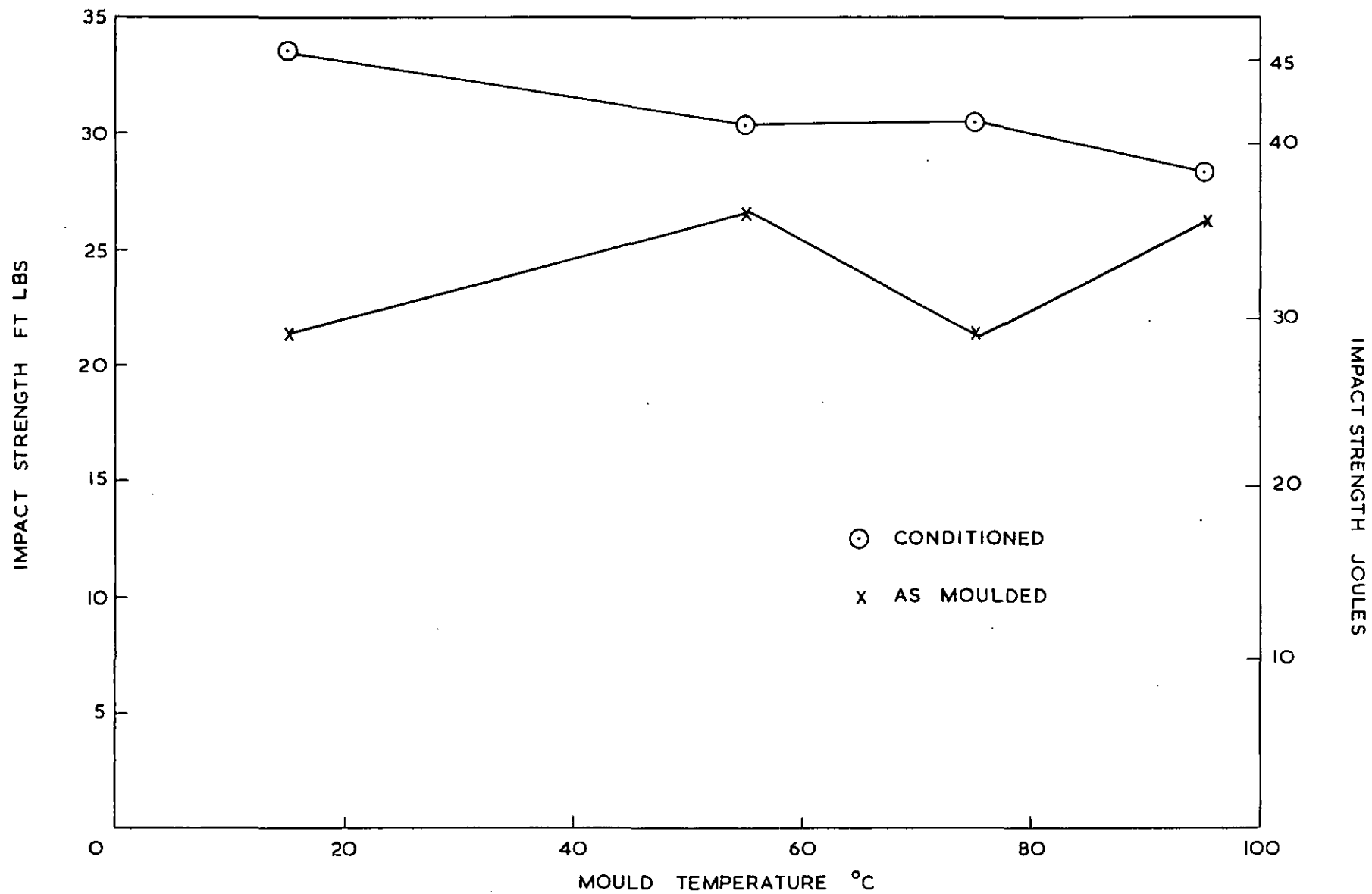
MOULD TEMPERATURE °C	AS MOULDED PSI (MN/m ²)	CONDITIONED PSI (MN/m ²)
15	179,100 (1,235)	172,600 (1,190)
55	193,100 (1,331)	167,500 (1,134)
75	203,700 (1,405)	178,900 (1,234)
95	200,600 (1,383)	188,800 (1,302)

Accelerated weathering has brought the flexural modulus figures of "as moulded" and conditioned samples much nearer as happened with the tensile yield figures, the "as moulded" samples giving slightly higher values than the conditioned samples. The overall tendency is for a higher mould temperature to give a higher flexural modulus even though there are some discrepancies e.g. 75°C and 95°C for "as moulded" and 15 and 55°C for conditioned samples.

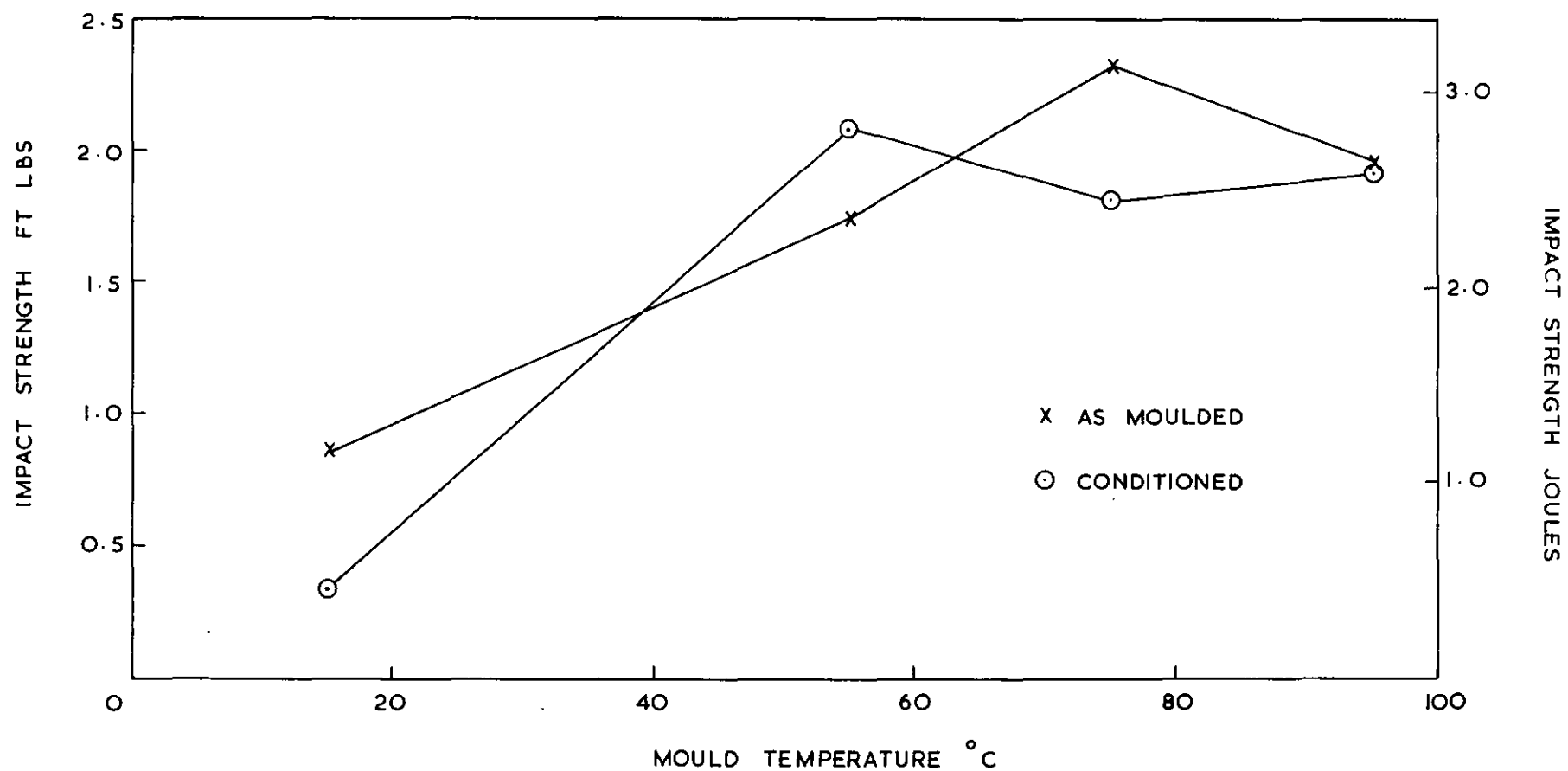
The conditioned samples give higher flexural modulus figures after accelerated weathering than before. This is most likely to be due to the accelerated samples containing less water in the surface region than the conditioned samples. Another factor is the increased density of the samples due to increased crystallinity causing the samples to be stiffer. The flexural moduli figures obtained at various mould temperatures and after treatments are summarised in Graph 2.

4.1.3 Impact

Falling weight impact strengths were determined using 2" (51 mm) diameter discs 1/16" (3 mm) thick. Twenty discs were used for each test and the results are shown in Table 5.



GRAPH . 3 . IMPACT STRENGTH vs. MOULD TEMPERATURE.



GRAPH. 4. IMPACT STRENGTH vs. MOULD TEMPERATURE
WEATHERED SAMPLES.

TABLE 5. IMPACT STRENGTH vs MOULD TEMPERATURE

MOULD TEMPERATURE °C	IMPACT ft lbs (JOULES)			
	BEFORE WEATHERING		AFTER WEATHERING	
	AS MOULDED	CONDITIONED	AS MOULDED	CONDITIONED
15	21.55 (29.21)	33.6 (45.55)	0.86 (1.166)	0.34 (0.461)
55	26.62 (36.09)	30.32 (41.11)	1.73 (2.345)	2.08 (2.82)
75	21.48 (29.12)	30.45 (41.29)	2.32 (3.146)	1.70 (2.304)
95	26.34 (35.72)	28.41 (38.52)	1.97 (2.671)	1.91 (2.589)

Before weathering both "as moulded" and conditioned samples gave high impact strengths, the conditioned samples containing more water than the "as moulded" samples giving the higher figures. There appeared to be no direct relationship between mould temperature and impact strength.

After weathering the impact strengths fell drastically. Since the disc surfaces were covered with cracks the low impact figures obtained are not surprising since the specimens could be likened to "notched samples". The impact strengths of samples moulded at 15°C were about 50% below those at the other mould temperatures. Possible explanations are that these samples had higher frozen-in stresses and/or were more severely degraded than the samples obtained at other mould temperatures.

Graphs 3 and 4 summarise the impact strength data before and after accelerated weathering.

4.1.4 Wear

Initial tests using the A/F rig were undertaken using samples cut from flexural bars. The sample dimensions were 1" x $\frac{1}{2}$ " x $\frac{1}{4}$ " (25.4 mm x 12.7 mm x 6.3 mm) and the load on the samples was 100 psi (0.6895 MN/m²). The average results for 22 hours running are shown in Table 6.

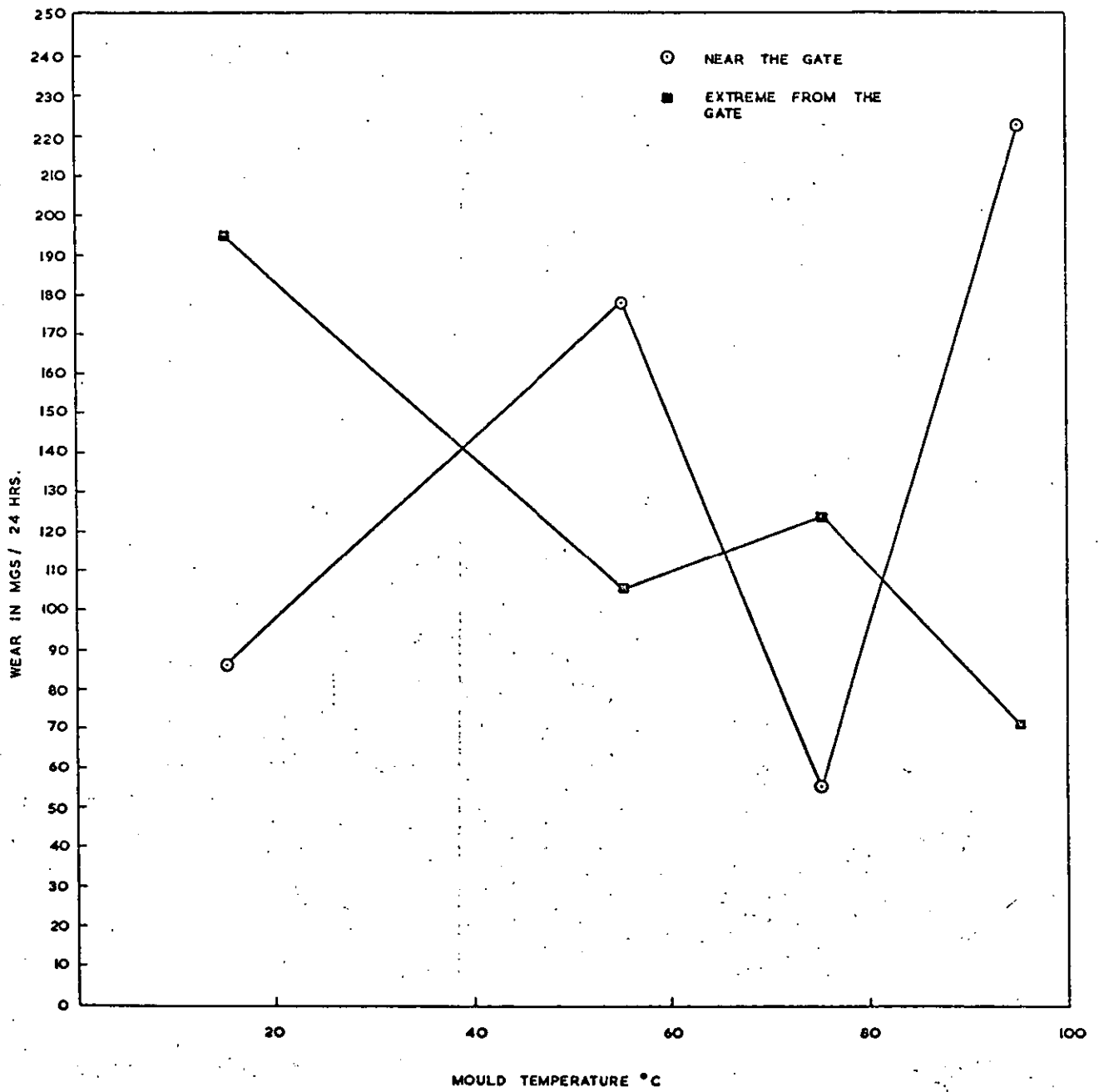
TABLE 6. WEAR vs MOULD TEMPERATURE

SAMPLE	MOULD TEMPERATURE °C	WEAR EXPRESSED AS WEIGHT LOSS (mgs)
Conditioned	15	19
"	55	19
"	75	25
"	95	83
As Moulded	15	33
"	55	25
"	75	15
"	95	12

These results indicate that for "as moulded" samples the wear increases as the mould temperature decreases while for conditioned samples the opposite is true.

Later tests using the A/F rig on specimens cut from water absorption discs as shown in Fig. 4 used a load of 100 lbs (45.4 kg) giving a load of 200 psi (1.379 MN/m²) on the specimen. Table 7 shows the average wear and dynamic coefficient of friction results obtained after 24 hours running using samples near to and extreme from the gate.

GRAPH . 5.



GRAPH . 5. WEAR vs. MOULD TEMPERATURE.

TABLE 7.

MOULD TEMP °C	WEAR EXPRESSED AS WEIGHT LOSS (mgs)		COEFFICIENT OF DYNAMIC FRICTION	
	NEAR THE GATE	EXTREME FROM THE GATE	NEAR THE GATE	EXTREME FROM THE GATE
95	222.9	70.6	0.55	0.55
75	55.2	123.3	0.55	0.55
55	178.4	105.6	0.55	0.56
15	86.3	194.3	0.57	0.51

These results are plotted in Graph 5 and show that the dynamic coefficient of friction is fairly constant and not affected by variations in mould temperature.

Wear measurements were also obtained using a rotating shaft rig a diagram of which is shown in Fig. 5. It was found that scar width was also a convenient measure of wear as well as weight loss as shown by the following figures.

WEIGHT LOSS (mgs)	SCAR WIDTH (inches)
5.8	0.570
11.2	0.754
11.4	0.770
24.9	1.093
46.6	1.216
53.4	1.258

However it was decided to use weight loss as this was easier to measure.

Specimens were cut from water absorption discs as shown in Fig. 4 but the cut surfaces were worn not the moulded surface. The two surfaces worn were the cut surface (Surface 1) nearest the gate in the sample nearest the gate and the furthest cut surface (Surface 2) of the sample extreme from the gate.

Table 8 shows the weight loss after 96 hours together with the water content of the samples after the wear tests.

TABLE 8.

MOULD TEMPERATURE °C	CUT SURFACE 1		CUT SURFACE 2	
	WEIGHT LOSS IN mgs	WATER CONTENT %	WEIGHT LOSS IN mgs	WATER CONTENT %
95	4.0	1.4	4.1	1.4
75	3.7	1.4	4.8	1.4
55	3.7	1.9	4.1	1.4
15	3.4	1.5	4.3	1.7

For the position near the gate it appears that the wear decreases as the mould temperature is decreased. For the wearing surface away from the gate no trend is shown for mould temperature, but the wear for specimens from this position is greater than for samples near the gate.

Further wear tests were undertaken using the rotating shaft apparatus but wearing against the moulded surface as with the A/F rig. The specimens were glued to polypropylene blocks to facilitate fixing in the specimen holder. Specimens were run for 168 hours using only the specimens taken from near to the gate.

The results obtained are shown in Table 9.

TABLE 9. WEIGHT LOSS vs MOULD TEMPERATURE

MOULD TEMPERATURE °C	WEIGHT LOSS (mgs)
95	5.7
75	5.1
55	6.3
15	6.9

As can be seen no trend is emphasized, the only point being that possibly a higher mould temperature gives less wear.

The load on the surface specimens was 16.70 lbs (7.584 kgs) and the load on the cut surface samples was 12.74 lbs (5.784 kgs). Initially at the start of the tests the area of contact between the rotating shaft and the sample is small, hence the load on the sample is at its highest level. This load decreases as the test proceeds and the area of contact increases. For a scar width of 0.1 inches the load initially is approximately 334 psi (2.303 MN/m^2) for the surface specimens and approximately 1,336 psi (9.212 MN/m^2) for the cut surface specimens. In the majority of cases the wear figures quoted are an average for four samples.

4.2 PHYSICAL AND THERMAL PROPERTIES

4.2.1 Water Absorption

According to the general line of thought on the water absorption of crystalline polymers it is assumed that water will absorb preferentially

into the amorphous regions. The results obtained for water absorption discs moulded at four mould temperatures are given in Table 10. After moulding one set of discs for each temperature were conditioned, then both sets of discs were pre-dried according to BS 2782 before the water absorption test.

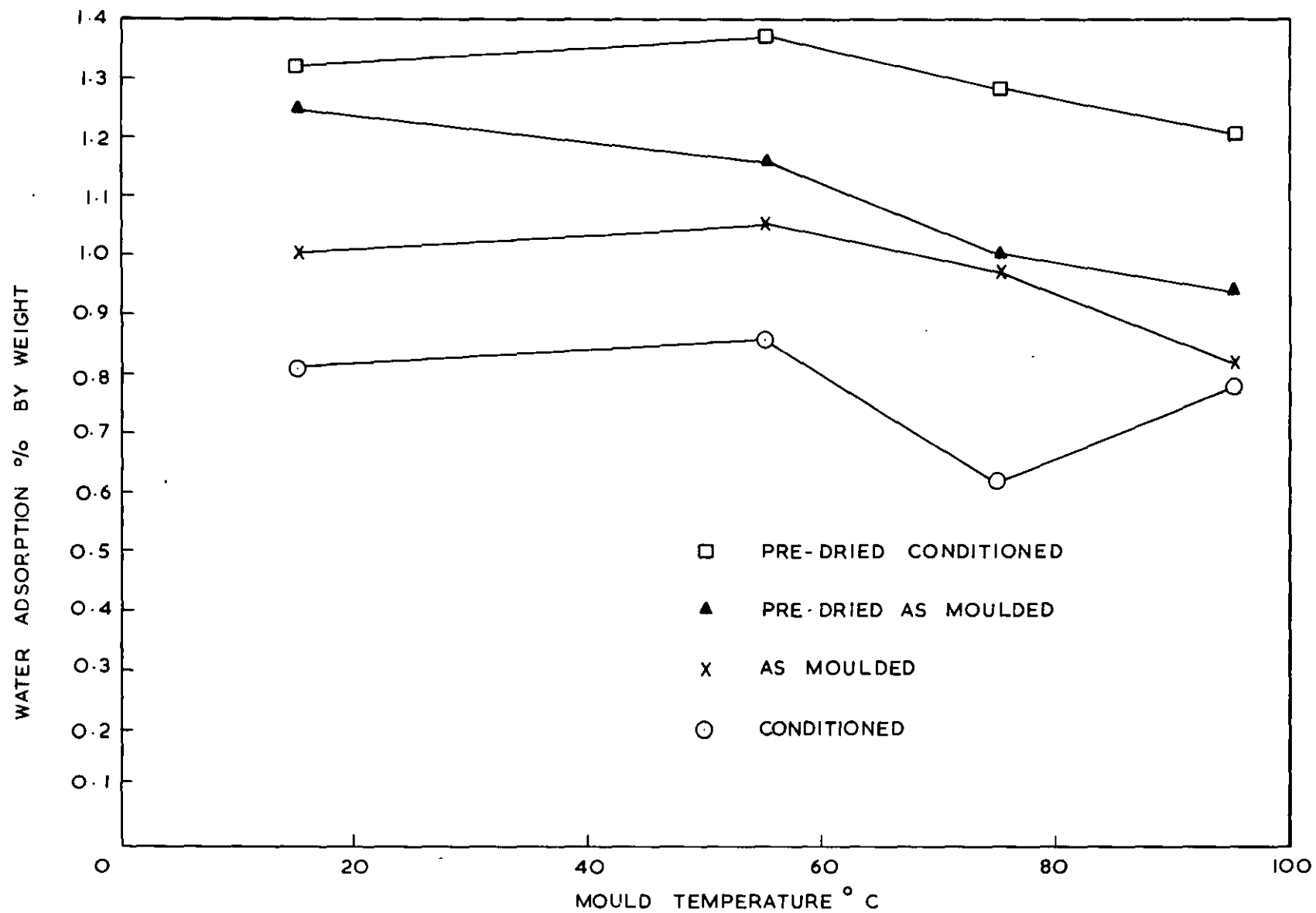
TABLE 10.

MOULD TEMPERATURE °C	WATER ABSORPTION % BY WEIGHT	
	AS MOULDED	CONDITIONED
15	1.00	0.81
55	1.05	0.86
75	0.97	0.62
95	0.82	0.78

The "as moulded" samples conform to the general picture, a greater water absorption for a lower mould temperature. The conditioned samples gave unusual results which will be discussed later. Table 11 shows the results for samples which were predried in a vacuum oven at 50°C.

TABLE 11.

MOULD TEMPERATURE °C	24 HOUR WATER ABSORPTION (%)	
	AS MOULDED	CONDITIONED
15	1.25	1.32
55	1.16	1.37
75	1.00	1.28
95	0.94	1.21



GRAPH. 6. WATER ABSORPTION vs. MOULD TEMPERATURE.

These results apart from the conditioned figures at mould temperatures of 15 and 55°C are as would be expected, i.e. (i) a higher mould temperature gives a lower water absorption. (ii) Conditioned samples give higher absorption figures than "as moulded".

The effect of mould temperature on water absorption is illustrated in Graph 6.

4.2.2 Inherent Viscosity

Inherent viscosity determinations as described in section 3.4.2 were carried out on moulded samples and similar samples after accelerated weathering. Initially on weathered tensile and flexural samples all the sample was used for viscosity determinations. The figures obtained are shown in Table 12.

TABLE 12. INHERENT VISCOSITY vs MOULD TEMPERATURE

MOULD TEMPERATURE °C	INHERENT VISCOSITY	
	AFTER WEATHERING	BEFORE WEATHERING
15	0.9817 (16,600)	1.0778 (18,700)
55	0.9324 (15,550)	1.0136 (17,300)
75	0.9413 (15,750)	1.0328 (17,750)
95	0.9383 (15,650)	1.0136 (17,300)

The figures in brackets are estimated molecular weight figures obtained from figures obtained by end group analysis.¹⁹⁷

Inherent viscosity figures (molecular weight figures in brackets) obtained on weathered impact discs are shown in Table 13 and for weathered flexural bars in Table 14.

TABLE 13. INHERENT VISCOSITY OF WEATHERED IMPACT DISCS

MOULD TEMPERATURE °C	INHERENT VISCOSITY	
	SURFACE SKIN (.005")	INTERIOR (CENTRE OF MOULDING)
15	0.7064 (11,400)	1.0763 (18,700)
55	0.8152 (13,150)	1.0436 (18,000)
75	0.8192 (13,200)	1.0552 (18,250)
95	0.7230 (11,650)	1.0193 (17,400)

TABLE 14. INHERENT VISCOSITY OF WEATHERED FLEXURAL BARS

MOULD TEMPERATURE °C	SURFACE SKIN (.005")	INTERIOR (CENTRE OF MOULDING)
15	0.741 (11,900)	1.091 (19,000)
55	0.654 (10,750)	1.070 (18,550)
75	0.753 (12,050)	1.071 (18,550)
95	0.600 (10,100)	1.064 (18,450)
15	0.6508 (10,650)	1.0157 (17,350)
55	0.7562 (12,150)	0.9992 (17,000)
75	0.7949 (12,750)	1.034 (17,800)
95	0.7406 (11,900)	1.035 (17,800)

From the figures obtained it can be seen that accelerated weathering has drastically reduced the inherent viscosity and hence molecular weight of the surface of the nylon samples while the interior of the mouldings have remained essentially unchanged.

4.2.3 Density

Densities of various samples were obtained using a density gradient column of carbon tetrachloride and toluene at 23°C. Crystallinity figures can be obtained from density measurements using known values of the density of completely amorphous and 100% crystalline nylon 66. The crystallinity results quoted were obtained using the density values given by Starkweather et al²⁶, using the figures quoted by Muller and Pflunger⁹⁷ crystallinity values obtained are approximately 50% higher.

TABLE 15 (a)

DENSITY g/cc (% CRYSTALLINITY) AT 23°C
OF FLEXURAL SAMPLES

MOULD TEMPERATURE °C	AFTER MOULDING	AFTER ACCELERATED WEATHERING
15	1.1385 (32.3)	1.1445 (36.3)
55	1.1410 (34.0)	1.1457 (37.1)
75	1.1403 (33.5)	1.1465 (37.7)
95	1.1416 (34.4)	1.1470 (38.0)

TABLE 15 (b)

DENSITY g/cc (% CRYSTALLINITY) OF IMPACT
AND WATER ABSORPTION SAMPLES

MOULD TEMPERATURE °C	DENSITIES AFTER MOULDING	
	IMPACT SAMPLES	WATER ABSORPTION SAMPLES
15	1.1365 (31.0)	1.1387 (32.5) ;
55	1.1397 (33.1)	1.1406 (33.7)
75	1.1403 (33.5)	1.1410 (34.0)
95	1.1409 (33.9)	1.1415 (34.3)

TABLE 15(c) DENSITY (% CRYSTALLINITY) OF WEATHERED IMPACT SAMPLES

MOULD TEMPERATURE °C	DENSITY g/cc
15	1.1441 (36.1)
55	1.1450 (36.7)
75	1.1455 (37.0)
95	1.1458 (37.2)

TABLE 15 (d) DENSITY OF WEAR SAMPLES TAKEN FROM WATER
ABSORPTION DISCS

MOULD TEMPERATURE °C	DENSITY g/cc (% CRYSTALLINITY)	
	NEAR GATE	EXTREME FROM GATE
15	1.1440 (36.0)	1.1435 (35.7)
55	1.1457 (37.1)	1.1456 (37.1)
75	1.1468 (37.9)	1.1466 (37.7)
95	1.1470 (38.0)	1.1470 (38.0)

TABLE 15 (e) DENSITY (% CRYSTALLINITY) OF WEATHERED
IMPACT DISCS

MOULD TEMPERATURE °C	DENSITY g/cc	
	SURFACE SKIN	INTERIOR (CENTRE OF MOULDING)
15	1.1521 (41.4)	1.1434 (35.6)
55	1.1517 (41.1)	1.1411 (34.1)
75	1.1508 (40.5)	1.1431 (35.4)
95	1.1488 (39.2)	1.1478 (38.5)

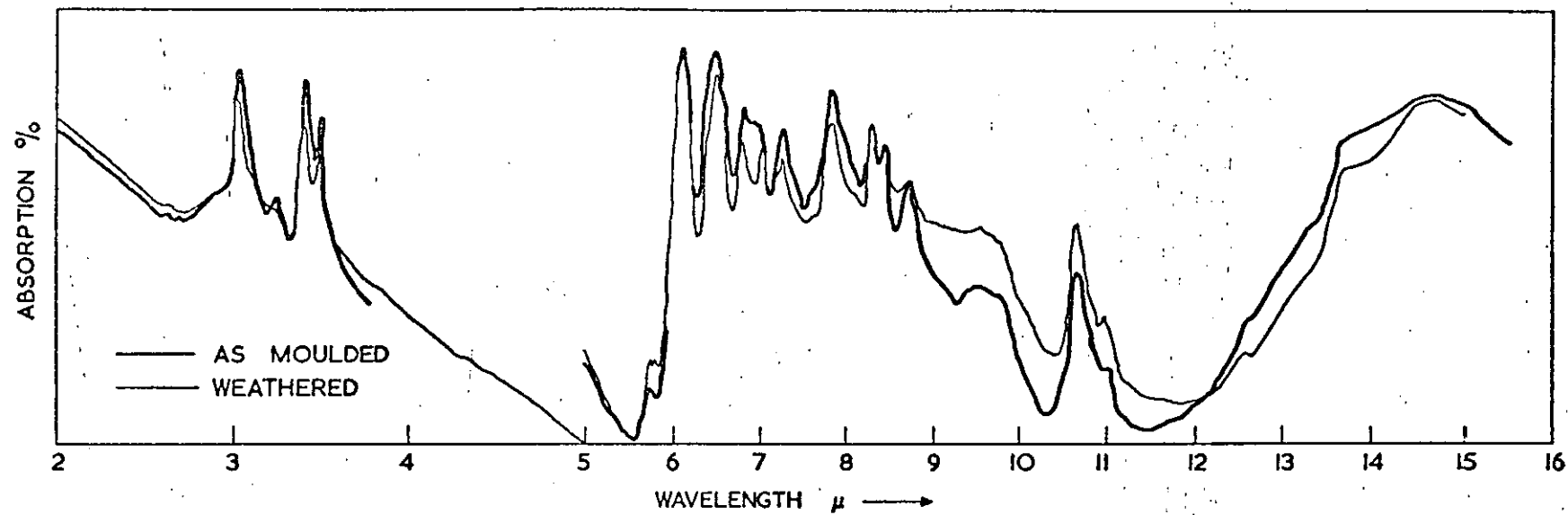


FIG 13. ATR SPECTRA FOR IMPACT SPECIMENS MOULD TEMPERATURE 95°C

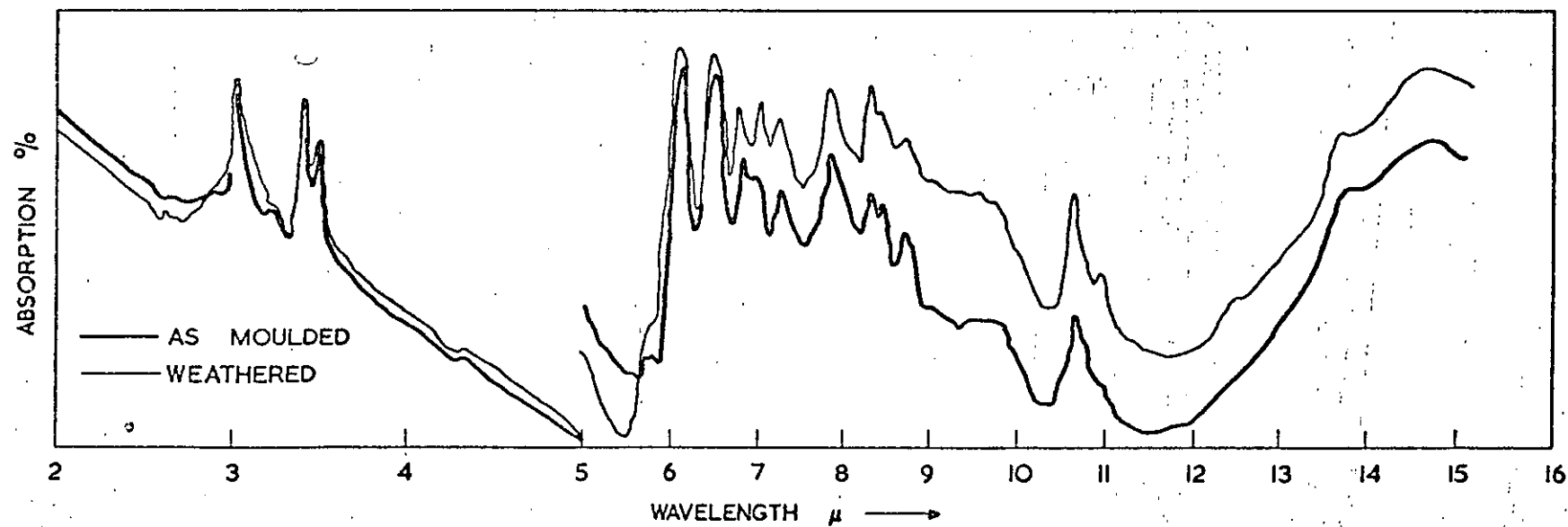


FIG 14. ATR SPECTRA FOR IMPACT SPECIMENS MOULD TEMPERATURE 75°C

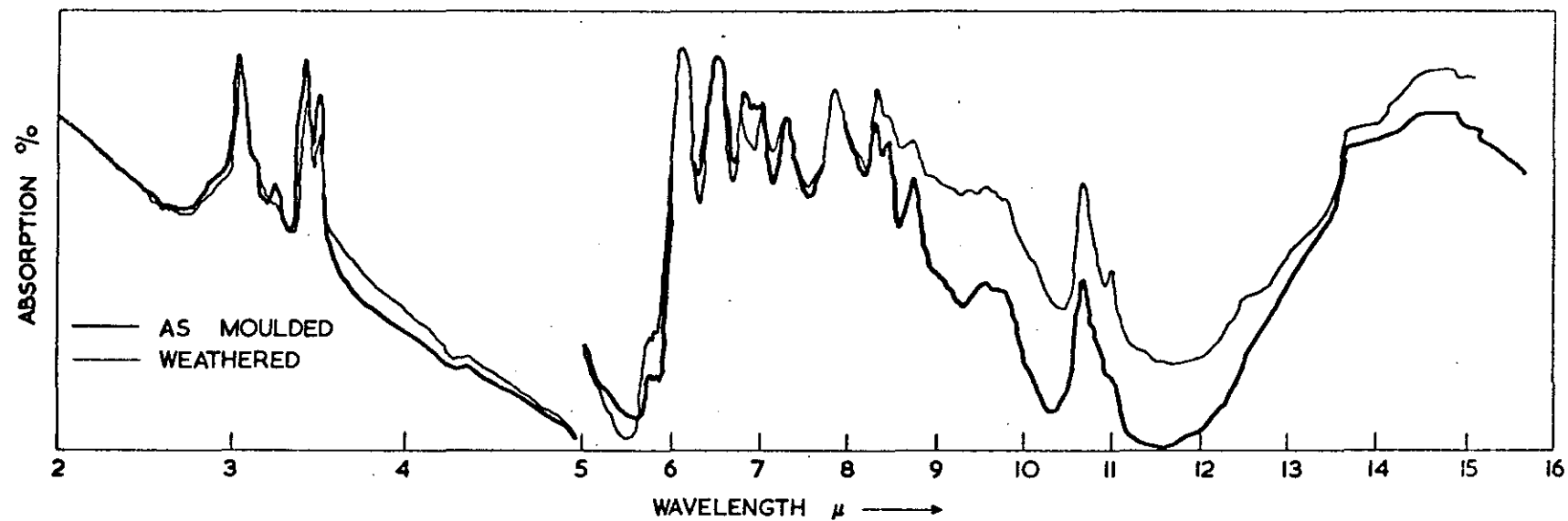


FIG 15 ATR SPECTRA FOR IMPACT SPECIMENS MOULD TEMPERATURE 55°C

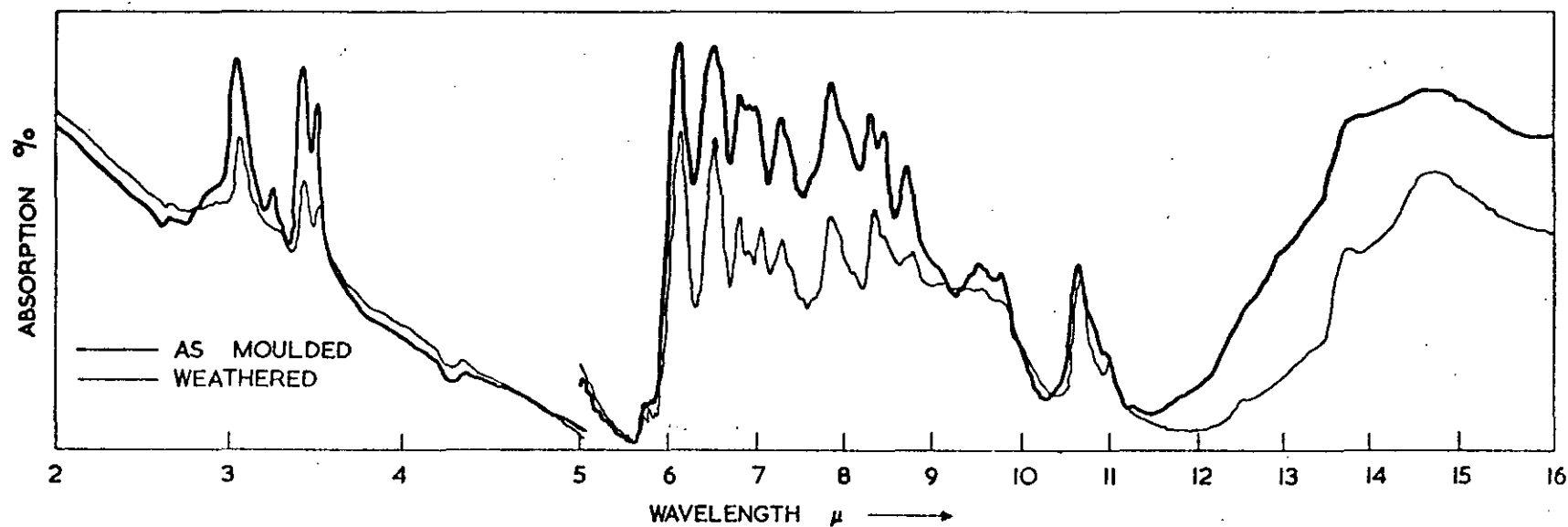


FIG 16 ATR SPECTRA FOR IMPACT SPECIMENS MOULD TEMPERATURE 15°C

As can be seen from Tables 15a and 15c the density increases with increasing mould temperature. The density also increases after accelerated weathering, but decreases the difference in density between samples moulded at different mould temperatures.

The densities of water absorption discs are higher than for impact discs moulded under the same conditions. This is to be expected due to the slower cooling of the thicker water absorption samples.

Table 15d shows that a slight difference in density exists for samples moulded at the same temperature but taken from different positions relative to the gate. The samples nearer the gate having a slightly higher density, this difference however appears to decrease as the mould temperature increases.

For weathered impact discs when specimens were taken from the moulding surface and from the interior large differences in density were obtained the surfaces being substantially higher. The higher density (higher crystallinity) giving a more brittle material as shown in Table 5.

4.2.4 Attenuated Total Reflectance (ATR)

The spectra obtained for weathered and unweathered impact samples are shown in Figs. 13, 14, 15, 16. As can be seen after weathering several changes have taken place the absorptions at $3.25\ \mu$, 5.7μ , 5.8μ , (doublet), $6.8\ \mu$, 7.05μ , $8.3\ \mu$, 8.45μ , 8.72μ (9.3μ , 9.5μ , $9.8\ \mu$), 11μ either being increased/decreased or being additional.

Some of the increased absorption could be attributed to hexamethylene diamine, and there is also evidence of a carboxylic acid being present, but not necessarily adipic acid.

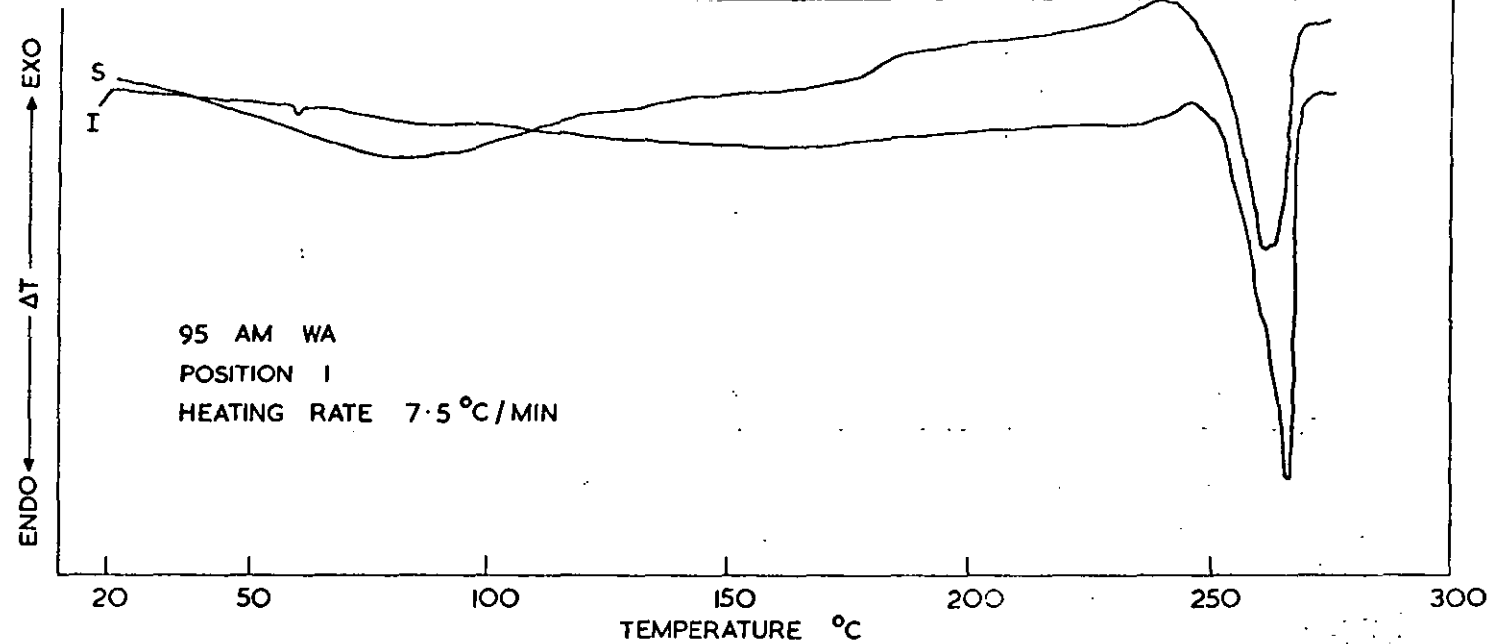


FIG 17a DSC THERMOGRAM FOR SAMPLE MOULDED AT 95 °C

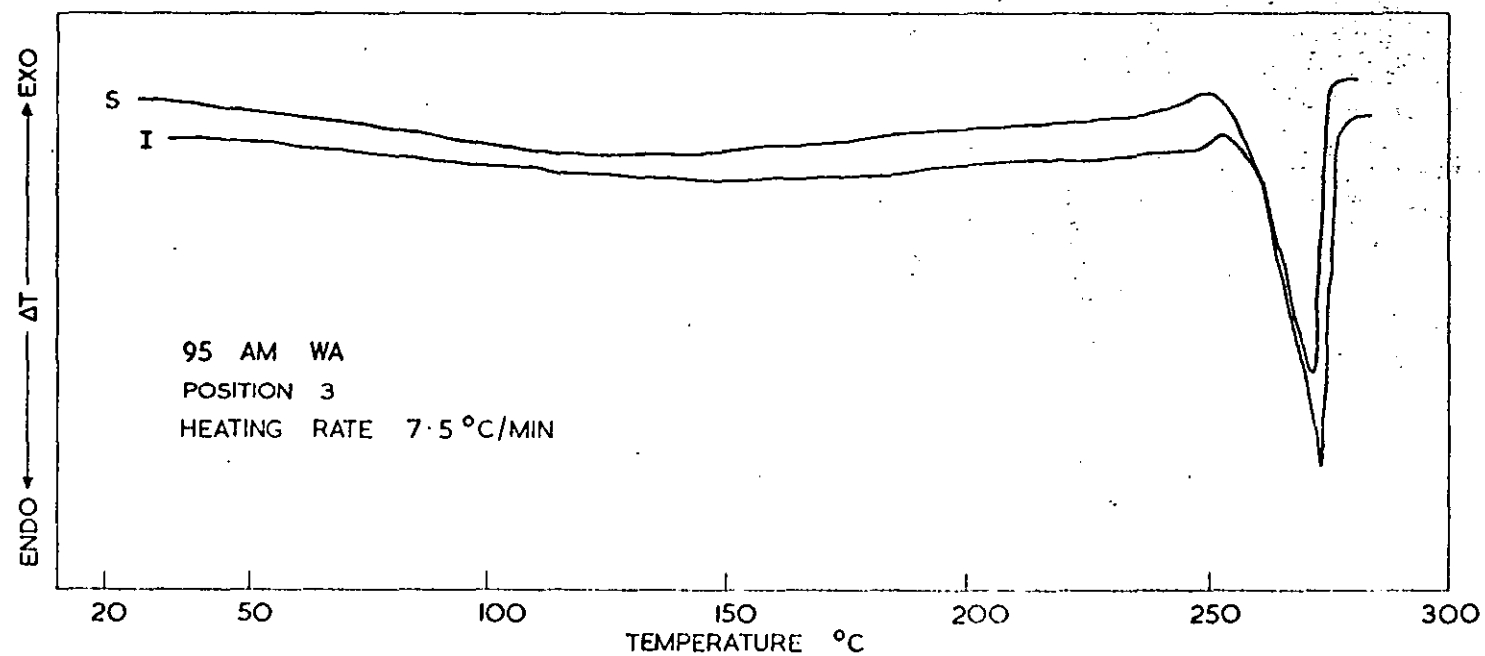


FIG 17b DSC THERMOGRAM FOR SAMPLE MOULDED AT 95 °C

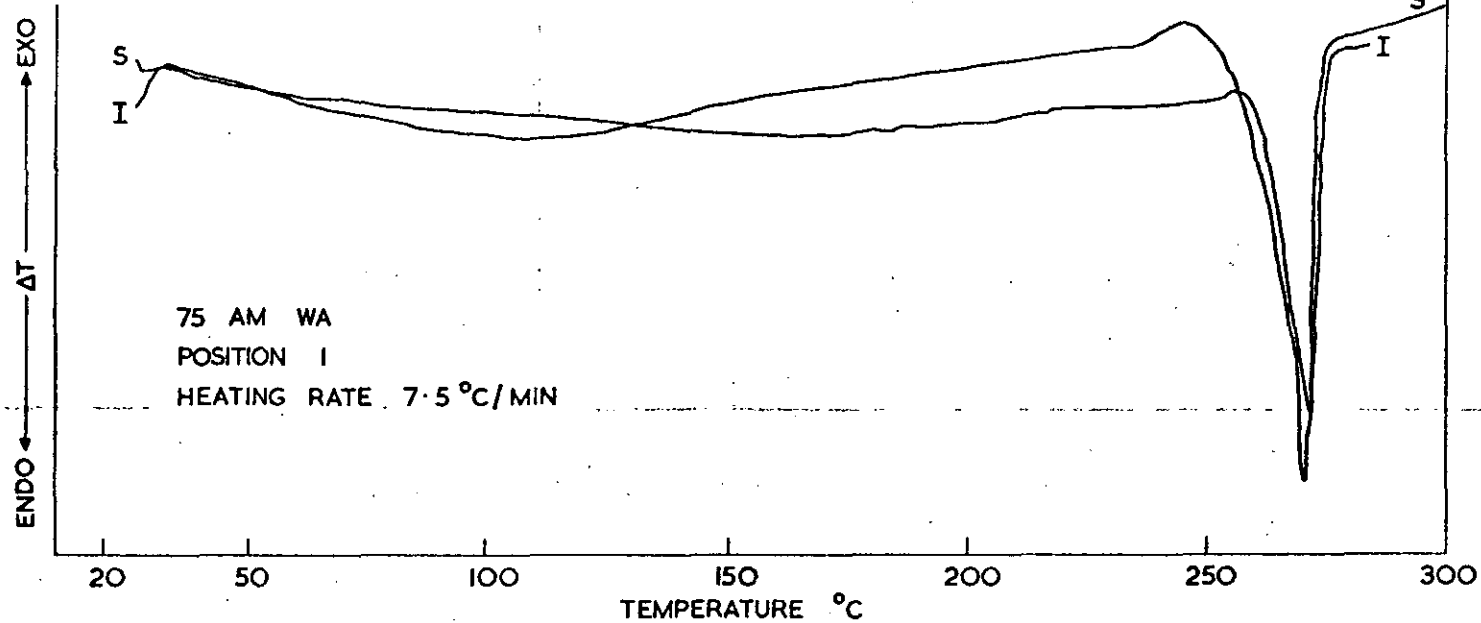


FIG 18a DSC THERMOGRAM FOR SAMPLE MOULDED AT 75 °C

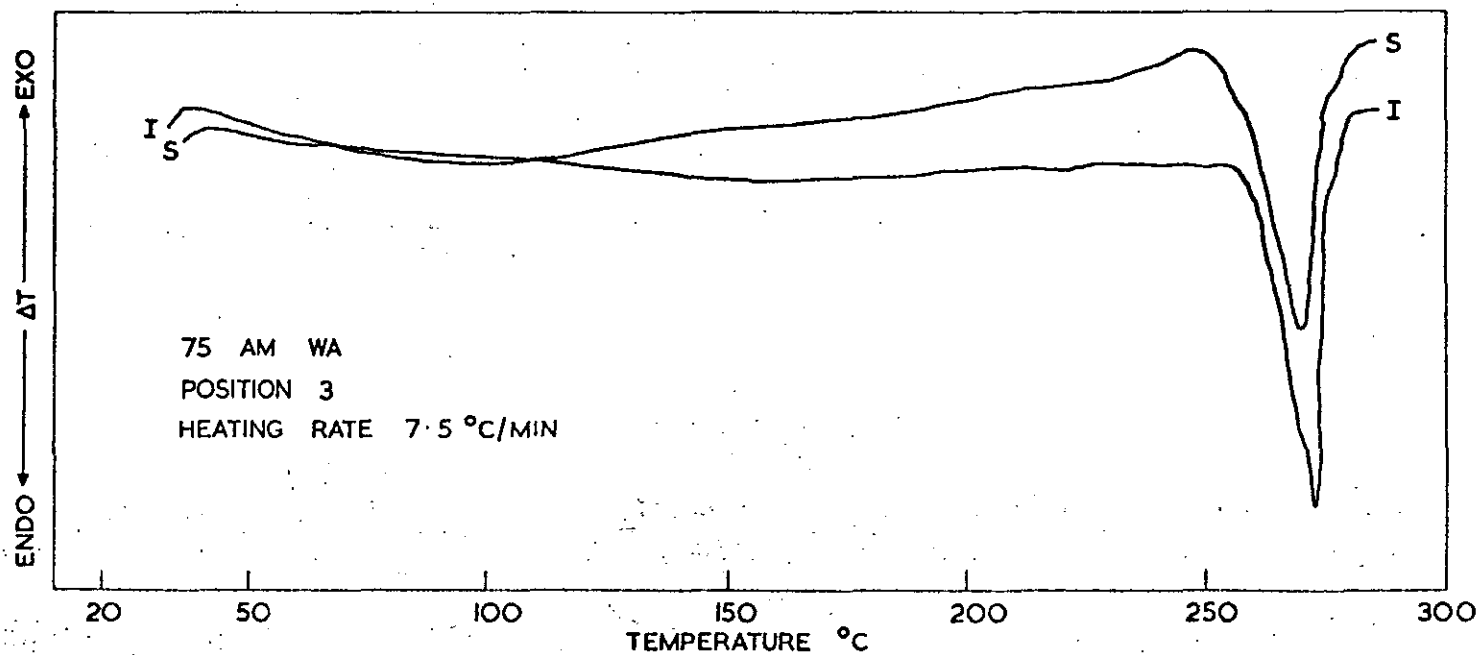


FIG 18b DSC THERMOGRAM FOR SAMPLE MOULDED AT 75 °C

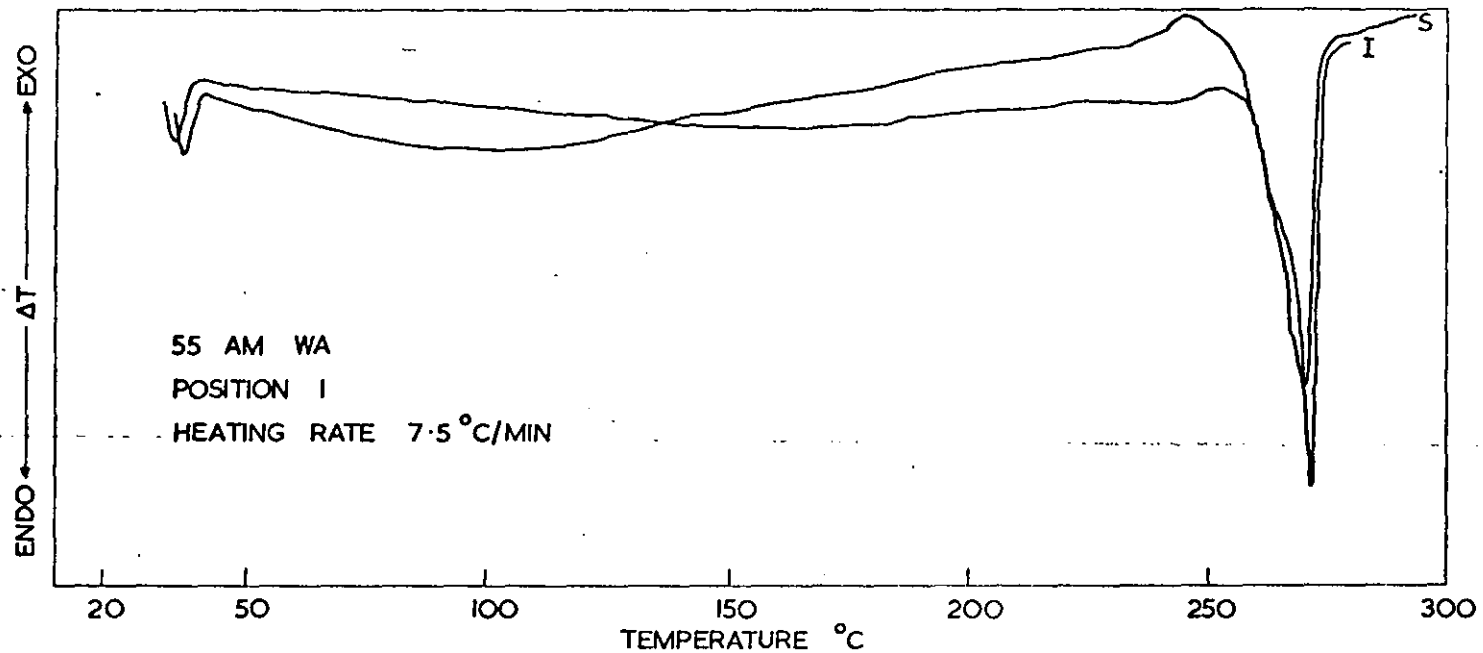


FIG 19a DSC THERMOGRAM FOR SAMPLE MOULDED AT 55 °C

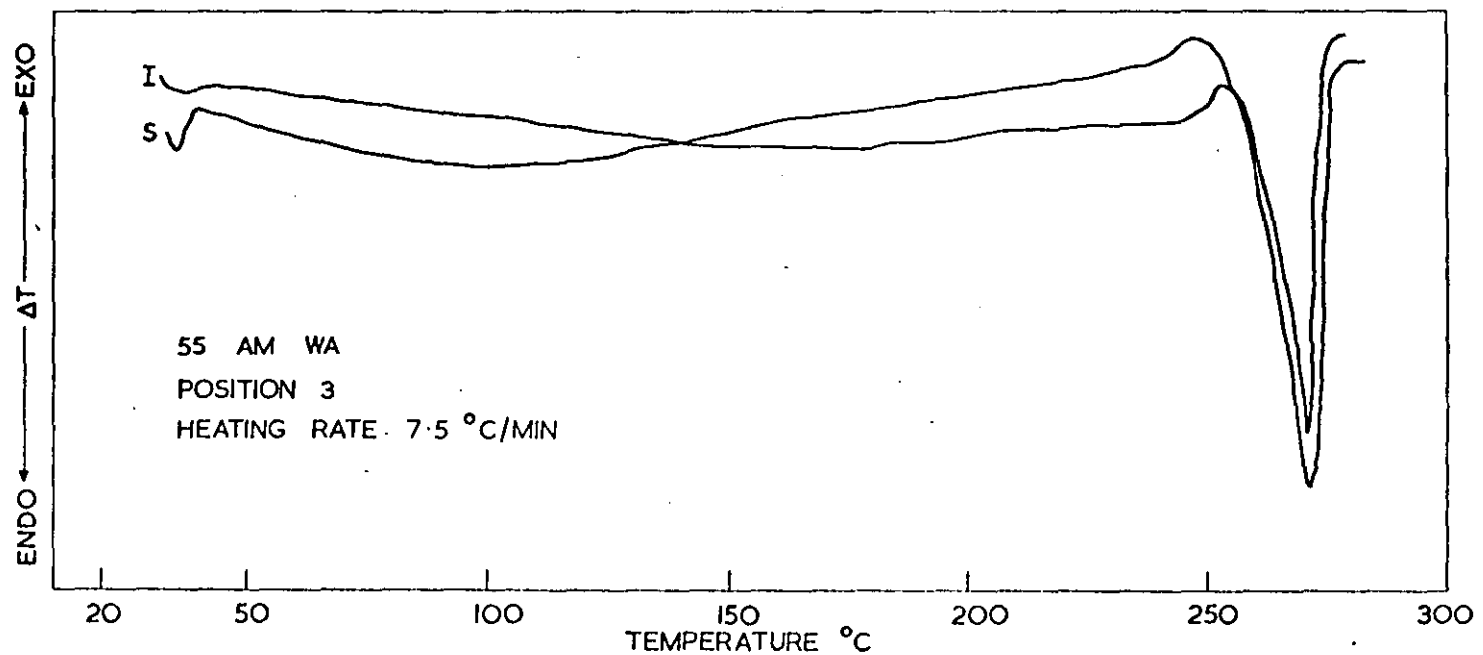


FIG 19b DSC THERMOGRAM FOR SAMPLE MOULDED AT 55 °C

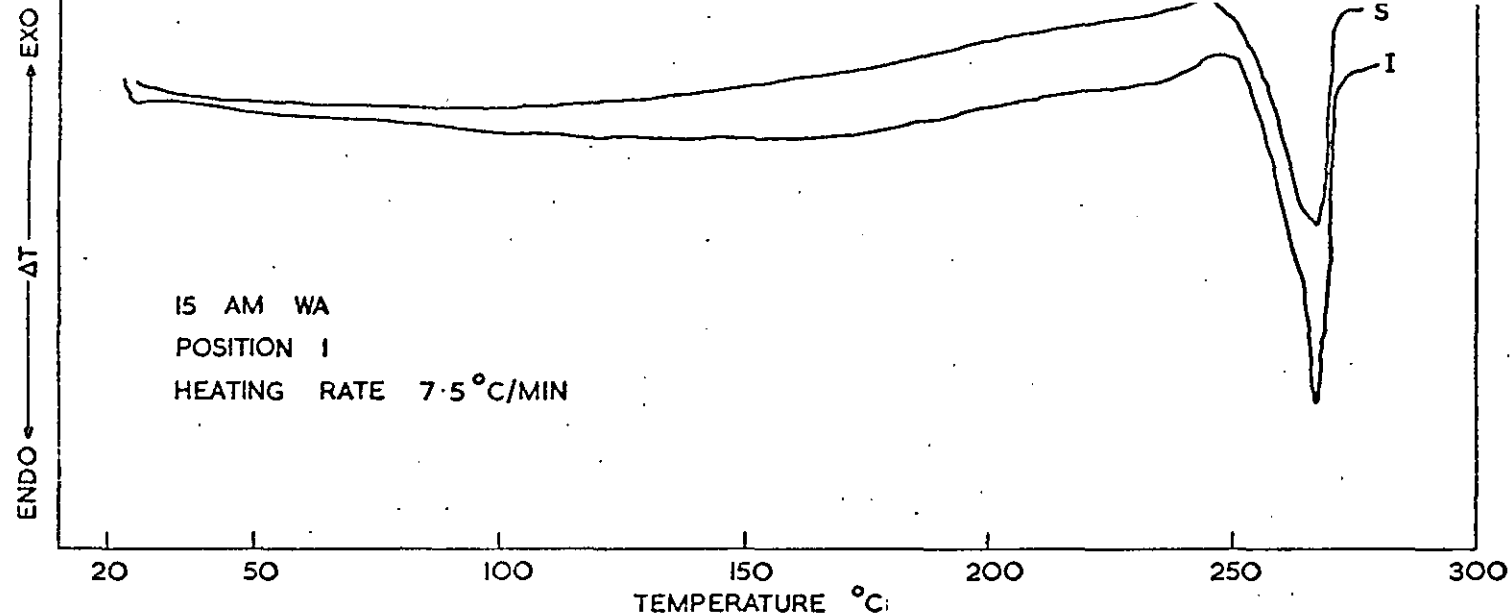


FIG 20a DSC THERMOGRAM FOR SAMPLE MOULDED AT 15 °C

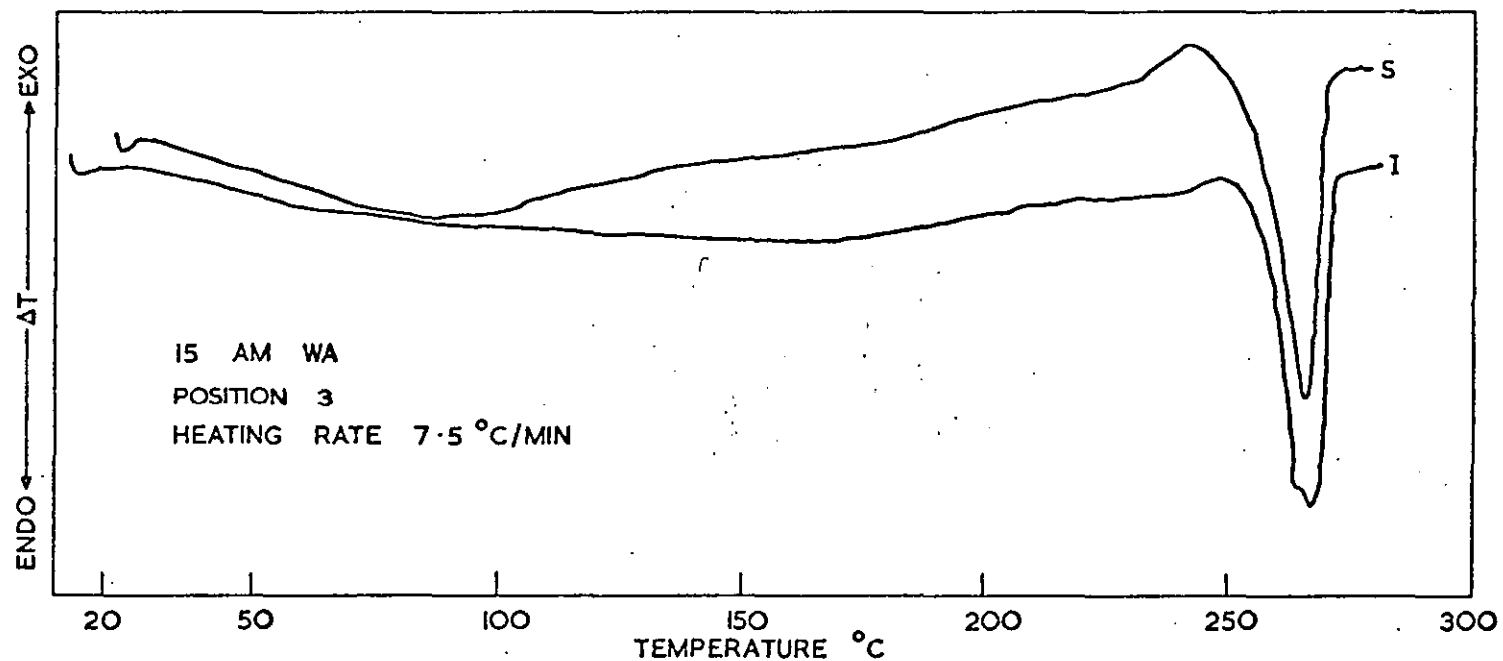


FIG 20b DSC THERMOGRAM FOR SAMPLE MOULDED AT 15 °C

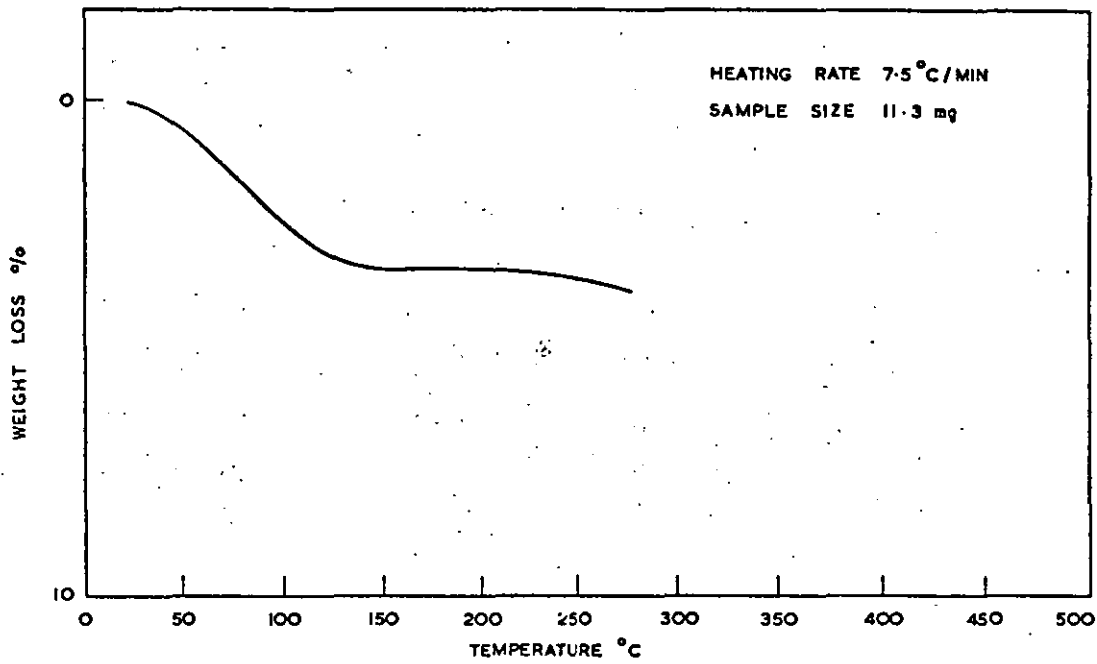


FIG. 21. TYPICAL TGA THERMOGRAM SHOWING WATER LOSS.

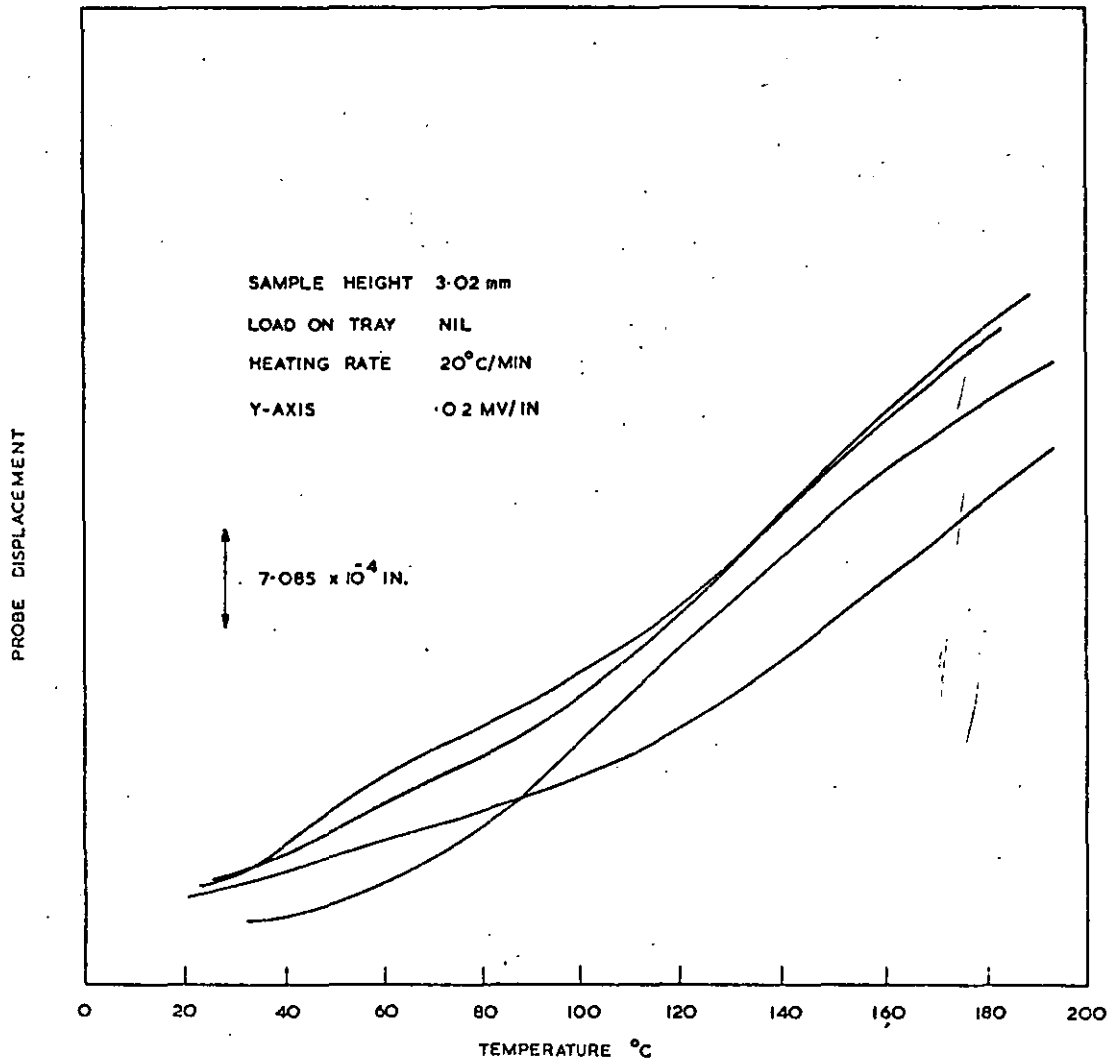


FIG. 22. TMA EXPANSION THERMOGRAM WATER ABSORPTION
SAMPLE MOULD TEMPERATURE 95°C

4.2.5 Differential Scanning Calorimetry (DSC)

From the thermograms (Figs. 17, 18, 19, 20) it can be seen that samples taken from the surface start melting at a lower temperature than those taken from the interior and also have a lower melting point (peak temperature).

The broadness of the melting peak is greater for surface samples than for interior samples probably due to imperfect crystals. There appears to be little if any difference between samples taken from the same position in mouldings obtained at different mould temperatures.

4.2.6 Thermogravimetric analysis (TGA)

Fig. 21 shows a typical TGA trace for nylon 66. This technique was used to obtain the water content of various samples. Table 16 shows the water content of various samples which have been subjected to accelerated weathering. Some unusual results are obtained in that the water content inside the samples was larger than on the outside. Water content was also determined on various wear specimens after testing.

TABLE 16. WATER CONTENT FOR ACCELERATED TENSILE BARS

MOULD TEMPERATURE °C	WATER CONTENT % <i>wgt</i>			
	SURFACE		INTERIOR	
	AS MOULDED	CONDITIONED	AS MOULDED	CONDITIONED
15	2.9	2.8	3.1	2.8
55	3.5	3.3	4.0	2.8
75	3.6	3.4	2.9	3.5
95	3.2	3.1	2.4	2.4

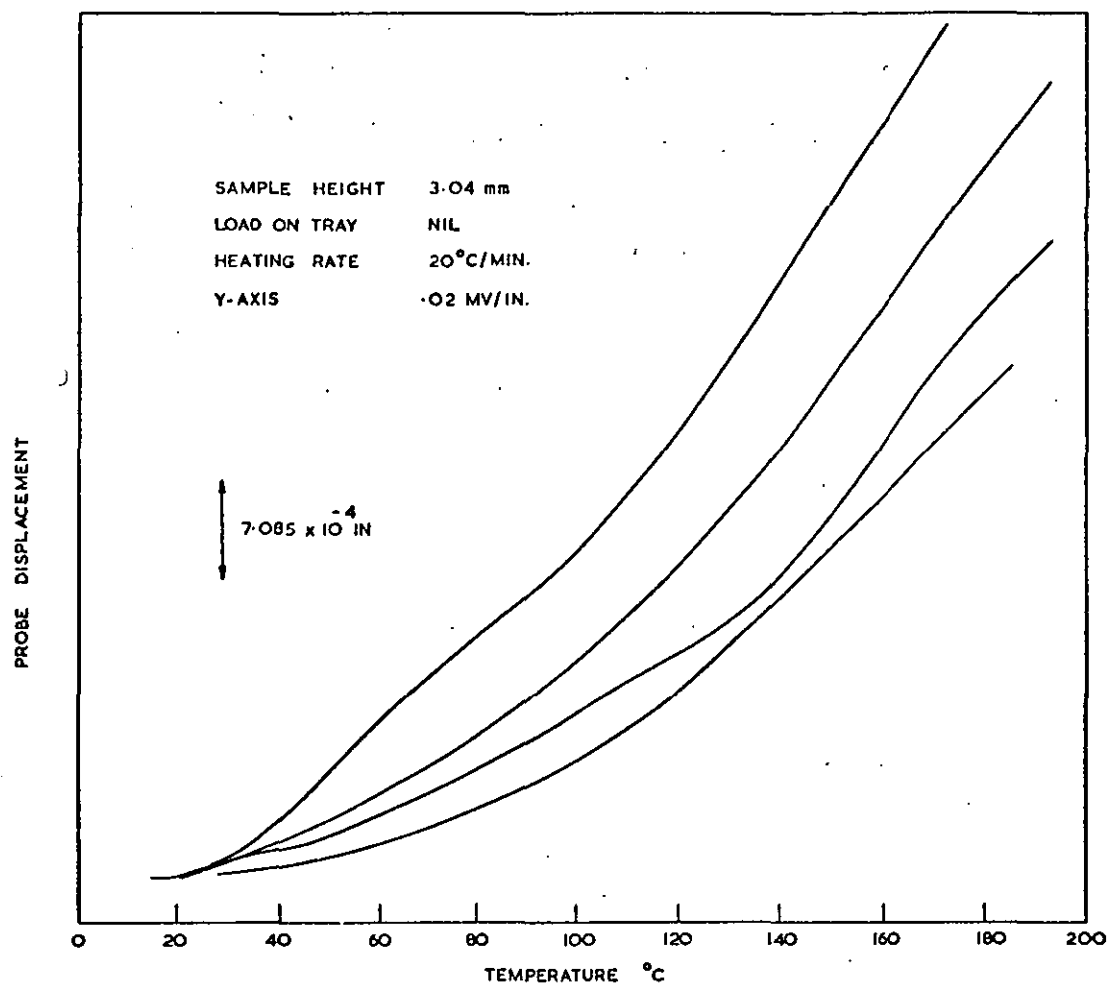


FIG. 23. TMA EXPANSION THERMOGRAM WATER ABSORPTION
 SAMPLE MOULD TEMPERATURE 75°C

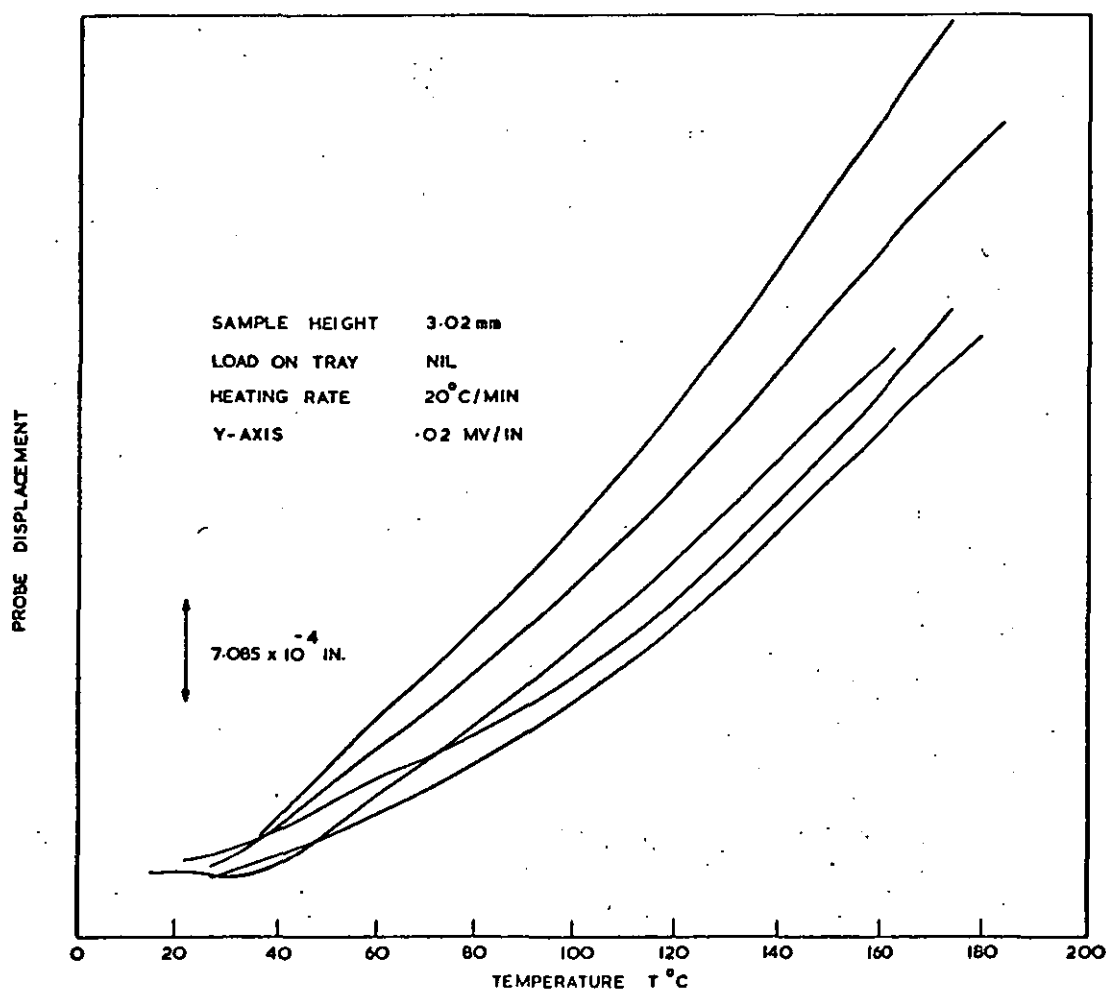


FIG. 24. TMA EXPANSION THERMOGRAM WATER ABSORPTION
 SAMPLE MOULD TEMPERATURE 55°C

FIGS. 25. & 26.

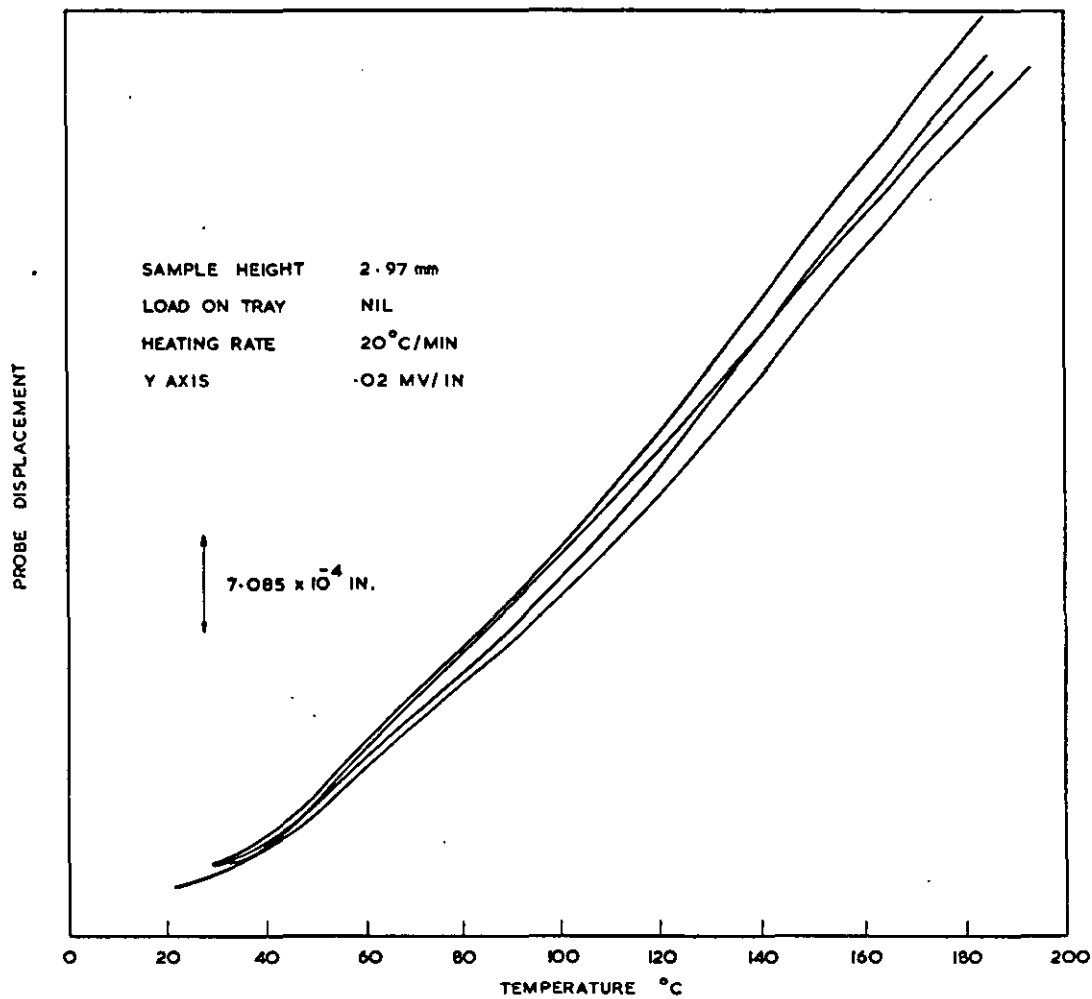


FIG. 25. TMA EXPANSION THERMOGRAM WATER ABSORPTION SAMPLE
MOULD TEMPERATURE 15°C.

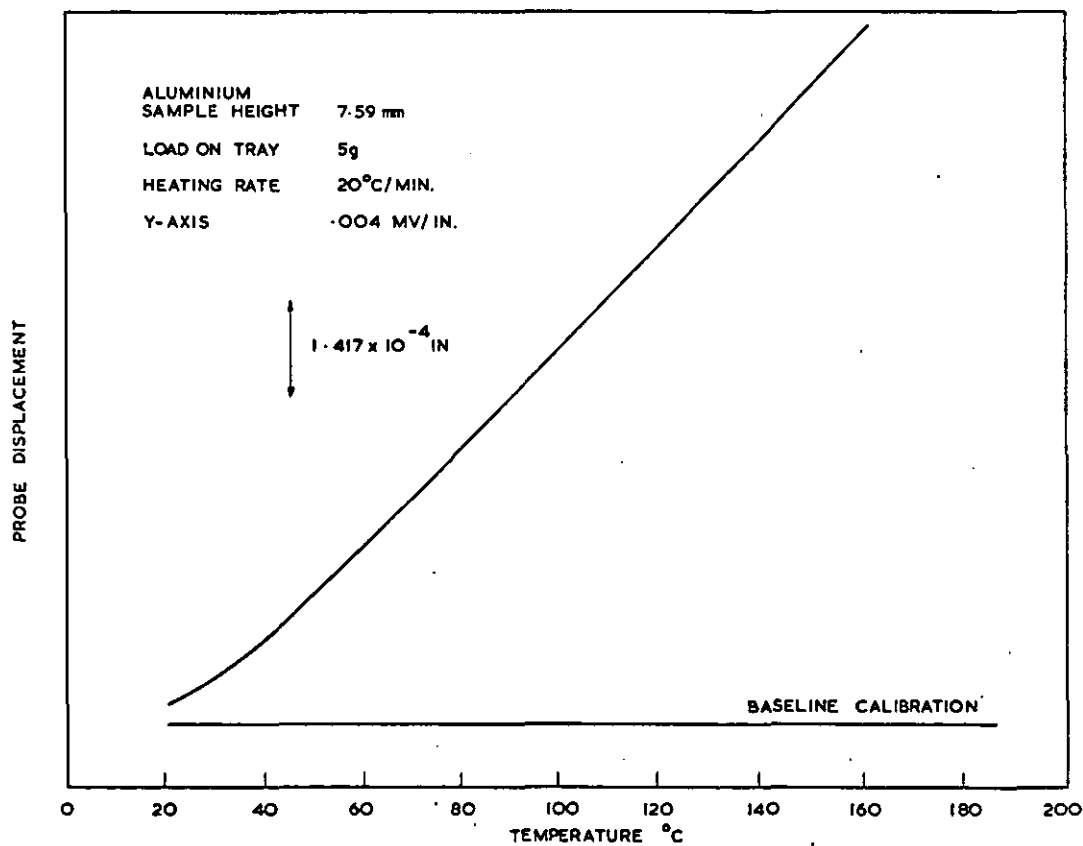


FIG. 26. TMA EXPANSION THERMOGRAM FOR STANDARD ALUMINIUM CYLINDER.

4.2.7 Thermal Mechanical Analysis (TMA)

Both penetration and expansion probes were used. TMA has been used to determine thermal transitions in polymers, e.g. neoprene, using the penetration probe while coefficients of linear expansion can be obtained using the expansion probe.

With the penetration probe variable results were obtained for samples moulded at any one temperature. Various heating rates and different weights were tried. More consistent results were obtained using the expansion probe. Figs 22, 23, 24, 25 show determinations for four different mould temperatures. The instrument was first calibrated using a standard aluminium cylinder. Since the sensitivity is independent of temperature, it is only necessary to determine the expansion profile over a temperature range sufficient to calculate the slope at a temperature where the expansion coefficient of aluminium is reported. The aluminium expansion profile used is shown in Fig. 26. Before the run the height of the aluminium cylinder was measured to the nearest thousandth of an inch. The slope of the recorded expansion was determined in units of inches of chart paper/ $^{\circ}\text{C}$. The sensitivity was obtained using the following formula :

$$S = \frac{\alpha_T h}{\text{Slope}_T}$$

S = sensitivity of instrument for a given Y-axis scale setting, mils defection/in. of chart paper.

α_T = linear expansion coefficient at temperature T ($^{\circ}\text{C}$) $^{-1}$

Slope_T = slope of metal expansion profile at temperature T inch of chart paper/ $^{\circ}\text{C}$.

h = height of sample (mils).

For aluminium at +77°C using a Y axis setting of 0.004 mils/inch.

$$S = \frac{24.1 \times 10 \times 299 \text{ mils/inch}}{5.08 \times 10}$$

$$= 0.1417 \text{ mils/inch}$$

Since the nylon 66 scans were made at a sensitivity of .02 mv/inch it is necessary to multiply 0.1417 by $\frac{.02}{.004}$

Sensitivity (at .02 mv/inch) = Sensitivity (at 0.004 mv/inch) x 5

$$= .7085 \text{ mils/inch of chart paper.}$$

For nylon 66

$$\alpha_T = \frac{.7085 \times \text{slope}_T (^{\circ}\text{C})}{h}$$

Using the above formula the values shown in Table 17 were obtained for samples moulded at different mould temperatures. As can be seen lower coefficients of expansion are obtained for higher mould temperatures.

TABLE 17. COEFFICIENT OF APPARENT LINEAR EXPANSION FOR
DIFFERENT MOULD TEMPERATURES

MOULD TEMPERATURE °C	COEFFICIENT OF APPARENT LINEAR EXPANSION $\times 10^5$	
	AT 100°C	AT 140°C
15	31.3	41.6
55	26.1	35.8
75	23.4	37.3
95	19.7	27.4


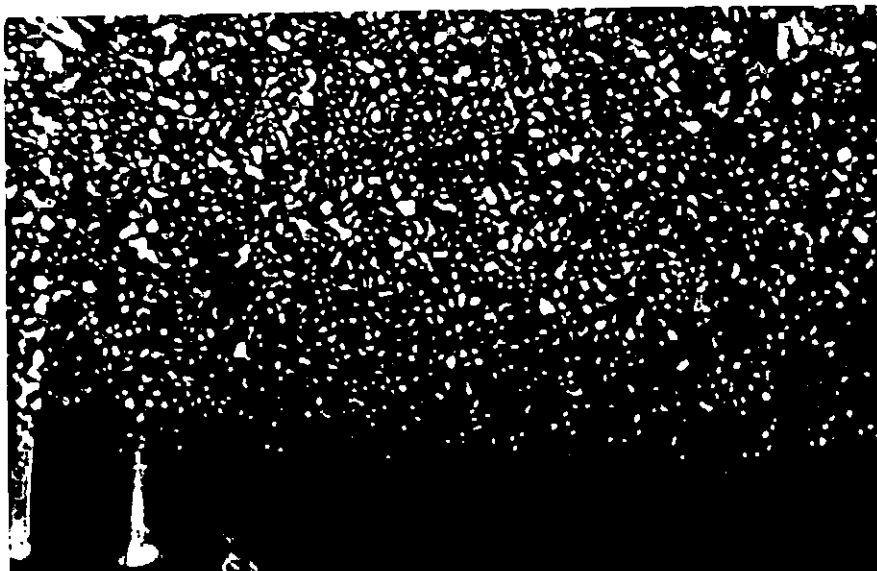
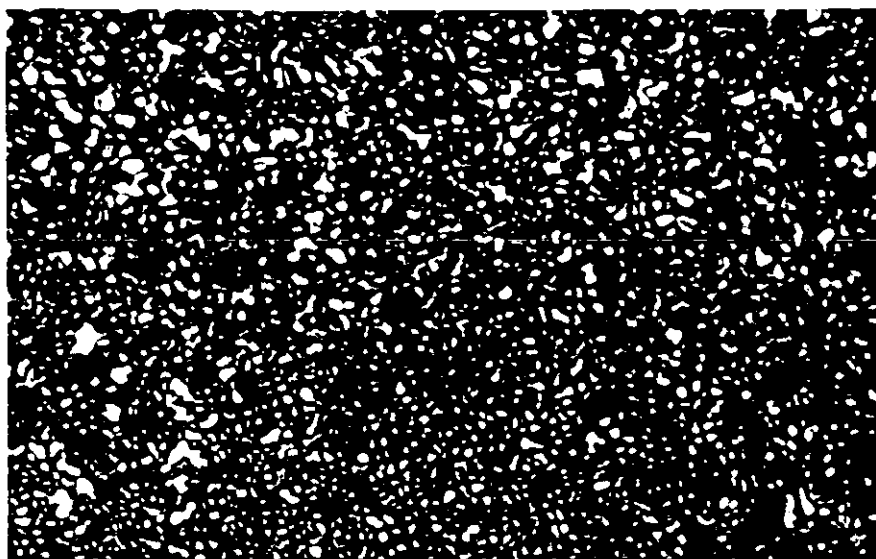
 Fig. 27 Optical Micrograph showing surface skin of a tensile sample obtained at a mould temperature of 55°C

Fig. 28 Spherulitic structure further into the sample than shown in Fig. 27

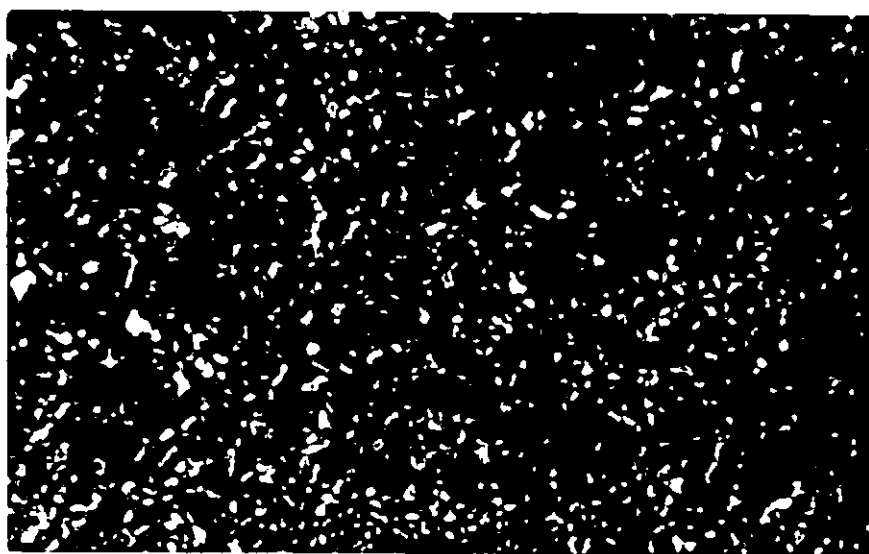
Fig. 29 Disturbed crystalline structure near centre of moulding



25 μ m



25 μ m



25 μ m



D7310/ 317/ 17

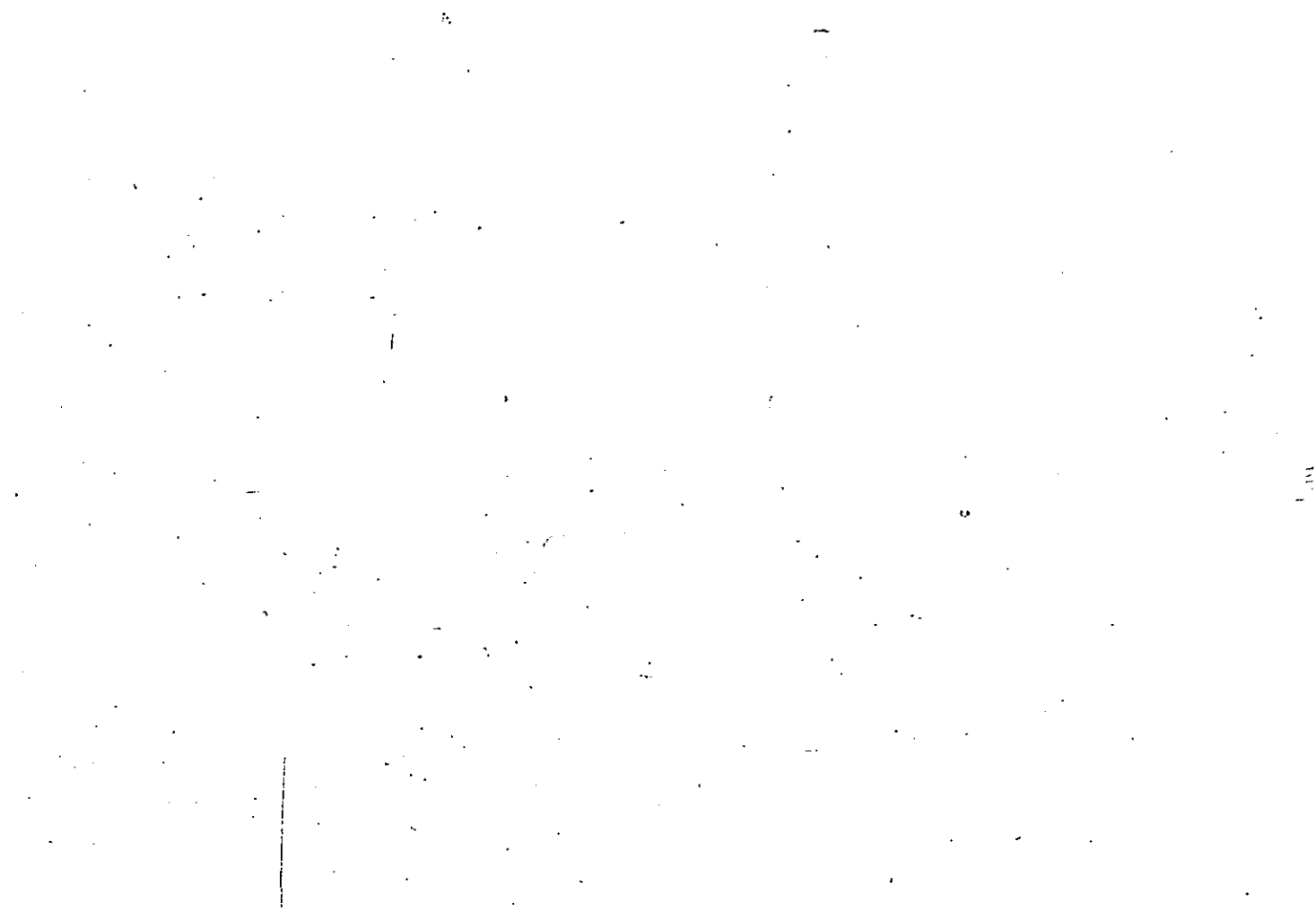
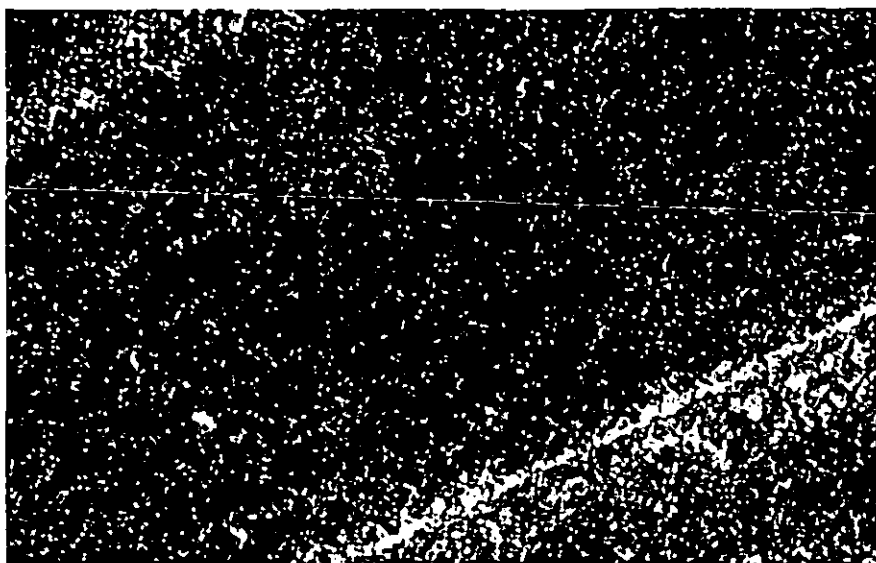


Fig. 30 Section cut parallel to the surface of a sample obtained at a mould temperature of 55°C.



25 μm

4.3 MICROSCOPY

4.3.1 Optical Microscopy

The majority of microscopy work undertaken in this project was optical using polarised light. In all, over 800 micrographs were taken, hence only a few will be shown to illustrate trends. The gating system used for the tensile and flexural samples was such as to cause the melt flow to impinge on the opposite cavity wall before filling the cavity.

With the impact and water absorption discs the gates were positioned so that the flow was directly across the cavity. The depth of the gate was the same as that of the cavity. Through a moulding the structure varies, the surface of the moulding being influenced by the temperature of the cavity wall. As we progress through the moulding the temperature of the mould has less influence, the temperature of the melt governing the structure. This is a consequence of the poor heat conduction of polymers.

Another factor appears to be flow within the cavity causing in certain instances definite crystalline (spherulite) bands.

Sections cut perpendicular to the face of the mouldings show at first a non-crystalline structure passing into a spherulitic structure. However, this spherulitic structure can then change into a malformed or disturbed crystalline structure before becoming spherulitic again. This is shown in Figs. 27, 28, 29. Fig. 30 shows a section cut parallel to the surface of the moulding. The following sketch illustrates the structure through the moulding.

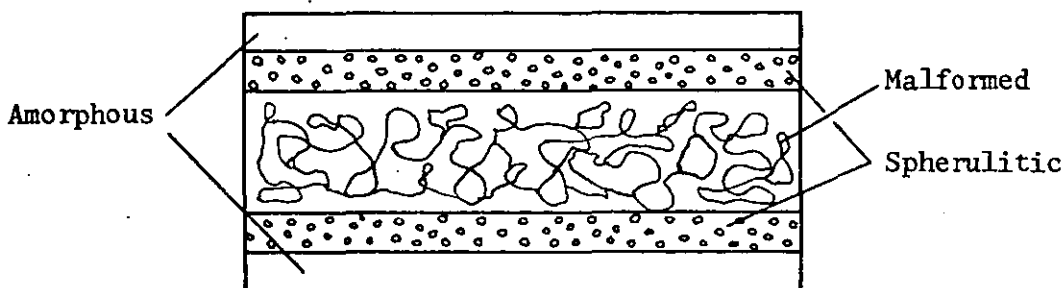


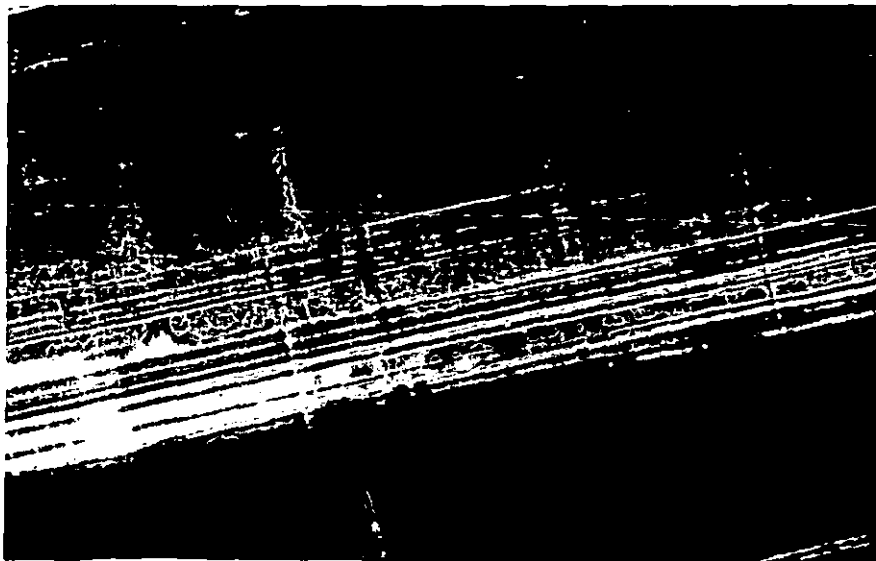
Fig. 31. Banded spherulitic structure of impact sample in position 1
obtained at 75°C.

Fig. 32. Structure further into moulding than shown in Fig. 31.

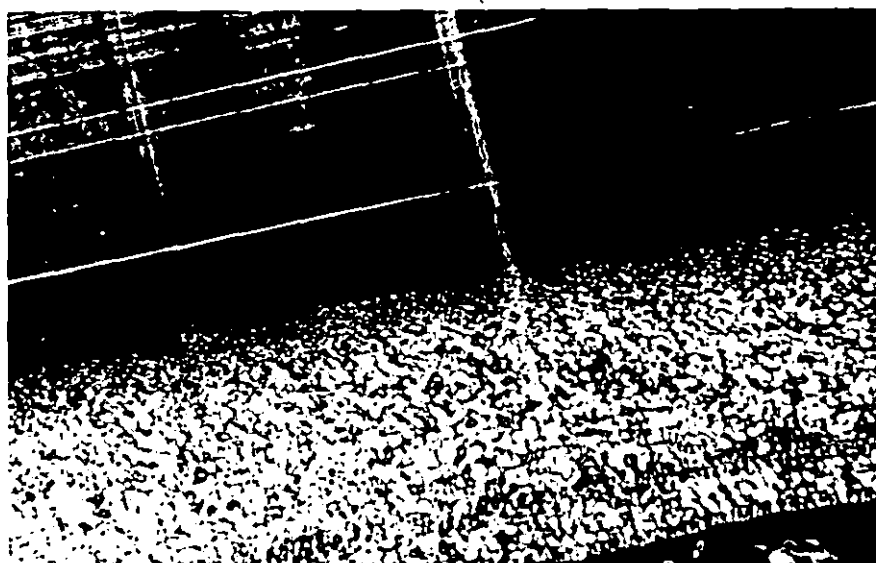
Fig. 33. Spherulitic banded structure near other surface of
sample



50μm



50μm



50μm

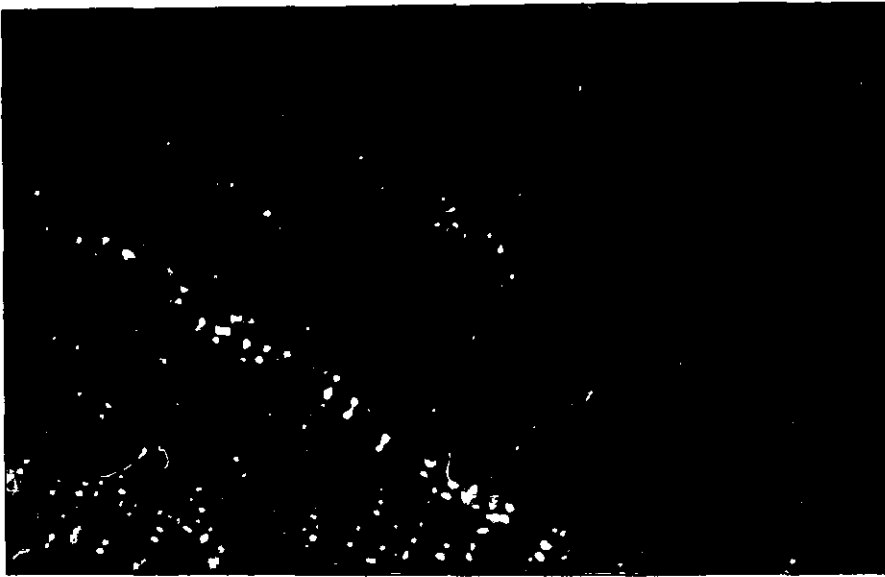


D7310/ 317/ 16

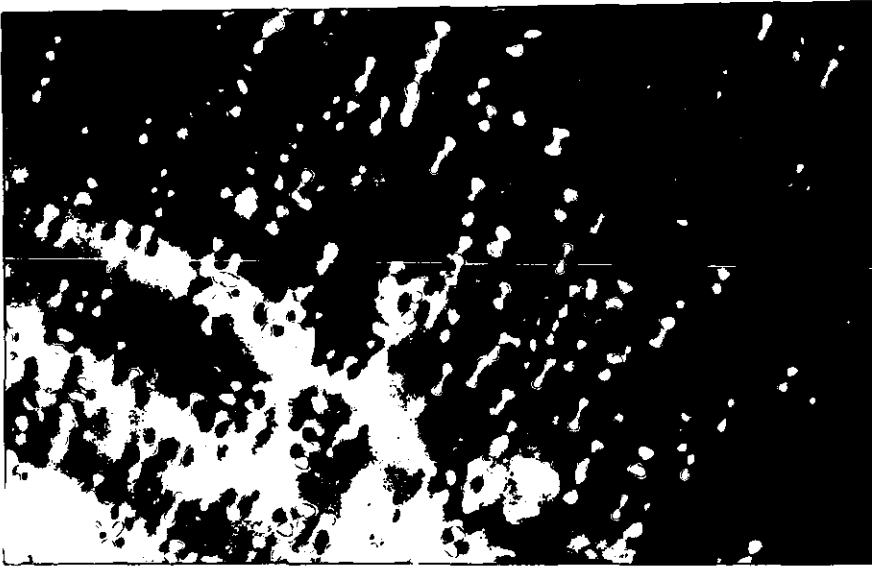
Fig. 34. Structure obtained near the surface of a tensile sample
obtained at 15°C.

Fig. 35. Higher magnification of Fig. 34.

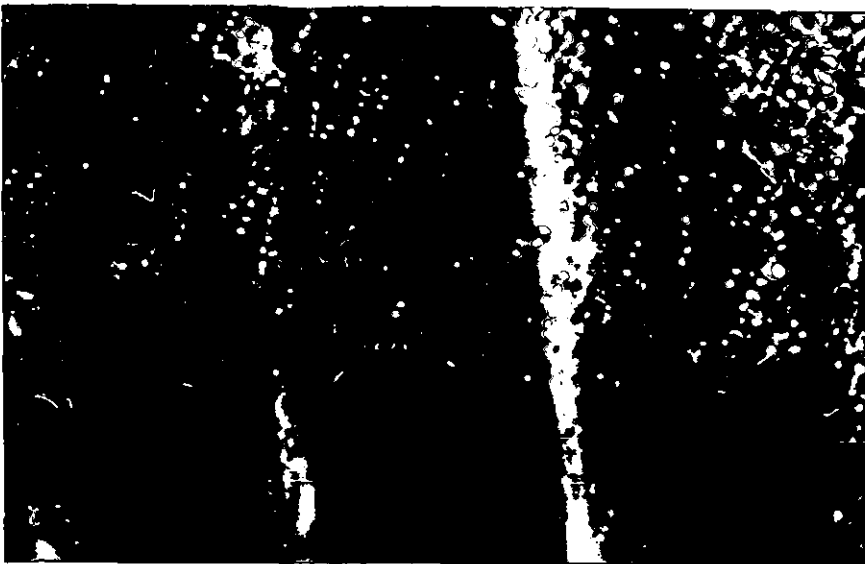
Fig. 36. Structure near surface of a flexural sample obtained at
55°C.



25 μ m



25 μ m



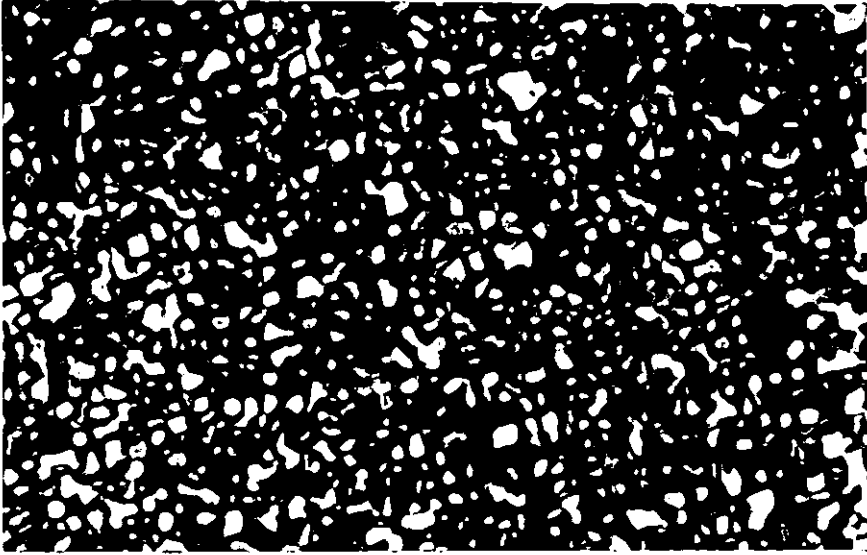
25 μ m



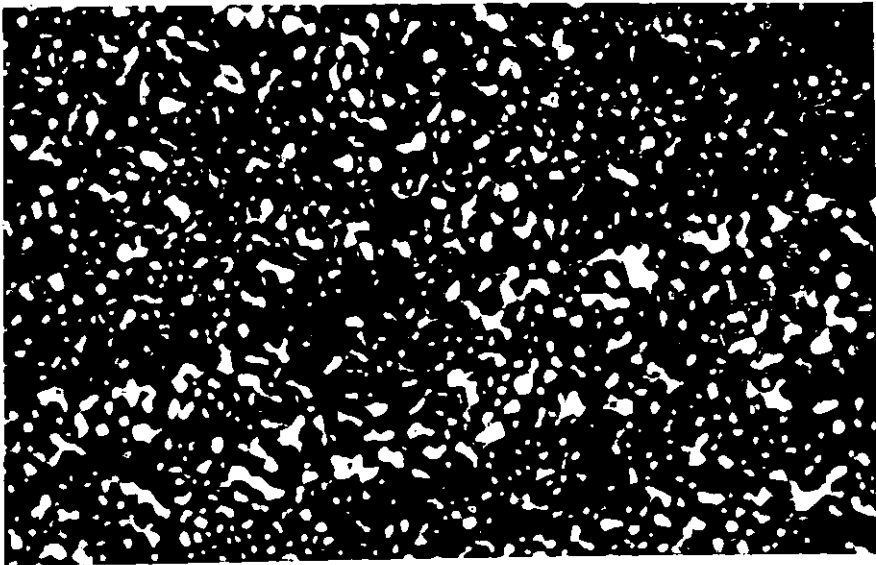
073401 3171 A

Fig. 37. Structure near surface of a flexural sample obtained at 75°C.

Fig. 38. Surface structure of tensile sample, mould temperature 95°C.



25 μm

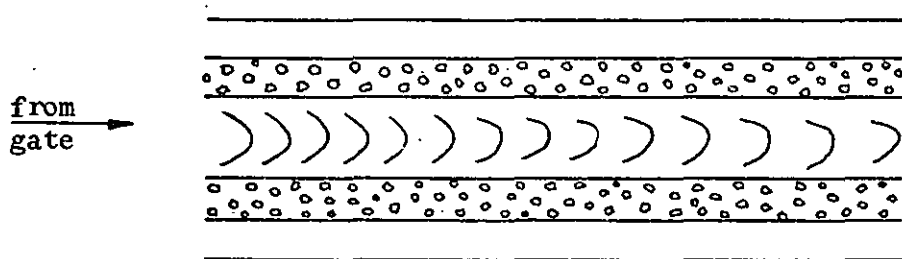


25 μm

D7310/ 317/ 15

Position from the gate

Whereas samples taken from Position 1 and 2 on tensile and flexural samples (see Fig. 11) showed little structural difference if any; water absorption and impact disc specimens showed definite changes in structure in positions 1, 2 and 3. Definite band structure was obtained as shown in Figs 31, 32, 33. This banded spherulite structure is still present in position 2 but not to such a large extent as in position 1. In position 3 very unusual structure is shown, spherulites being present in very thin bands and being much smaller than those in position 1 and 2.

Position 1

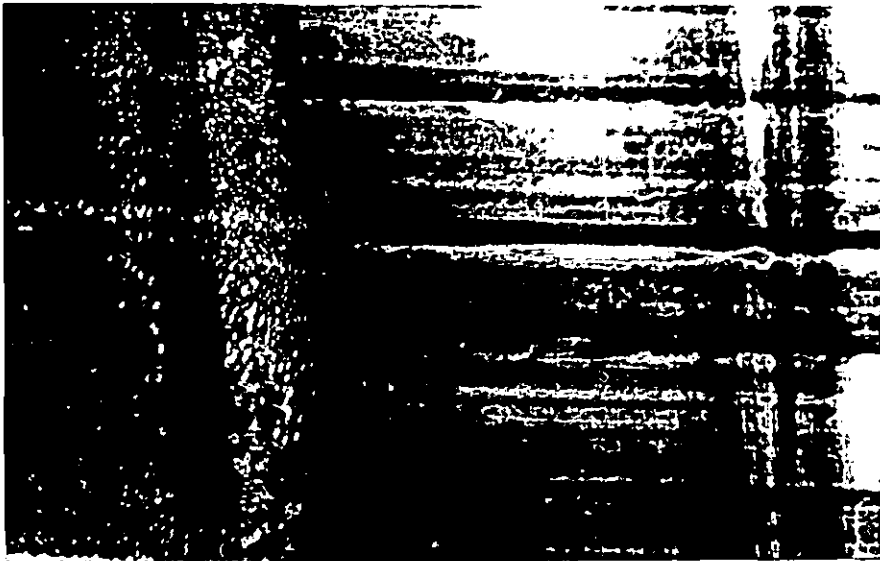
This illustrates the effect the position of the gate has on mouldings when one considers that the gate size for the tensile and flexural bars is the same as for the water absorption discs.

There appears to be little difference in the structure as shown by optical microscopy through mouldings obtained at different mould temperatures for tensile and flexural samples except near the surface of the mouldings where the structure obtained at 15°C and in some cases at 55°C is different for that obtained at mould temperatures of 75 and 95°C. This is shown in Figs. 34, 35, 36 when compared with Figs. 37, 38. However for impact and water absorption samples the spherulite structure is not as pronounced at 15°C as at other mould temperatures. The spherulite diameter being a maximum of $\approx 7\mu\text{m}$ compared to $\approx 22\mu\text{m}$.

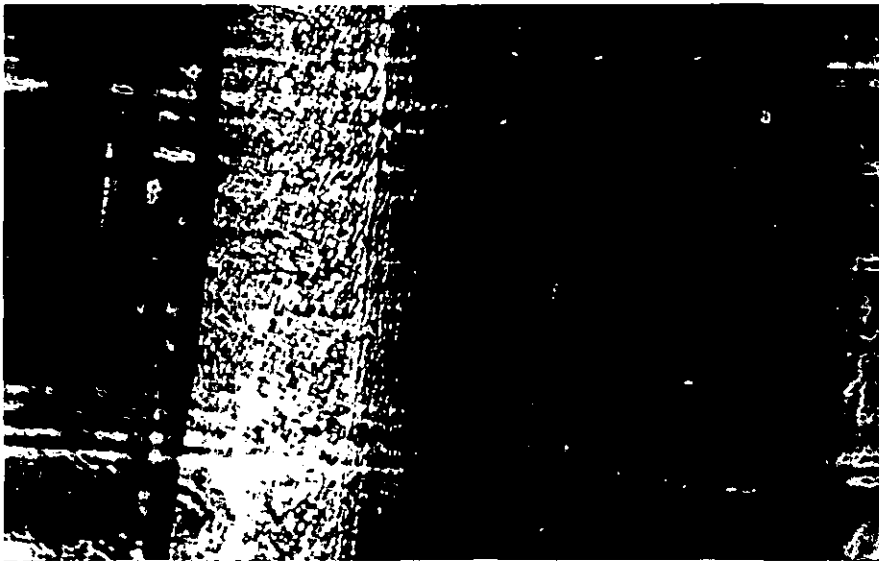
Fig. 39. As moulded impact sample, position 1, mould temperature
15°C.

Fig. 40. As Fig. 39 but sample conditioned.

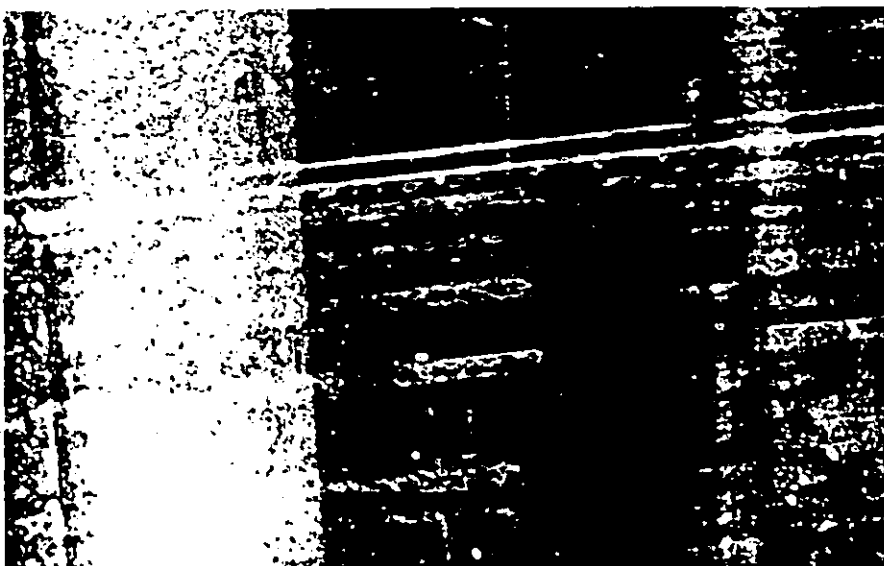
Fig. 41. As sample in Fig. 39 but after accelerated weathering.



25 μ m



25 μ m



25 μ m



DECEMBER 31 1971 5

It appears that both conditioning and accelerated weathering cause no change in structure as observed by optical microscopy. This is shown by comparing Figs. 39, 40, 41.

Examination of micrographs showing sections cut from weathered samples of tensile and flexural samples gave depth of cracks (caused by weathering) ranging from 15 - 140 μ m. It was found to be quite difficult to measure crack depths from micrographs so the depth of cracks were measured directly under the microscope using an eyepiece graticle. The table below shows some values obtained :-

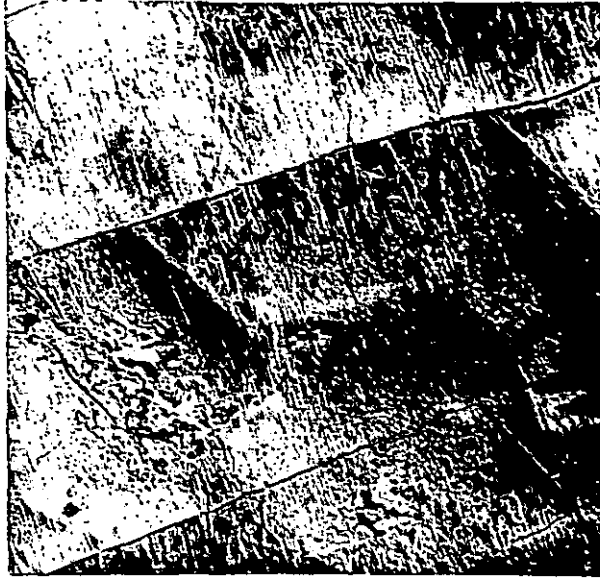
MOULD TEMPERATURE °C	POSITION	AVERAGE DEPTH OF CRACK IN MICRONS	RANGE OF DEPTH OF CRACKS IN MICRONS
15	1 Flexural	33	24 - 65
	2 Flexural	56	17 - 86
55	1 Tensile	19	9 - 45
75	1 Tensile	39	12 - 60
95	1 Flexural	19	5 - 167
	1 Tensile	20	5 - 155

4.3.2 Transmission Electron Microscopy

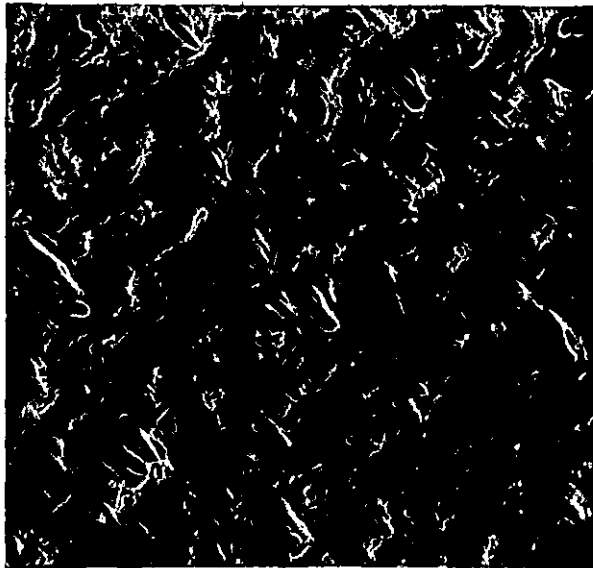
After obtaining many optical micrographs from various moulded samples it was decided to use transmission electron microscopy to examine the surface structure of mouldings in greater detail. Examination of the as moulded surface showed no structure, therefore various etchants were tried with the idea that these would remove any low molecular weight material and preferentially attack the non-crystalline regions leaving the crystalline regions for examination. Of the various etchants tried m-cresol/methanol

Fig. 42. Replica of sample etched with 80/20 V/V m-cresol/
methanol.

Fig. 43. Replica of sample etched with 30/70 W/W m-cresol/
methanol.



10 μm



5000 \AA

D7310/ 317/ 1

Fig. 44. Replica of cut and etched sample showing fibrillar structure.

Fig. 45. Replica of cut and etched sample showing tie fibrils

Fig. 46. Lower magnification of Fig. 45.



1 μm



2000 Å



1 μm

D7310/ 317/ 14

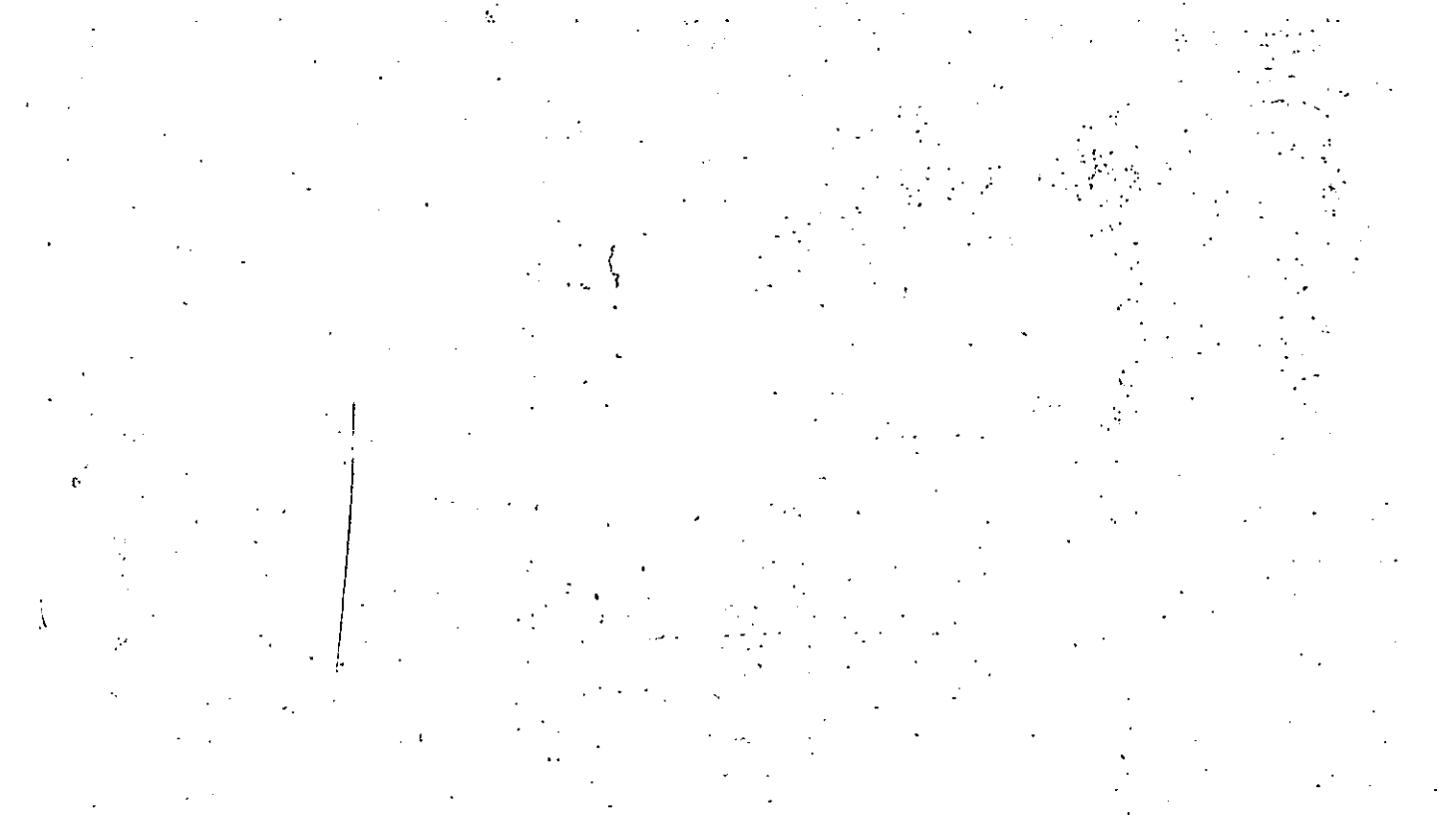


Fig. 47. Fibrillar type structure on cut and etched sample.

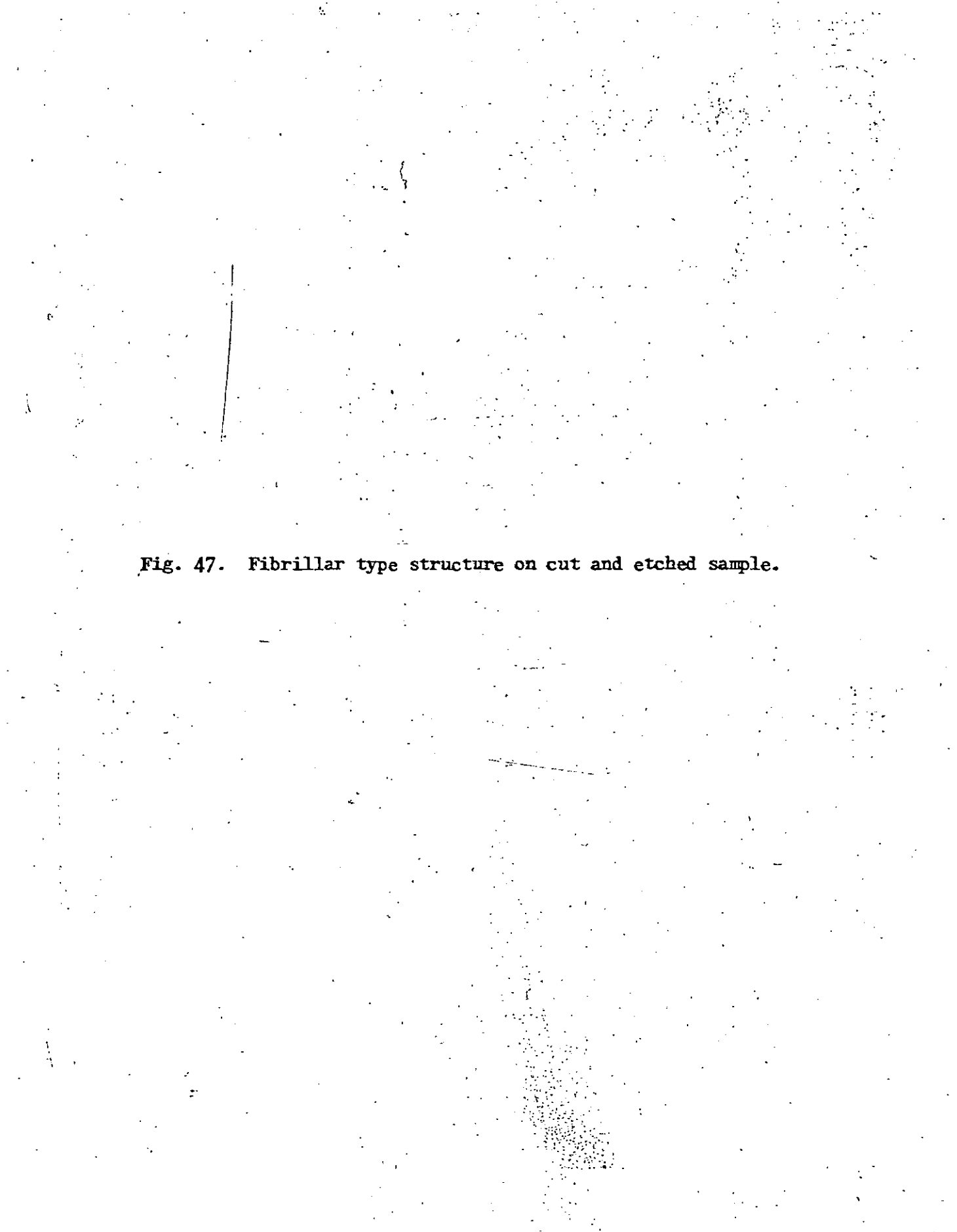


Fig. 48. Lamellae type appearance sample again cut and etched with m-cresol/methanol.



1 μ m



1 μ m

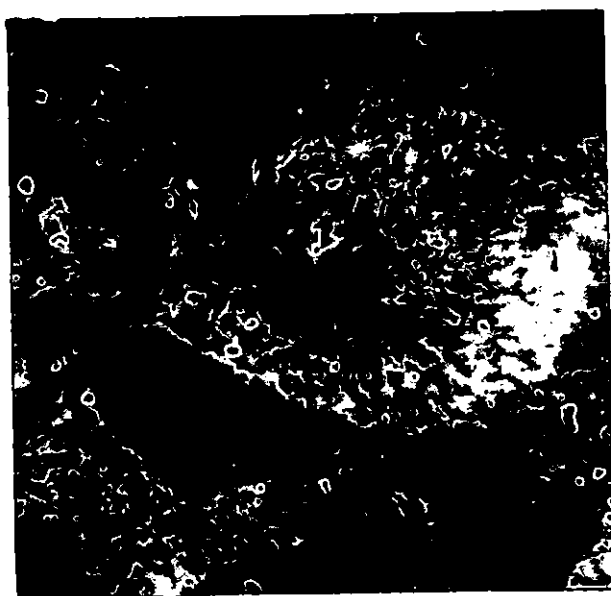
D7310/ 317/ 8

Fig. 49. Spherulites obtained on thin sectioning and staining with phosphotungstic acid.

Fig. 50. Spherulites obtained in thin sections stained with phosphotungstic acid.



10 μm



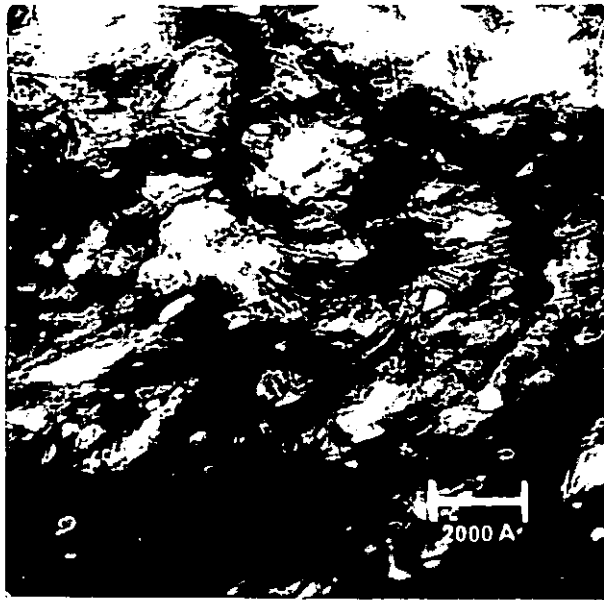
2 μm

D7310/ 317/ 10

Fig. 51. Stained section showing fibrillar structure

Fig. 52. Banded structure obtained on stained section.

Fig. 53. Higher magnification of Fig. 52.



D7310/ 317/ 12

mixtures were the most successful, 20% calcium chloride in methanol was too severe while glacial acetic acid, 10% orthophosphoric acid, and 10% formic acid (v/v) did not effect the nylon. The technique used by Khoury²⁹ was tried but difficulties were encountered, on washing the etched sample reprecipitation of the dissolved polymer occurred. Fig. 42 shows a replica obtained by etching with 80/20 v/v m-cresol/methanol for 5 minutes, rinsing with methanol and then etched for one minute with 80/20 v/v m-cresol/methanol before finally rinsing with methanol. This etching gave a poly-hedral structure but further attempts to reproduce this structure failed. Fig. 43 shows the structure obtained using 30/70 w/w m cresol/methanol mixture. This appears to show a twisting fibrillar structure. Etching on cut surfaces using the procedure as for Fig. 42 gave micrographs as shown in Figs. 44, 45, 46 showing a fibrillar type structure and also tie fibrils.

Figs 47, 48, show fibrillar type structures. Towards the end of the project an ultramicrotome became available and hence ultrathin sections were prepared and examined directly under the electron microscope after staining with phosphotungstic acid vapours. This technique gave some encouraging results as is shown in Figs. 49 and 50. Various structures were obtained :-

Fig. 51 shows fibrillar structure (lamellae)

Fig. 52 shows banded structure

Fig. 53 shows a higher magnification of Fig. 52 but tends to lose definition.

Unfortunately time did not allow for this technique to be fully exploited.

4.3.3 Scanning Electron Microscopy (SEM)

In the early stages of the project the scanning electron microscope was used to examine surfaces of nylon obtained by fracturing at liquid nitrogen temperatures. Fibrillar structure was shown to be present as is shown in

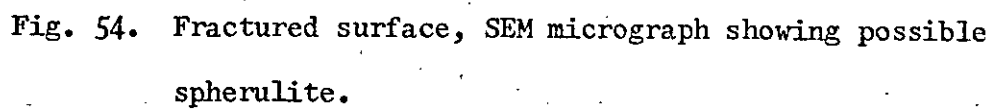
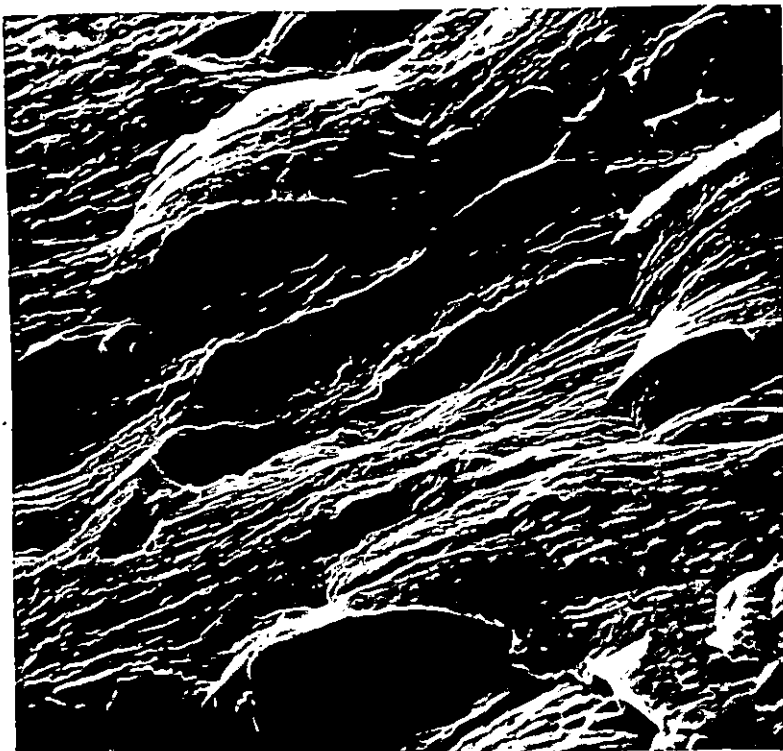
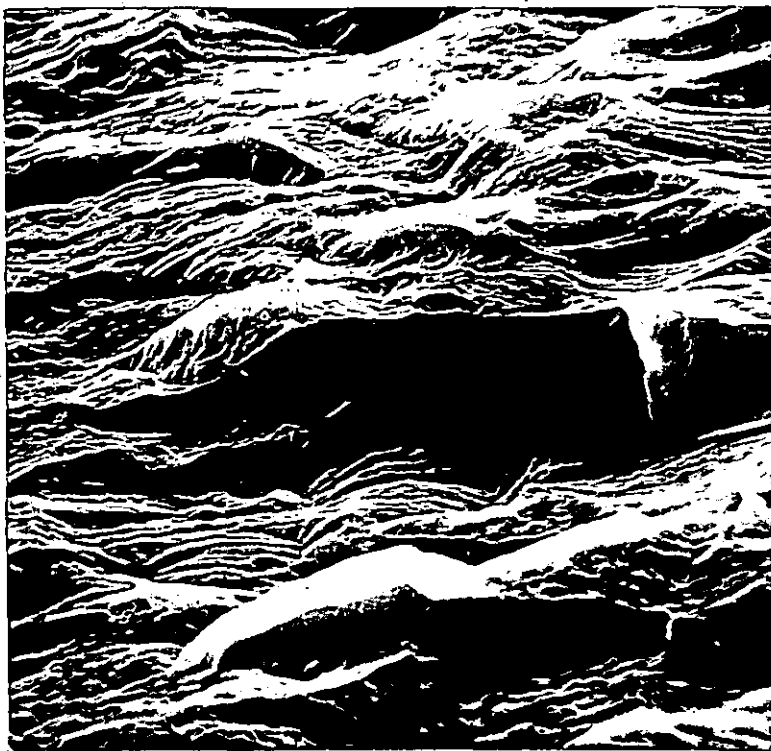
The image is a scanning electron micrograph (SEM) showing a fractured surface. The surface is characterized by a rough, irregular texture with various sized particles and features. A prominent, somewhat circular or spherulitic structure is visible, which is the focus of the caption. The overall appearance is that of a microscopic view of a material's fracture process.

Fig. 54. Fractured surface, SEM micrograph showing possible spherulite.

Fig. 55. Similar to Fig. 54.



10 μ m

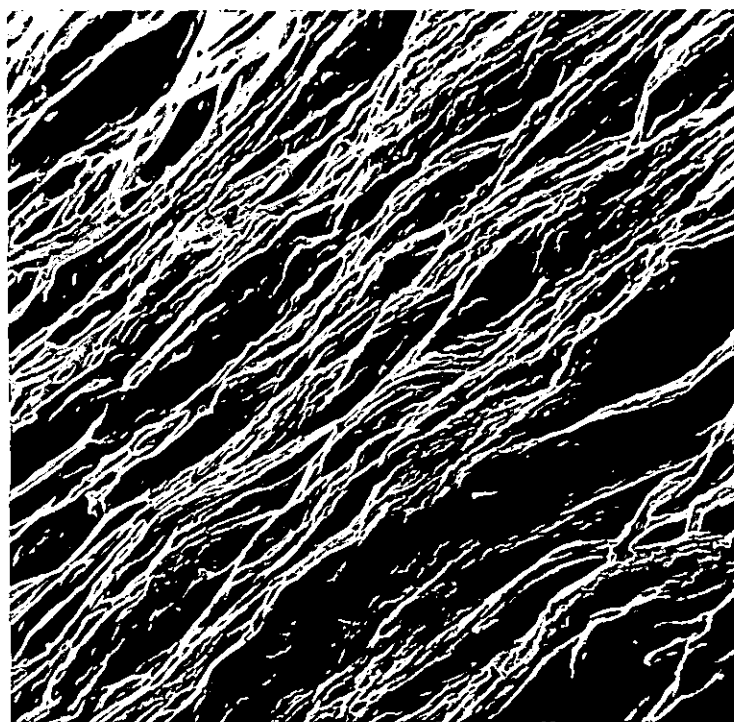


10 μ m

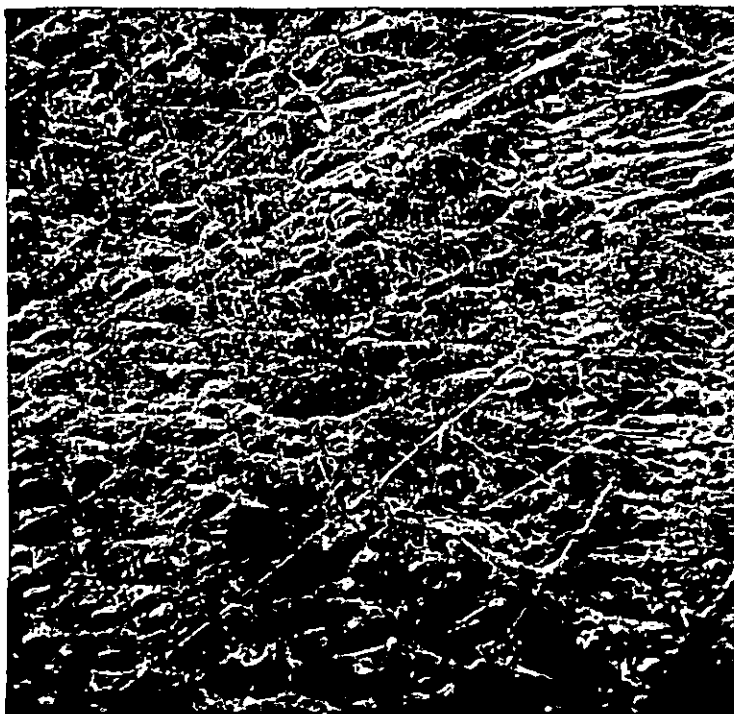
D731 0/ 3 17/ 9

Fig. 56. Fractured surface showing fibrillar structure.

Fig. 57. Paratoluene sulphonic acid etched sample showing "mole hills", SEM micrograph.



10 μm

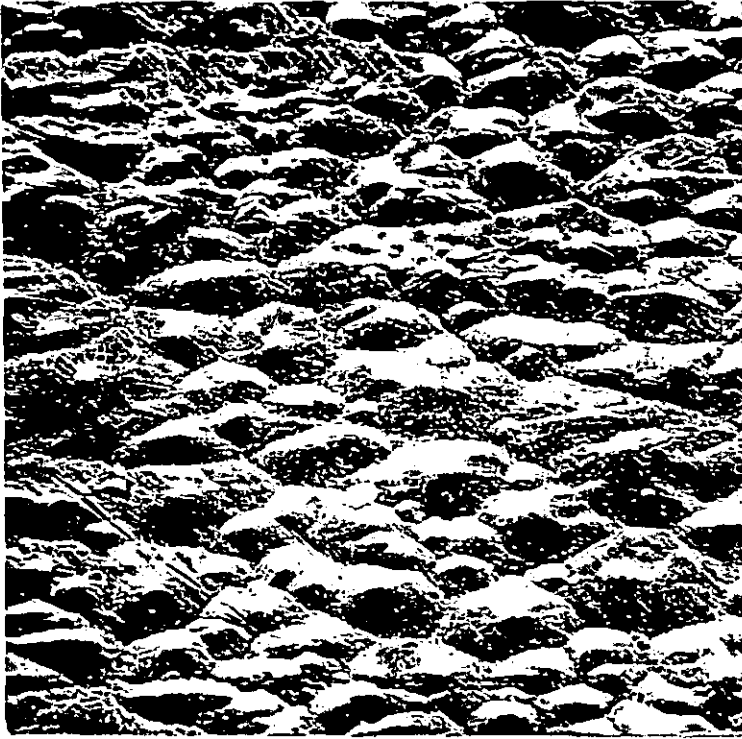


10 μm

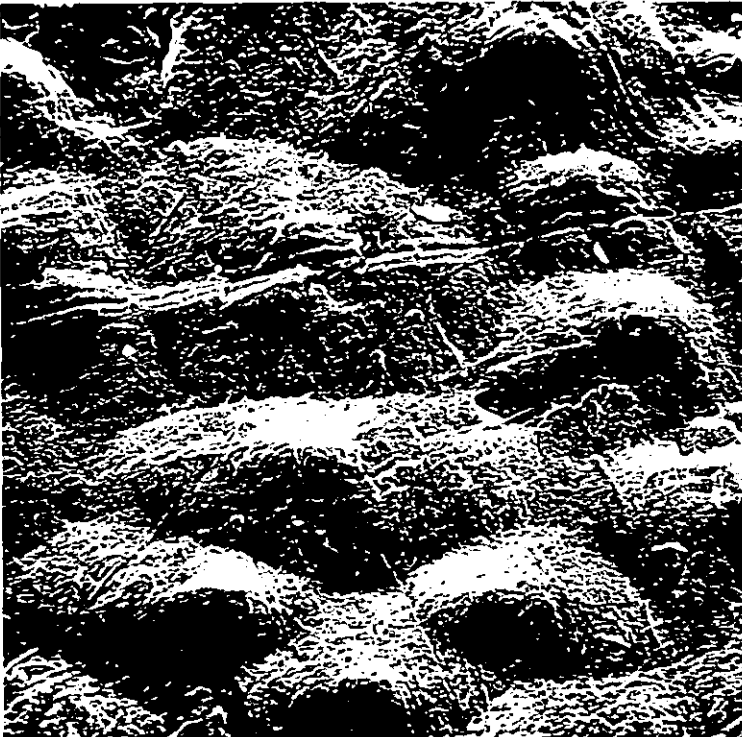
D731 0/ 317/ 3

Fig. 58. Paratoluene sulphonic acid etched sample

Fig. 59. Higher magnification of Fig. 58.



50 μ m



10 μ m



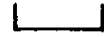
D731 0/ 317/ 6

Fig. 60. Crack patterns for weathered impact sample obtained at 55°C, position 1.

Fig. 61. Similar to Fig. 60 but in position 2.



250 μm



500 μm



D7310/ 317/ 1

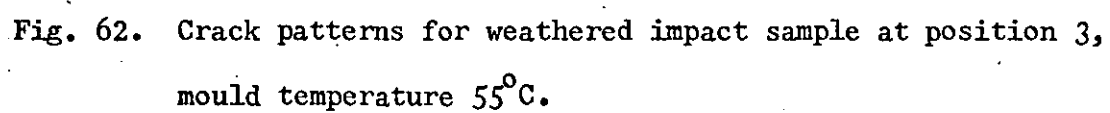
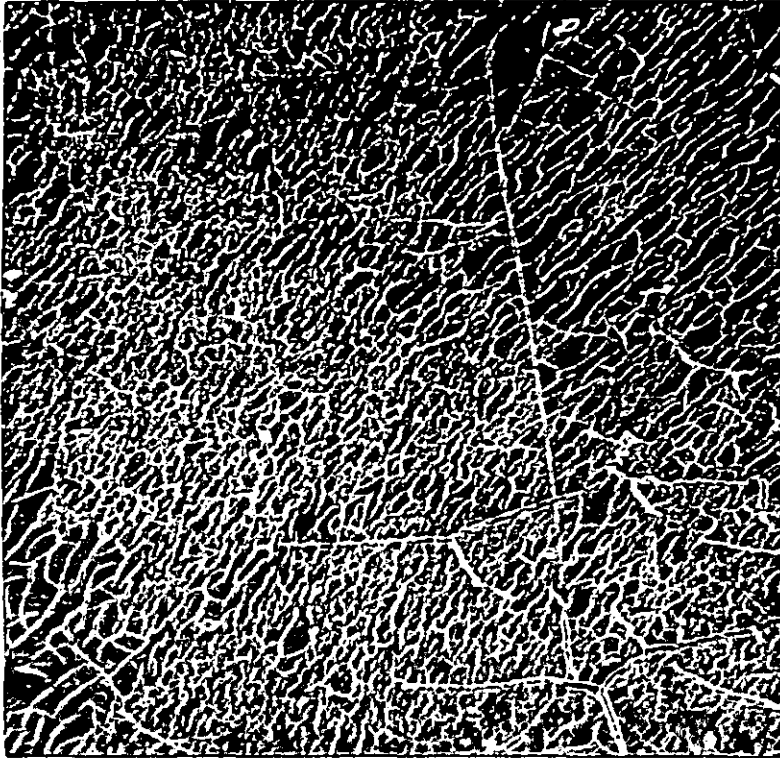
The image area above the caption is mostly blank with some faint, scattered noise or artifacts, likely from the scanning process. There is no visible crack pattern or sample image.

Fig. 62. Crack patterns for weathered impact sample at position 3,
mould temperature 55°C.



500 μ m

27201 2424

Figs. 54, 55, 56. It was thought however that sufficient information could be obtained from optical microscopy on sections cut through the moulding.

Towards the end of the project para-toluene sulphonic acid was tried as an etchant and the surfaces were examined by SEM. A very unusual structure was observed as shown in Figs. 57, 58, 59. These structures which are like "mole hills" have sizes ranging from 25 - 70 μ m which are in excess of the diameters recorded for spherulite diameters as observed by optical microscopy. Grubb¹³¹ has suggested that these are the result of beam damage and are in fact artifacts.

Scanning electron microscopy was used to examine the surface of weathered impact specimens. The actual crack pattern was observed at various positions with reference to the gate and also the inside of the crack walls were examined.

The cracks patterns were seen to vary with position from the gate as can be seen in Figs. 60, 61, 62 which show the patterns obtained for samples moulded at 55°C.

Examination of the crack walls revealed in most instances a fibrillar structure. The structure obtained in cracks of samples obtained at a mould temperature of 95°C appears to have a coarser structure than the cracks obtained at other mould temperatures, the layers of platelets being more parallel to the moulding surface than other samples where the structure tends to be perpendicular to the moulded surface. The tendency appears to be of a change from a fine to a coarse structure as the mould temperature increases and also the direction of the fibrillar structure changes from parallel to the crack walls to perpendicular to crack walls as the mould temperature is increased.

Crack widths as well as distance between cracks were measured from micrographs. These results are tabulated in Tables 18 and 19.

TABLE 18DISTANCE BETWEEN CRACKS PRODUCED ON MOULDED SURFACES BY ACCELERATED WEATHERING

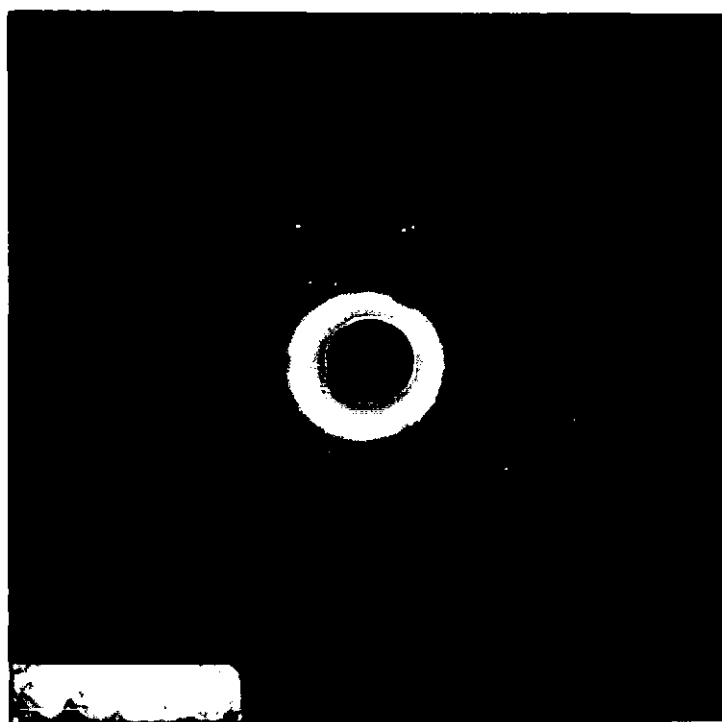
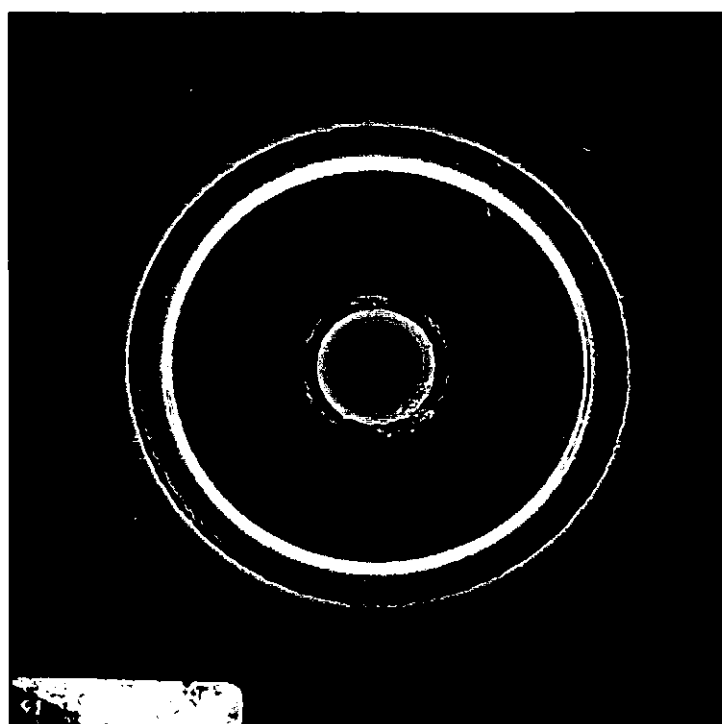
MOULD TEMPERATURE °C	POSITION MOULDING	DISTANCE BETWEEN WIDER CRACKS IN MICRONS	DISTANCE BETWEEN SMALLER CRACKS IN MICRONS
15	1	107 - 161	27 - 98
15	2	90 - 160	
15	3	120	36 - 109
55	1	135 - 250	10 - 38
55	2	185 - 352	18.5 - 56
55	3	Few wide cracks	18.5 - 56
75	1	109 - 273	27 - 73
75	2	127 - 309	18 - 64
75	3	127 - 345	18 - 45
95	1	115 - 154	19 - 58
95	2	135 - 288	19 - 67
95	3	135 - 385	10 - 29

TABLE 19. CRACK WIDTHS PRODUCED ON MOULDED SURFACES BY ACCELERATED WEATHERING

MOULD TEMPERATURE °C	POSITION IN MOULDING	CRACK WIDTH IN MICRONS
15	1	3.6
15	3	4.3
55	1	3.1
55	2	3.3
55	3	1.5
75	1	0.7
75	2	6.5
75	3	2.1
95	1	3.2
95	2	2.1
95	3	1.5

Fig. 63a. X-ray pattern showing rings due to $110 + 010$, 100 and 002 planes.

Fig. 63b. X-ray pattern only showing rings due to $110 + 010$ and 100 planes.



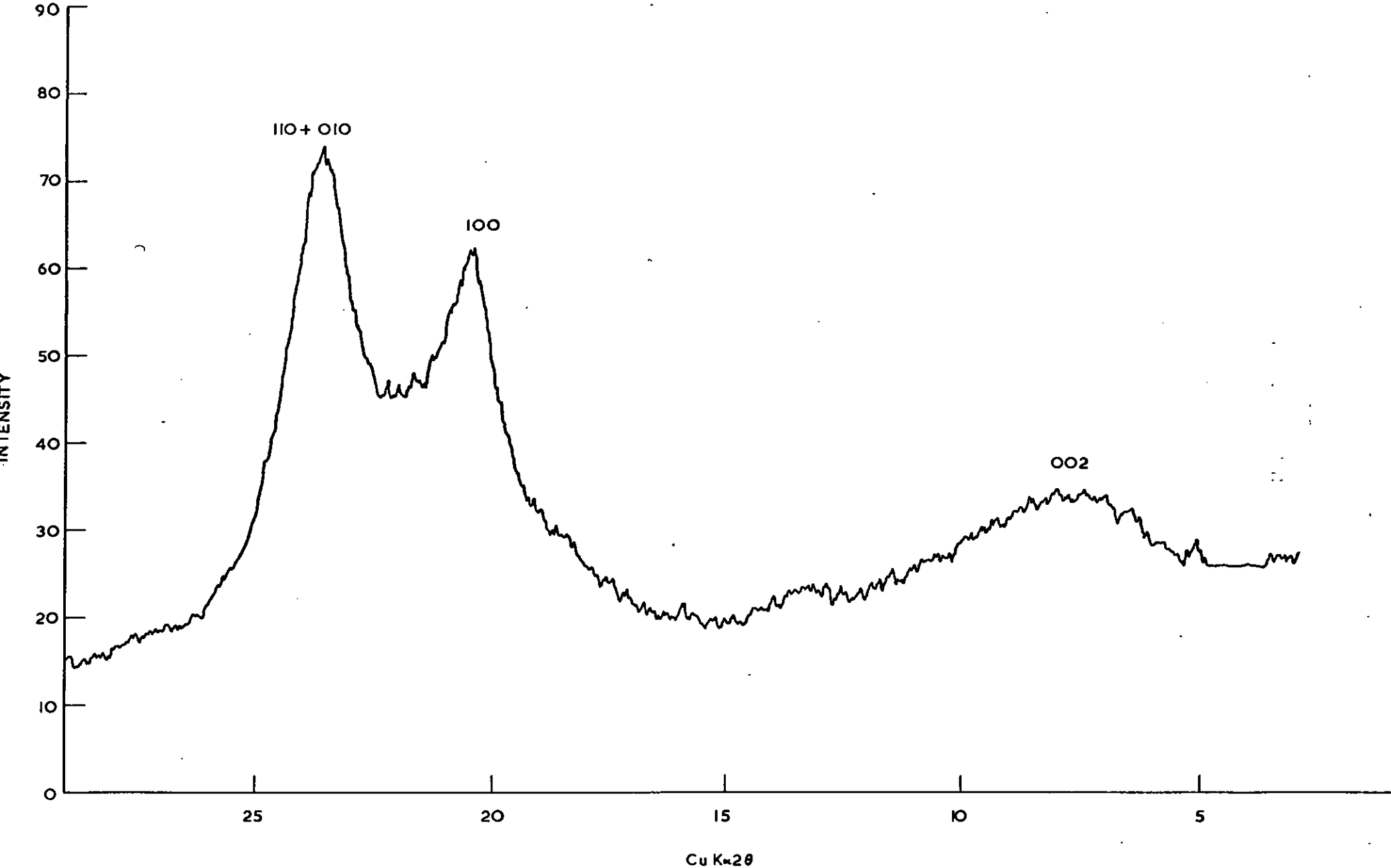


FIG. 64.

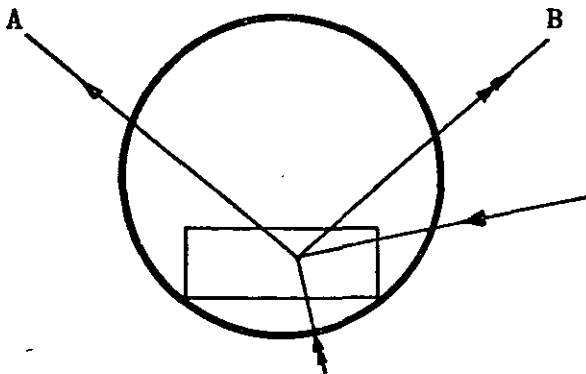
FIG. 64. DIFFRACTOMETER TRACE FOR A SAMPLE OBTAINED
AT A MOULD TEMPERATURE OF 75°C

4.4 X-RAY DIFFRACTION

X-ray diffraction was carried out on samples cut from water absorption discs as shown in Fig. 4. The samples were taken near to the gate.

Initially diffraction patterns were obtained with the X-ray beam passing through the sample perpendicular to the mould surface.

Very little preferred orientation was shown from these diffraction patterns as can be seen in Fig. 63a. The four rings starting from the outside are due to the 110 plus 010, the 100, the 002 and the 001 planes respectively. Fig. 63b shows just the two outer rings, Fig. 63a being over developed to show reflections due to the 001 and 002 planes. Diffractometer curves show differences in samples turned through 90° . For samples moulded at a mould temperature of 15°C the 110 plus 010, and 100 reflections in the diffractometer traces are of similar intensity. For samples moulded at 55°C stronger intensities are obtained in the A direction while samples moulded at 75°C and 95°C give stronger intensities in the B direction.



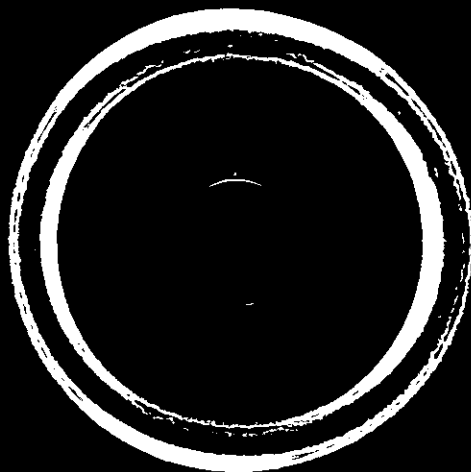
A diffractometer trace for a sample obtained at a mould temperature of 75°C is shown in Fig. 64.

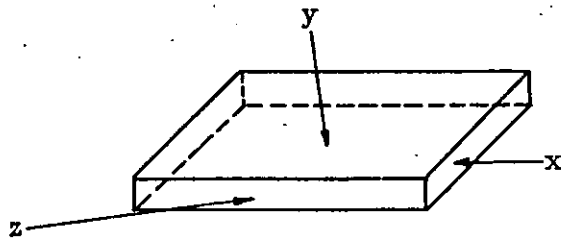
Later in the programme of work further X-ray diffraction patterns were obtained by passing the X-ray beam in the three directions shown
overleaf:-

Fig. 65. X-ray pattern obtained in x direction (see Page 90) for sample obtained at 15°C.

Fig. 66. X-ray pattern for sample obtained at 95°C, in x direction

Nº 5 Red face





The exposure times were reduced to one hour and the double film technique was not used. The z direction is parallel to the gate direction. The preferred orientation of the 002 plane with the beam in the x direction is shown in Fig. 65. This is for a sample obtained at a mould temperature of 15°C .

No preferred orientation of the 002 plane was shown for samples obtained at other mould temperatures as shown by comparing Fig. 65 with Fig. 66, the latter being for a sample obtained at a mould temperature of 95°C .

CHAPTER 5 DISCUSSION OF PRACTICAL WORK AND EXPERIMENTAL RESULTS

5.1 TENSILE YIELD STRENGTH, FLEXURAL MODULUS AND IMPACT PROPERTIES

With nylon 66 one must always remember that water is present in the polymer and this plays an important part in the properties obtained and also complicates interpretation of results. Considering the "as moulded" state then the water content of nylon 66 is fairly low $\approx 0.04\%$, whereas the normal equilibrium value is $\approx 2.4\%$.

The tensile yield values obtained in this study increase for "as-moulded" samples as the mould temperature increases, the greatest difference being between samples obtained at mould temperatures of 15 and 55°C, there after the value only increasing slightly. One assumes that higher mould temperatures cool the nylon slower than low mould temperatures leading to mouldings of higher crystallinity which have a greater resistance to yielding since more H-bonds and Van der Waal forces have to be overcome.

Density figures on "as moulded" samples give corresponding crystallinity figures of 32.3, 34, 33.5 and 34.4% for samples obtained at 15, 55, 75 and 95°C respectively. (This is using the amorphous and crystalline densities given by Bunn and Garner¹⁰⁹). The conditioned samples give much lower tensile strengths as one would expect due to the uptake of moisture. The water could be considered as acting as a plasticiser and thus enabling the chains to slide past each other. The general trend is for the higher mould temperature to again give the highest tensile strength due to the samples obtained at these temperatures having a higher crystallinity and probably a lower water content. Starkweather et al²⁶ obtained a crystallinity difference of 4 to 5% for "as moulded" samples obtained at mould temperatures of 50 and 100°C. This difference dropped to about 2% after.

the samples had been conditioned at 75°C and 53% RH for two weeks. In their work spherulites ranging 30 to 50 μ m in diameter were obtained in the interior of 0.125" thick test bars. The size of these spherulites is far in excess of those obtained in our own experiments. Starkweather used a 6 oz Watson/Stillman injection moulding machine in his experiments which could have been a plunger type machine, no nozzle temperature was given but the barrel temperatures were higher than those used in our experiments as was the cylinder pressure (presumably injection pressure). A higher melt temperature should give a slower cooling rate and hence larger spherulites and an increase in density, but no increase in spherulite size was observed with increase in mould temperature in the present study, this is surprising but may be due to the high crystallisation rate of nylon 66. However, an increase in tensile strength with crystallinity was obtained in agreement with the findings of Starkweather et al²⁶.

After accelerated weathering the samples obtained at a mould temperature of 75°C gave brittle failures when tensile tested, no specimens actually gave a tensile yield stress. Including brittle failures, the tensile strength figures at yield were lower for "as moulded" samples than conditioned samples. This is probably due to the conditioned samples being in a "stress-relieved" condition compared with the "as-moulded" samples. Another important result was that the spread in values obtained for samples from any one mould temperature was less for conditioned samples indicating a more consistent product.

Less brittle failures were obtained with conditioned samples after weathering compared with "as moulded" samples.

Flexural modulus figures show "as-moulded" samples obtained at mould temperatures of 15, 55 and 75°C to give similar values only the flexural modulus figure for samples moulded at 95°C showing any significant increase, yet the tensile strength at 55, 75 and 95°C is similar. However, for conditioned samples the trend is a higher flexural modulus for a higher

mould temperature. The conditioned samples show a vast reduction in flexural modulus compared to the "as-moulded" samples, obviously the water content being a major influence. This is important if nylon 66 is used in a humid environment and in fact if a high flexural modulus is required then nylon 66 should not be used.

The accelerated weathered samples bring the "as-moulded" and conditioned values closer together the "as moulded" figures being slightly higher.

The general trend is again for a higher mould temperature to give a higher flexural modulus. The conditioned samples give higher values after weathering than before probably due to the surface of the samples being more crystalline and hence more rigid. The generally held view is that the surface has a more pronounced effect in flexural than in tensile conditions.

The impact results obtained in this study show the good impact properties of nylon 66 compared with other crystalline polymers. For impact specimens the normal thought is that a higher crystallinity (density) gives a lower impact strength. However, for the samples tested this is not the case, the impact strengths for samples moulded at 55 and 95°C being similar and higher than those obtained for samples moulded at 15 and 75°C which are also similar. Density figures as presented in Table 15(b) show the differences between samples moulded at different mould temperatures. The density of samples moulded at 15°C is much lower than densities of samples moulded at other mould temperatures. Conditioned samples give impact figures in the order expected i.e. a higher impact strength for samples moulded at a lower mould temperature but this is probably influenced more by the water content of the samples than the crystallinity. (It probably would be worthwhile to find the impact strength at say -5°C on these samples, because it would be more likely to show up differences).

The water has increased the impact figures above those obtained for the "as moulded" samples. The samples obtained at lower mould temperatures having a lower crystallinity should have a more "open structure" so that water can penetrate the samples more easily and hence give higher impact figures than samples obtained at higher mould temperatures which have a higher crystallinity and a more "packed or closed structure".

After accelerated weathering there is a drastic reduction in impact strength. This is not surprising however when one considers that the surface of the samples contained many cracks after weathering and all these must act as notches. It is often stressed in technical literature on the design of items how important is the absence of sharp corners and notches. Inherent viscosity figures given in Table 13 show the large decrease in molecular weight for the surface of impact samples after accelerated weathering, while Table 15 (e) shows the large density increase of the specimen surface due to secondary crystallisation. These two parameters namely molecular weight reduction and density increase are major factors responsible for the reduction in impact strength after accelerated weathering.

The low figures for samples obtained at 15°C compared with other mould temperatures could be due to high crystallinity of the surface and frozen-in stresses but not reduction in molecular weight since Table 13 shows the inherent viscosity to be similar to that obtained on the skin of samples moulded at 95°C.

Vinogradskaya and Ozolin⁹⁶ believe that the supramolecular structure changes during ageing, they are of the opinion that this change is caused by relaxation of the internal residual stresses and secondary crystallisation. On ageing at room temperature they found that larger spherulites were produced in nylon 66. This does not agree with the findings of the present

study in which the spherulite size did not alter during accelerated weathering. Muller and Pflunger⁹⁷ state that the temperature to which the melt is raised before solidification has no direct influence on the crystallinity of solid polyamide but it does affect the morphological structures (does for polyethylene). No changes in the morphological structures detectable by optical polarisation were observed alongside recrystallisation by Muller and Pflunger. This is in agreement with the present study but disagrees with the work of Vinogradskaya and Ozolin.

Every polyamide passes through a maximum crystallinity as the temperature rises. Two opposing mechanisms operate, on the one hand there is the increasing mobility of the polymer chains and the related increasing probability of the formation of regions of order and on the other hand the growing tendency towards the dissolution of the lattice structure with rising temperature. Muller and Pflunger⁹⁸ found impact strength to be higher for a higher mould temperature. These workers also state that higher crystallinity gives greater resistance to atmospheric oxidation and chemical attack. Mouldings containing a variety of morphological forms must be considered as of inferior quality owing to their anisotropy and greater tendency to produce internal stresses.

5.2 WEAR PROPERTIES

Initial tests using the A/F rig (as described in the Experimental Section) gave results indicating that increasing the mould temperature increased the wear resistance of "as moulded" samples. One would expect this, a higher crystalline material having a harder surface and hence being more resistant to wear. The conditioned samples gave an opposite result i.e. increasing the mould temperature gives a lower wear-resistance. This is in disagreement with the thinking that a sample obtained at a lower mould temperature should absorb more moisture than one obtained at a higher mould temperature due to its lower crystalline content. Conditioned samples having a greater water

uptake and hence being softer should wear more. Later tests using specimens cut from water absorption discs showed an alternating behaviour, samples moulded at 15 and 75°C having superior wear resistance to those obtained at mould temperatures of 55 and 95°C. This was for samples obtained near to the gate. Extreme from the gate the opposite was true, samples moulded at 95 and 55°C having the better wear-resistance. The dynamic coefficient of friction was not influenced by changing the mould temperature.

Using the rotating shaft rig the general trend is shown that lower wear occurs for samples taken near to the gate then those taken extreme from the gate. These results however were obtained on cut and not moulded surfaces. Rotating shaft wear tests on moulded surfaces indicated that a higher mould temperature gave a higher wear resistance.

It can be seen that conflicting results have been obtained in this study with regard to wear properties. One would think that since a crystalline material is more densely packed and in nylon 66 more H-bonds are formed then greater energy is required to wear the nylon away. One would therefore expect a higher mould temperature to give better wear properties due to a higher crystallinity. This is shown in some but not all our results.

Giltrow¹⁵² has related the wear properties to their chemical constitution and states that the cohesion between portions of polymer chains is greater in crystalline regions than in amorphous regions. However, Giltrow found that changing the surface roughness of 37 μ m of the abrasive paper to one of 6 μ m does not give the correlation between rate of wear and cohesive energy. Lancaster¹⁵⁴ has shown that plastic deformation only becomes predominant during wear processes when the surface roughness of the counterface is of the order of 25 μ m. Hence in this study since the surface of the counterface is of the order of 16 μ m factors other than cohesive energy are coming into play.

Polymers with low elongation are very sensitive to counterface roughness. It could be that the surface roughness of the polymer is affected by the mould temperature and hence gives different wear rates.

In our study it would have been interesting to have tried different annealing procedures in an attempt to produce gross morphological differences and then examine the wear properties.

According to Fedorchuk¹⁷⁶ the degree of crystallinity and the modification of the crystalline phase greatly affect the wear resistance of polyamides. Fedorchuk studied nylon 6 and found that the wear resistance decreased with increasing crystallinity to about 39% crystallinity and then increased as the crystallinity increased to 47% there after decreasing as the crystallinity increased to a maximum of 52%.

Fedorchuk found that an increase in the size or number of spherulites leads to a fall in wear resistance but with spherulites of $3-4\mu$ m the maximum wear resistance was obtained, however in this study no spherulites were obtained in the surface. The whole question of wear raises many contradicting views. In certain instances polymeric materials will be given a wear resistance rating in one test and then another test will rank the materials in a completely different order.

Lancaster¹⁵⁴ is of the opinion that even in the relatively simple situation of wear on coarse abrasive papers, it has not yet been possible to obtain convincing correlations between wear rates and fundamental molecular and structural properties. The effects of crystallinity on wear can therefore be somewhat conflicting and the situation is complicated even further by the fact that molecular orientation produced in the surface layer by the wear process itself will influence the stress-strain relationship of this layer. The effects of lubricating oils also give a conflicting picture on the wear rate of polyamides.

Mitrovich¹⁵⁹ found the wear rate increased above 80°C while Lancaster¹⁶⁹ found the wear rate decreased at $\approx 80^{\circ}\text{C}$ and dropped to a minimum at $\approx 115^{\circ}\text{C}$ before increasing again. It would appear that each bearing application must be considered separately since a polyamide bearing for instance may be precisely manufactured and found to be satisfactory while for another application a change in the abrading surface may require the bearing to be made under different processing conditions.

Farberova et al.¹⁶¹ state that there is a correlation between wear obtained against metal mesh and that obtained on a smooth metal surface. These workers support the view that wear is connected to the product of strength and elongation to break. Water may act as a partial lubricant and oil annealing gives a lower elongation and hence a maximum wear.

Another important factor is the transfer of polymer onto the abrading surface. This then gives a polymer/polymer abrasion which generally leads to a higher wear due to thermal degradation, local heating can in extreme cases cause the polymer to melt and flow.

Since polymers are time and temperature dependent it is reasonable to suppose that changes in wear are going to occur with change in temperature. If during wear a polymer passes through its glass transition temperature then changes in wear would be expected. If conditions due to a failure of some kind cause very high loads on a polymer in service then the polymer may melt. Another important factor is that if the structure of a crystalline polymer changes as one moves from the moulded surface into the interior of the moulded part then changes in wear rate may occur.

5.3 WATER ABSORPTION

The undried samples give very unusual results the "as-moulded" samples are almost in agreement with the general thinking that a higher mould

temperature gives a higher crystallinity and hence a lower water absorption since water does not penetrate the crystalline regions. The undried conditioned samples give somewhat variable and inexplicable results. The predried samples give figures as one would expect except that the values obtained for conditioned samples obtained at mould temperatures of 15 and 55°C would be expected to be reversed.

The figures obtained for the water content after accelerated weathering show the water content in some instances to be higher in the interior than in the surface of samples. This appears to be somewhat controversial but may be explained if one considers that on accelerated weathering cracks are formed on the surface thus allowing water to penetrate easily into the polymer below the surface.

On accelerated weathering the surface increases in density and hence has a higher crystallinity. It is usually accepted that water penetrates the more amorphous regions of a polymer and hence as the surface crystallises the water content decreases.

5.4 INHERENT VISCOSITY

Initially with tensile and flexural samples all the specimen was used to obtain inherent viscosity values after weathering. While this gave a reduction in the viscosity the reduction was quite low because both the degraded surface and the protected interior were taken together, the interior of the accelerated weathered samples being undegraded the skin acting as a "UV shield".

However with accelerated weathered impact discs and other flexural samples since the exposed surface material was removed by filing for viscosity determinations the extent of the degradation was clearly shown. However, inaccuracies must exist with this method. Many specimens are required

to obtain enough exposed material for carrying out inherent viscosity determinations and unexposed material which is unavoidably included gives a higher inherent viscosity.

5.5 ATTENUATED TOTAL REFLECTANCE

For all the samples accelerated weathering produced changes in the ATR spectra indicating chemical and physical changes. Carbonyl absorption increased indicating degradation which is substantiated with the inherent viscosity data. The samples also increased in crystallinity on accelerated weathering as can be seen by the ratio of the 10.7μ peak to the 8.7μ peak. Density increases also indicate higher crystallinity values after accelerated weathering. The decrease in molecular weight on accelerated weathering should make crystallisation easier^{kinetically} since shorter chains can pack better than longer ones and hence an increase in crystallinity would be expected. Optical microscopy using X-polars showed no changes in spherulitic structure (or crystalline structure) after weathering. Other accounts of work in this field report conflicting findings some workers found no change in spherulite structure while others have reported considerable changes.

It may be that changes in structure do take place on ageing but these are so small that they cannot be resolved by optical microscopy. However electron microscopy and small angle X-ray diffraction should show up these small changes if they exist. Various workers have shown changes in lamella thickness after various treatments e.g. lamellae thickening on annealing; but these treatments are more special research techniques rather than treatments during and/or after plastic processing. Also discrepancies have been shown to exist between small angle X-ray diffraction and electron microscopy figures obtained for lamellae thickness.

The water conditioning treatment given to certain of the test specimens is a standard technique used in processing nylon 66. Certain oil annealing treatments are sometimes used and it is likely that this type of treatment will effect the structure more than water conditioning because of the higher temperatures involved. Steam treatment would however probably cause degradation due to hydrolysis.

It has been suggested that certain changes in the ATR spectra after accelerated weathering could be due to inorganic materials,¹⁷⁷ these originating from the deionised water used as a water spray in the accelerated weathering cycle. Increased intensity of the carbonyl band near 5.8μ is no doubt due to oxidation. The decreased intensity of the amorphous band at 8.7μ and the sharper better defined character of the crystalline band between 10.5μ and 11.0μ and also the better resolution obtained on the $-NH$ band at 3.2μ in the weathered sample indicate a more crystalline surface.

5.6 THERMAL ANALYSIS

As stated earlier in the results section samples taken from the surface of mouldings melt at a lower temperature than those taken from the interior and also melt over a wider range, hence the broadness of the melting peak is greater for surface samples than for interior samples.

There appears to be little if any difference between samples taken from the same position in mouldings obtained at different mould temperatures. On the basis of differential thermal analysis (DTA) work Ke and Sisko¹⁷⁸ suggest that orientated crystallites become disoriented before they melt. In a thermogram of a nylon 66 monofilament a doublet was obtained. According to Ke and Sisko the first endothermic peak is attributed to disorientation followed by a normal melting point. A doublet peak in oriented yarns has

been previously observed by White¹⁷⁹. Arakawa et al¹⁸⁰ found that larger crystals gave a higher melting point.

Matsuoka et al¹⁸¹ studied transcrystalline regions in polyethylene. DSC showed a smaller heat of fusion for transcrystalline material compared with spherulites indicating a lower degree of crystallinity. In addition a lower melting point of transcrystalline material is indicative of smaller crystallite sizes in these structures (cf Arakawa)¹⁸⁰

In the present study it can be seen by examining Figs. 17 to 20 that prior to melting the surface samples give a larger exotherm than the interior samples, this would appear to indicate a recrystallisation before melting. This can be explained if one considers that the surface contains less crystalline material than the interior and hence is more likely to recrystallise. In the thermograms obtained no transition was seen in the region 40 to 50°C the generally accepted glass transition temperature of polyamides. However certain workers believe the glass transition to be below 0°C, Rybníkar¹⁸² is one of these workers and he obtained a value of - 65°C. Hartley, Lord and Morgan²⁵ proved that nylon 66 still crystallises at -36°C and therefore believe the glass transition must be below this figure, in the region -40 to -50°C.

Gordon¹⁸³ found that annealing nylons at 75°C for 24 hours gave another transition at 92°C which after leaving to rest in a dessicator for five days gave two transitions one at 43°C and the other at 92°C.

With nylon 11 Gordon found that the only difference in the thermograms after allowing the sample to pick up moisture was a reduction in the transition temperature by 5°C. Gordon explains these results by suggesting a network built up of hydrogen bonds in the amorphous regions of the polymer.

Inflexions in the thermograms especially those with surface samples indicate a transition in the region of 85 - 100°C.

No multiple endothermic melting peaks were found in this study although they have been reported elsewhere. One or two peaks have shoulders but no splitting of the one melting peak into two was observed.

An interesting observation is that a shoulder is obtained on samples moulded at 75°C opposite the injection point, both with surface and interior samples. This shoulder is obtained at 271°C. It can be just seen in Fig. 18b which is a reduction of the original thermogram.

Bell et al¹⁸⁴ considered the two endothermic melting peaks to be due to two morphological species forms I and II. Form I is fixed in melting and form II varies with annealing conditions. They state form I results from rapid cooling while form II results from slow cooling. They attribute the variability of the melting of form II to variable crystal size/or perfection.

Later Bell and Dumbleton¹⁸⁵ suggested that form I is due to folded chain crystals while form II are extended chain crystals. These give vastly different stress/strain properties form II being unable to extend. In this work isothermal crystallisation was carried out just below the melting point and hence it is possible that extended chain crystals are formed. In the present study it would seem unlikely that chain extended crystals are formed due to the mould temperature being between 15 and 95°C. Hence it is difficult to explain the shoulders on the melting endotherms in terms of extended chains crystals since shoulders are produced in endotherms for all the samples examined unless extended chain crystals are present in both the surface and interior of the mouldings.

Bell and Dumbleton¹⁸⁵ found that material at the higher temperature endotherm can by annealing be converted to the material represented by the lower melting endotherm. After about 90 hours at 220°C only form II is left. In the work of Bell and Dumbleton thin nylon 66 film 0.005" thick was used hence temperature changes should affect the whole sample whereas in the

present study only the surface of the samples should be appreciably affected. Magill¹⁸⁸ and Cannon et al¹⁹⁸ have found that different types of nylon 66 spherulites have different melting points.

The inflexions in the thermograms at around 150 to 160°C may be connected with the Brill transition¹⁸⁶. At this temperature rearrangement in the packing of the molecules takes place. Blount¹⁸⁷ has also observed this transition and found it to decrease to a lower temperature as the water content of the nylon increased. Nylon 66 can form four different types of spherulites.

According to Magill¹⁸⁸ the optical melting point of positive nylon 66 spherulites is 265°C. This is the most prevalent kind encountered in the crystallisation of nylon 66. Non birefringent spherulites are formed just below 265°C. Negative spherulites grow between 251 and 264°C. These spherulites have a higher optical melting point than the positive spherulites being in the region 269 - 271°C. Spherulitic aggregates normally grow with negative spherulites when sections of polymer chip are rapidly heated to temperatures between 256 and 264 and subsequently held between 251 and 264 until crystallisation occurs. Typical melting points for these aggregates are between 270 - 272°C.

Positive ringed spherulites are obtained from crystallisation between 240 - 245°C.

Generally in polyamides a high incidence of nucleation and comparatively fast rates of crystallisation are the main obstacles towards achieving the entire range of these temperature controlled multifarious textures within a single spherulite. In the present work the shoulders on the melting peaks at 271°C shown in Fig. 18b, may be due to negative spherulites or spherulitic aggregates.

In the injection moulding process the polyamide melt cools from above its melting point to the mould temperature and eventually to room temperature. Since according to Magill only positive spherulites are produced below a crystallisation temperature of 251°C then one would expect mainly/or only positive spherulites in an injection moulding sample. In an injection moulding only the central interior of the moulding has any chance to form other than positive spherulites and it may be that the samples moulded at 75°C in position 3 cooled sufficiently slowly between 251 and 264°C for spherulitic aggregates or negative spherulites to be produced.

Considering the TMA work the tests carried out using the penetration probe gave inconsistent results. While a neoprene sample gave a well defined glass transition using the penetration probe no glass transition could be determined for the nylon 66 samples. The consistency of the thermograms obtained on samples obtained at any one mould temperature was poor. May be further trial and error methods varying the heating rate and the load applied on the sample may give some useful results with nylon 66.

The expansion probe gave more consistent results and apparent coefficients of linear expansion were obtained as can be seen in Table 17.

It can be seen that a lower expansion is obtained for samples moulded at a higher mould temperature. This is in accordance with a higher crystalline material being more resistant to expansion since greater forces such as Van der Waal and H-bonding are present than in amorphous regions. This is very important if one considers using a moulded item in close tolerance conditions at elevated temperatures. It can be seen that items moulded at high mould temperatures would be more suitable. The coefficient of expansion figures quoted in Table 17 are higher than the normal quoted figures in the literature since the latter are for normal room temperatures.

The results obtained from the microscopy work give an overall picture of the structure throughout the mouldings. However for examination of the structure below the size of spherulites electron microscopy and X-ray work are essential. In the present work both these techniques have been used to a limited extent, the X-ray work mainly to study orientation and the electron microscopy to look for structural entities such as lamellae and shish-kebabs.

The gating system used for the flexural and tensile bars was such as to try and reduce orientation. With the disc samples this could not be arranged. In the present study a slow injection speed was used to try and limit orientation effects.

Ideally to study the influence of mould temperatures one should examine thin films, less than 0.2 mm, since the polymer can be rapidly cooled to the mould temperature. However the majority of nylon mouldings are much thicker than 0.2 mm so it is only the surface of the moulding which is cooled initially to the mould temperature. The poor heat conduction properties of polymers hence cause the interior of mouldings to cool more slowly the "surface skin" action as an insulating layer. In injection moulding shear effects are present on filling the mould and these alter the nature of the moulding.

5.7 MORPHOLOGY & MOULDING

5.7.1 Influence of Moulding Conditions

In injection moulding the processing stresses on the flowing or cooling melt are high and heat removal during cooling is fast but uneven. The transition from cylinder (barrel) to mould is a function of both viscosity, i.e. temperature, and pressure, but excessive use of one variable to

offset the other leads to component and processing deficiencies. In injection moulding the polymer is sheared during passage through the nozzle, runners and gates as well as in the mould. In general practice the melt temperature is usually chosen as low as possible, but this can lead to orientation effects which in turn gives rise to anisotropy of properties.

The rate of cooling of the moulding while affecting crystallinity should also influence surface finish and the amount of orientation relaxation. As crystalline polymers begin to cool the molecular chains approach each other and begin to crystallise. If cooling is slow then the number of chains that have time to organise themselves into the crystal form is large. As the degree of crystallinity achieved rises so also do the density dependent properties. With nylons it is quoted⁹⁹ that extreme conditions can give variations of 40 to 50% crystallinity although post-moulding crystallisation substantially increases the density from initially low levels of crystallisation. In practice injection mouldings have density variations much less than these extreme values.

Increases in thickness of the moulding and cylinder temperature favour increased relaxation of orientation stresses. The melt density varies as the pressure drops along the cavity whilst packing pressure increases the density in the gate area as shown in Table 15d. This density gradient results in differences in shrinkage and causes formation of internal stresses. Additional cooling at the gate in the mould reduces this.

After moulding the density of mouldings and properties are modified by post-moulding crystallisation. This can take place naturally through ageing or artificially by annealing. In the present study this is caused to some extent by water conditioning, but mainly by accelerated weathering. However these final density values are largely influenced by the initial density and moulding conditions. Since the extremities of the moulding have lower

initial density than the centre, these will have a faster rate of post-moulding crystallisation and this is borne out when one examines the density values in Table 15e. On cooling the surface of the moulding will shrink less than the interior and hence compressive stresses are set up in the surface.

As polymer flows through the system the velocity of the inner core of the polymer will be higher than that of the outer layers due to drag between the melt and mould walls and a higher viscosity due to cooling.

The polymer chains in the melt are in a random coiled form but since one part of the chain may be in a lower velocity region than another there is a tendency to stretch the chain out of its normal coil and into a more linear form.

The degree of orientation will depend upon the shear rate and the temperature of the melt. A slow shear rate allows time for relaxation as does a high melt temperature. However if the shear rate is low then the viscosity will probably be higher due to lack of shear heating.

Usually as polymer fills the cavity, the high velocity material in the core flows out across the face of the flow front and makes contact with the cool walls of the mould where it is immediately frozen. Since this material is at a high temperature and has only been exposed to a low degree of shear it is only slightly orientated and thus the very immediate surface of the moulding itself may have a low orientation. However further material laid immediately behind this skin will not solidify immediately being thermally insulated in the mould by the first layer, but as the material loses heat it steadily becomes more viscous. Under the influence of injection pressure, this viscous material will continue to flow, although more slowly than the hot central core. Shear under these conditions leads to a high degree of orientation. This probably accounts for the banded structure obtained

Fig. 67. X-ray pattern showing orientation near top surface of sample obtained at 15°C.

Fig. 68. X-ray pattern near centre of same sample as in Fig. 67.

Fig. 69. As Fig. 67 but near bottom surface of sample

through the water absorption and impact discs, the crystallisation and orientation being caused by shear effects. The centre core of the moulding has time to relax and is not subjected to these high shearing forces. However in the present study X-ray pictures show that there is more orientation in the centre of the moulding. Figs. 67, 68 and 69 show this for a water absorption sample obtained at 15°C . This may mean that the centre core is not having time to relax and may be the slow injection speed is causing some surging effect in the centre core. More work is obviously needed in this area using micro X-ray beam techniques to obtain a precise picture of orientation through the moulding thickness.

Transcrystallisation produced by orientated cooling in one direction is shown in Fig. 33.

The orientation pattern along the mould will also be affected by the formation of the highly sheared layers adjacent to the mould face. The thickness of these layers will be least at the flow front since they have been formed and cooled for the shortest period, whilst those near the gate would be the thickest since they were formed first. However the constant passage of hot fresh material and heat derived from high shear in the gate raises the mould temperature in the feed region and thus retards cooling and hence orientation. Orientation should be lower for water absorption samples compared to impact samples since the former are thicker and cool slower giving more relaxation. By retarding cooling higher mould temperatures similarly lead to lower levels of orientation in the final moulding and this is shown in the X-ray diffraction patterns if one compares mouldings obtained at 15 and 95°C .

After flow has ceased in filling the chains attempt to revert towards their normal coiled form but the viscosity rises and slows the relaxation down. A lower molecular weight gives a lower melt viscosity and hence

a lower orientation. Orientation can have an effect on the flow of crystalline polymers in the mould. Under certain conditions alignment can lead to premature crystallisation and solidification in the flowing polymer at temperatures above the normal crystallisation temperature⁸⁸. This premature crystallisation in the flowing melt leads to a sudden increase in viscosity or even cessation of flow.

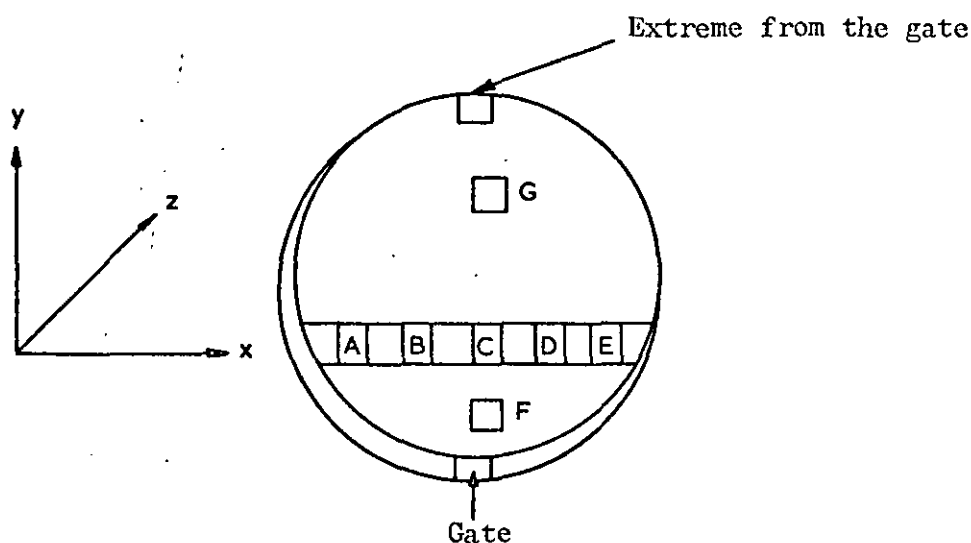
After injection moulding the majority of shrinking takes place in the first 24 hours. At temperatures above ambient the rate of post-crystallisation steadily increases. With hygroscopic materials such as nylon, absorbed moisture facilitates post crystallisation even at temperatures below ambient, but the resulting after shrinkage is compensated to a varying degree by the expansion due to uptake of water.

While the gating system on the tensile and flexural bars was such as to reduce orientation, orientation effects are still present. These effects must influence the flexural modulus and tensile results. The higher orientation at lower mould temperatures balancing the higher crystallinity at higher mould temperatures except for a mould temperature of 95°C with regard to flexural modulus values. With tensile figures the crystallinity is the overriding influence.

The X-ray diffraction patterns indicated preferred orientation of the 002 plane (also 100 plane) in samples obtained at a mould temperature of 15°C. One would expect more orientation at lower mould temperatures since the chains are more likely to be frozen in place, at higher mould temperatures the chains have more time to relax and possibly the shearing forces obtained in the mould are lower than at low mould temperatures.

5.7.2 Additional Experimental Work to check orientation

Further work on samples moulded at 15°C showed that the orientation varied across the moulding i.e. a strip taken perpendicular to the flow direction as shown overleaf :-



Samples taken at A and E showed some preferred orientation. While samples taken at B, C and D showed more preferred orientation in the x direction.

Samples taken at G and F showed different degrees of orientation, orientation being less at F than at G. Since F is very near the gate this area is one of the last to cool in the moulding and hence the chains have more time to relax whereas chains at G are frozen into a particular orientation. The lowest orientation was observed in the sample extreme from the gate.

From the X-ray pictures it appears that the preferred orientation is caused by the molecular chains being perpendicular to the flow direction. This disagrees with the work by Clark¹⁸⁹ who obtained chains // to the flow direction using polyoxymethylene. However it may be that different polymers can give different results as is suggested by Clark¹⁹⁰.

Keller^{24,48} has suggested that the orientation observed in nylon 66 mouldings and extrusions is due to crystalline units rather than the molecular chains.

5.7.3 Morphological Situations

Considering the structure obtained in the injection mouldings, it appears that spherulitic and disturbed spherulitic are the two most common forms.

Electron microscopy has indicated the presence of tie molecules, lamella and also fibril type structures. However much more work than that carried out in the present study on electron microscopy needs to be undertaken to obtain a better understanding of the morphology of injection moulded items. Small angle X-ray work would also help in obtaining an idea of lamella size and also changes in lamella structure after various heat treatments and ageing.

Speculating regarding the question of extended chain crystals; in normal injection mouldings it is very unlikely that these will be formed since they are usually formed at high pressures and high crystallisation temperatures.

Geil and others⁹⁰ have shown that polyethylene at 5300 atmospheres (5.37 kbars) gives extended chain crystals while polyethylene at 2000 atmospheres (2.03 kbars) gives chain folded crystals; this is because at higher pressures the surface energy of chain extended crystals is less than that of chain folded crystals.

According to Hoffman⁶³ the number of tie molecules increase the lower the crystallisation temperature, and on storage the interlamellae links tend to be removed giving higher crystallinity. Also it is stated that melting point variations are due to differences in lamellae thicknesses.

Anderson⁶⁴ is of the opinion that room temperature crystallised material consists mostly of chain folded lamellae plus a smaller amount of extended chain crystals.

Since shish-kebabs are intermediate between the previously mentioned structures then may be they are present in injection mouldings. According to Bassett¹⁹¹ extended chain crystals are only formed above 3 kbars below this pressure shish-kebabs are formed, however he believes that the formation of shish-kebabs in injection mouldings is doubtful. One must

not forget however the work undertaken on crystallisation under the effects of shear when shish-kebabs are formed. Also relaxation experiments on microtomed layers near the surface of injection mouldings have shown a 10 fold contraction¹⁹². This would tend to indicate the presence of shish-kebabs reverting to a folded chain structure. It would appear therefore that shish-kebabs may be present near the surface of injection mouldings.

5.7.4 Comparisons

With other engineering crystalline polymers such as polyoxymethylene and thermoplastic polyesters then different effects may occur. The morphological structure of injection moulded polyoxymethylene as observed by optical microscopy shows a very fibrous structure. This polymer also exhibits a high degree of crystallinity in injection mouldings. With thermoplastic polyesters the mould temperature has to be above the T_g or mainly amorphous mouldings are formed. Hence it can be seen that these polymers appear to be different from nylon 66. The behaviour of nylon 11 and 12 is probably different to that of nylon 66 due to the much smaller number of H-bonds and also the effect of the longer paraffinic units in the chain. Polypropylene has an interesting morphological structure and this effects the properties and causes changes from generally recognised trends¹⁹³.

5.8 Additional Note

While certain aspects of the work have proved to be especially interesting it must be stressed that this study has been an industrial project and therefore deviations from the main path of procedure that was originally planned, could not be followed in depth. The aim was to expose critical features in a comprehensive examination.

In particular the work on wear took up much time, inevitably as the investigation proceeded, but in retrospect this time could have been better spent on further electron microscopy and X-ray diffraction work.

CHAPTER 6. CONCLUSIONS

This study has provided the following conclusions.

6.1 For best overall properties of nylon 66 a high mould temperature is required. Using high mould temperatures good tensile stress, flexural modulus and impact properties are obtained, along with a good surface finish of the product.

6.2 The generally held view that a low mould temperature gives good impact properties probably holds shortly after moulding but on ageing the impact properties are drastically reduced so that a mould temperature of around 95°C is preferred for long term use.

6.3 With injection mouldings the question of orientation must always be considered along with mould temperature in regard to flexural modulus. This is borne out when one considers the negligible effect of mould temperature within the range 15 to 75°C on flexural modulus. Normally one would expect the flexural modulus to increase with mould temperature in compression mouldings where there is little orientation.

In the present study with injection mouldings and the presence of orientation, the highest flexural moduli were observed with mould temperatures near to 95°C.

6.4 Secondary crystallisation of the surface material takes place in mouldings over a period of time, surface samples having much higher densities after accelerated weathering than before.

6.5 The water conditioning treatment given to the mouldings changes the mode of failure after accelerated weathering (i.e. exposure to UV light and water). Conditioned mouldings fail in a ductile manner whereas unconditioned ones fail in a brittle manner. This is for tensile

samples. The use of a water conditioning treatment is therefore well justified.

6.6 If nylon 66 mouldings are to be used in service at high temperatures then high mould temperatures are recommended, since lower expansion occurs with samples obtained at high mould temperatures than with those obtained at low mould temperatures.

6.7 In this work no unambiguous correlations between wear and mould temperature have been established although there are indications that better wear properties are obtained at mould temperature around 95°C , and particularly nearer the gate.

6.8 Varying the mould temperature does not affect the morphology as viewed by optical microscopy but lower mould temperatures give samples with greater orientation.

6.9 The orientation indicated in mouldings obtained at low mould temperatures, about 15°C is unusual and not in accordance with the generally held theories, being significantly perpendicular to the surface. On stretching such samples at 0.2 cm/min to 150% elongation, orientation is induced at almost right angles to the original direction, i.e. in the direction of stretching.

6.10 The unusual orientation which has been discovered in the core requires more work before a fully satisfactory explanation can be obtained. However, as the mould fills and the temperature and pressure of the melt change, a skin might well be formed due to the slow injection speed, causing a back pressure which eventually forces melt material to break through the skin. A surging effect is considered to be the likely consequence, with abnormal orientation resulting.

6.11 The position of the gate and/or moulding shape affects the morphology as observed by optical microscopy. This is evident when one compares the micrographs obtained for flexural and tensile bars as opposed to those obtained for impact or water absorption discs.

6.12 On weathering, samples embrittled at their surfaces, so that impact strengths were drastically reduced.

6.13 A speculative conclusion with regard to the structure in the moulding, concerns the spherulites in disc samples. Spherulites are formed in two distinct bands between the outer skins and on either side of the inner core. Shish-kebabs are probably not present between these layers and the surface. The structure of the inner core is difficult to determine and may contain disturbed spherulites these being less than a few microns in diameter.

CHAPTER 7 RECOMMENDATIONS FOR FURTHER WORK

In any future work as has already been mentioned, more electron microscopy work should be carried out, and this includes work on etching.

Wide angle X-ray diffraction work has proved useful in the present study and this could be further exploited, use being made of a goniometer to obtain pole diagrams. A "mapping out" of the whole area of a moulding by wide angle X-ray work would be of interest since the present work has shown the different orientation in different areas of the moulding from the gate.

Small angle X-ray work would help to establish some idea of the lamellae thickness and the old metallurgical technique of microhardness would be useful to follow orientation changes across the moulding thickness¹⁹⁹, microbeam X-ray techniques would also be useful for this purpose.

As far as moulding conditions are concerned the effect of melt temperature and injection speed on morphology would be interesting areas for study since one would expect orientation to change significantly.

The moulding itself should be more complex so that thickness changes are present and flow around inserts or cores would be interesting variables. The main problem of using a complex moulding would be the difficulty in testing the moulding to obtain a property which could be correlated with the morphological changes.

The question of wear is in itself a topic for investigation. In view of the many variables which seem to affect wear, it would appear that to make say a bearing, and test this to find the effect of morphology on wear is a reasonable approach.

The effect of oil annealing or even high furnace temperatures for short times¹⁹², before water conditioning should be worthy of investigation since oil annealing usually involves much higher temperatures than used in water conditioning, and should change the structure in mouldings.

REFERENCES

1. L. Mandelkern, "Crystallisation of Polymers", p.21, New York (1964)
2. M. Dole and B. Wunderlich, Makromol. Chem., 34, 29 (1959)
3. R. Hill and E.E. Walker, J. Polym. Sci., 3, 609 (1948)
4. A. Sharples, "Introduction to Polymer Crystallisation", Edward Arnold, London (1966).
5. C.W. Bunn, J. Polym. Sci., 16, 323 (1955)
6. E.W. Fischer, Z, Naturforsch, 12a, 753 (1957)
7. A. Keller, Phil. Mag., 2, 1171 (1957)
8. P.H. Till, J. Polym. Sci., 24, 301 (1957)
9. A. Keller in "Growth and Perfection of Crystals" John Wiley, New York (1958)
10. A. Keller, Makromol. Chem., 3, 1 (1959)
11. B.M. Lindenmeyer, J. Polym. Sci., C1, 5 (1963)
12. A. Peterlin, J. Polym. Sci., C9, 61 (1965)
13. L.B. Morgan and P.G. Stern, Polymer, 9, 375 (1968)
14. D.V. Rees and D.C. Bassett, J. Mat. Sci., 6, 1021 (1971)
15. K. Hermann, O. Gerngross and W. Abitz, Z. Physik, Chem., B10, 371 (1930)
16. Standinger H and R. Signer, Z. Krist., 70, 193 (1929)
17. C.W. Bunn and T.C. Alcock, Trans. Faraday Soc., 41, 347 (1945)
18. W. Brenschede, Koll. - Z.Z. Polym., 114, 35 (1949)
19. J. Richards, J. Appl. Chem., 1, 370 (1951)
20. A.C. Cooper, A. Keller and J.R.S. Waring, J. Polym. Sci, 9, 215 (1953)
21. R.G. Scott, J. Appl. Phys, 28, 1089 (1957)
22. V.A. Kargin, J. Polym. Sci., 30, 252 (1958)
23. R. Eppe, E.W. Fischer and H.A. Stuart, J. Polym. Sci., 34, 721 (1959)
24. A. Keller, J. Polym. Sci., 17, 351 (1955)
25. F.D. Hartley, F.W. Lord and L.B. Morgan, Atti. del. Symp. Intern. Macromol. Chem., Milano - Turino, Ricerca Sci (Supplement), 25, 577 (1955)

26. H.W. Starkweather, G.E. Moore, E. Hansen, Th.M. Roder and R.E. Brooks, J. Polym. Sci., 21, 189 (1956)
27. A. Keller and J.R.S. Waring, J. Polym. Sci., 17, 447 (1955)
28. F.P. Reding and A. Brown, Ind. Engng. Chem., 46, 1962 (1954)
29. F. Khoury, J. Polym. Sci., 26, 375 (1957)
30. F. Bernauer, "Gedrillte Kristalle", Borntraeger, Berlin 1929, from Forschungen zur Kristallkunde, Heft 2.
31. B. Popoff, Lato, Farm. Zurn., 1, 1934
32. H.A. Stuart and B. Kahle, J. Polym. Sci., 18, 143 (1955)
33. A. Keller, J. Polym. Sci., 36, 361 (1959)
34. V. Peek and W. Kaye, J. Appl. Phys., 25, 1565 (1954)
35. G.C. Claver, R. Buchdahl and R.L. Miller, J. Polym. Sci., 20, 202 (1956)
36. A. Keller, Nature (London), 169, 913 (1952)
37. A. Keller, Nature (London), 171, 170 (1953)
38. A. Keller, J. Polym. Sci., 17, 291 (1955)
39. G. Schuur, J. Polym. Sci., 11, 385 (1953)
40. E. Jenckel, E. Teege and W. Hinrichs, Koll. - Z.Z. Polym., 129, 19 (1952)
41. M. Takayanagi and T. Yamashita, J. Polym. Sci., 22, 552 (1956)
42. E.H. Boasson and J.M. Woestenenk, J. Polym. Sci., 21, 151 (1956)
43. E.H. Boasson, and J.M. Woestenenk, J. Polym. Sci., 24, 57 (1957)
44. F. Khoury, J. Polym. Sci., 33, 389 (1958)
45. F.P. Reding & E.R. Walter, J. Polym. Sci., 21, 559 (1956)
46. W.M.D. Bryant, R.H.H. Pierce and C.R. Lindegren, J. Polym. Sci., 16, 131 (1955)
47. P.J. Flory and A.D. McIntyre, J. Polym. Sci., 18, 592 (1955)
48. A. Keller, J. Polym. Sci., 21, 363 (1956)
49. E. Sauter, Z. Physik. Chem., B18, 417 (1932)
50. F.C. Frank, Dis. Faraday Soc., 5, 48 (1949)
51. P.H. Geil, "Polymer Single Crystals", Interscience (1963)

52. A. Keller, Polymer, 3, 393 (1962)
53. A. Keller, Koll. - Z.Z. Polym., 231, 386 (1969)
54. A. Keller, Koll. - Z.Z. Polym., 197, 98 (1964)
55. D.A. Blackadder, J. Macromol. Sci., C1(2), 297 (1967)
56. P.H. Lindenmeyer, SPE Trans., 4, 1 (1964)
57. B. Lotz, A.J. Kovas, G.A. Bassett and A. Keller, Koll. - Z.Z. Polym., 209, 115 (1966)
58. A.J. Pennings and A.M. Kiel, Koll. - Z.Z. Polym., 205, 160 (1965)
59. A.J. Pennings, J. Polym. Sci., C16, 1799 (1967)
60. A. Keller and M.J. Machin, J. Macromol. Sci., B1, 41 (1967)
61. M.J. Hill and A. Keller, J. Macromol. Sci., B3 (1), 153 (1969)
62. H.D. Keith, Koll.-Z.Z. Polym., 231, 421 (1969)
63. J.D. Hoffman, SPE Trans., 4, 315 (1964)
64. F.R. Anderson, J. Appl. Phys., 35, 64 (1964)
65. H.D. Keith, F.R. Padden Jr. and R.G. Vadimsky, Science, 150, 1026 (1965)
66. Same authors J. Polym. Sci., A2, 4, 267 (1966)
67. Same authors J. Appl. Phys., 37, 4027 (1966)
68. M.J. Avrami, J. Chem. Phys., 7, 1103 (1939)
69. H.D. Keith and F.R. Padden Jr., J. Polym. Sci., 51, 84 (1961)
70. Same authors J. Appl. Phys., 34, 2409 (1963)
71. Same authors J. Appl. Phys., 35, 1270, 1286 (1964)
72. F.P. Price, J. Chem. Phys., 31, 1679 (1959)
73. J.T. Lauritzen, Jr., and J.D. Hoffmann, J. Chem. Phys., 31, 1680 (1959)
74. F.C. Frank and M. Tosi, Proc. Roy. Soc. (London)., A 263, 323 (1961)
75. J.D. Hoffman, J.F. Lauritzen, Jr., E. Passaglia, G.S. Ross, L.J. Frolen and J.J. Weeks, Koll. - Z.Z. Polym., 231, 564 (1969)
76. A. Peterlin, E.W. Fischer and Chr. Reinhold, J. Polym. Sci., 62, 859, (1962)
77. H. Zahn and W. Pieper, Koll. - Z.Z. Polym., 180, 97 (1962)

78. K. Kobayashi, p473 in "Polymer Single Crystals" ed P.H. Geil Interscience New York (1963)
79. M. Takayanagi, K. Imada and T. Kajiyama, J. Polym. Sci., C15, 263 (1966)
80. R.J. Samuels, J. Polym. Sci., A3, 1741 (1965)
81. P. Dreyfus and A. Keller, J. Polym. Sci., B8, 253 (1970)
82. A. Peterlin and E. Roeckl, J. Appl. Phys., 34, 102 (1963)
83. J.D. Hoffman and J.J. Weeks, J. Chem. Phys., 42, 4301 (1965)
84. D.A. Blackadder and P.A. Lewell, Polymer, 11, 125 (1970)
85. D.A. Blackadder and P.A. Lewell, Polymer, 11, 659 (1970)
86. E.P.H. Meibohm and A.F. Smith, J. Polym. Sci., 7, 449 (1951)
87. W.O. Statton, in "Newer Methods of Polymer Characteristion" ed. Bacon Ke p.238-239 Interscience. New York (1964)
88. A.K. Van der Vegt and P.P.A. Smit, Adv. Polym. Sci. and Tech., 26, 313 (1967)
89. R.S. Porter and J.F. Johnson, Trans. Soc., Rheol., 11, 259 (1967)
90. P.M. Geil, F.R. Anderson, B. Wunderlich and T. Arakawa, J. Polym. Sci., A2, 3707 (1964)
91. D.V. Rees and D.C. Bassett, Nature, 219, 368 (1968)
92. D.V. Rees and D.C. Bassett, J. Polym. Sci., B7, 273 (1969)
93. P.H. Lindenmeyer, J. Polym. Sci., C15, 109 (1966)
94. P.H. Lindenmeyer, Koll. - Z.Z. Polym., 231, 593 (1969)
95. J. Ch. F. Kessler, Trans. Plastics Inst., 25, 281 (1957)
96. E.L. Vinogradskaya and Ya K. Ozolin, Mekhanika polimerov, 1, 17 (1965)
97. A. Muller and R.Pfluger, Kunststoffe, 50, 203 (1960)
98. A. Muller and R. Pfluger, Plastics, 24, 350 (1959)
99. R. Th. Steinbuch Brit. Plast., 37, 676 (1964)
100. J. Ch. F. Kessler in Bulletin of Verenigd Plastic Verkoopkantoor N.V. (AKZO Plastics) No. 1/523/C (January 1967)
101. H.W. Starkweather and R.E. Brooks, J. Appl. Polym. Sci., 1, 236 (1959)
102. B. Maxwell, J. Polym. Sci., C9, 43 (1965)
103. S. Matsuoka and B. Maxwell, J. Polym. Sci., 32, 124 (1958)
104. T.I. Sogolova, Mekhanika polimerov, 1, 5 (1965)

105. V.A. Kargin, DAN SSSR, 142, 1084 (1962)
106. W.M.D. Bryant, J. Polym. Sci., 2, 547 (1947)
107. C.M. Langkammer and W.E. Catlin, J. Polym. Sci., 3, 305 (1948)
108. R.J. Barriault and L.F. Gronholz, J. Polym. Sci., 18, 393 (1955)
109. C.V. Bunn and E.V. Garner, Proc. Roy. Soc. (London), A189, 39 (1947)
110. Herbst, Z. Electrochem., 54, 318 (1950)
111. C.R. Lindegren, J. Polym. Sci., 50, 181 (1961)
112. H. Mark and A.V. Tobolsky, "Physical Chemistry of High Polymers" 2nd edition p.347 (1950)
113. N.K.J. Symons, J. Polym. Sci., C3, 109 (1963)
114. F.P. Chappel, M.F. Culpin, R.G. Gosden and T.C. Tranter, J. Appl. Chem., 14, No 1 12 (1964)
115. M.F. Culpin and D. Madoc Jones, J. Sci. Inst., 36, 28 (1959)
116. D.R. Fitchmun and S. Newman, J. Polym. Sci., B7, 301 (1969)
117. H. Schonhorn, Macromolecules, 1, No. 2 145 (1968)
118. S. Hoshino, E. Meinecke, J. Powers, R.S. Stein and S. Newman, J. Polym. Sci., 3, 3041 (1965)
119. J.R. Collier, Rubb. Chem. Technol., 42, 769 (1969)
120. J.H. Magill, J. Polym. Sci., A3, 1195 (1965)
121. J.H. Magill, J. Polym. Sci., A2 7, 123 (1969)
122. J.H. Magill, J. Polym. Sci., A2 9, 815 (1971)
123. J.H. Magill, J. Polym. Sci., A2 4 243 (1966)
124. J. Farmer & K. Little, Br. Polym. J., 1, 259 (1969)
125. J.A. Rusnock and D. Hansen, J. Polym. Sci., A3, 647 (1965)
126. L.I. Bezruk, G.A. Gorokhovskii and Yu. S. Lipatov, Vys. Soed., A10, No 6 1434 (1968)
127. R.G. Crystal and D. Hansen, J. Polym. Sci., A2 6, 981 (1968)
128. P.H. Harris, 5th International Congress for Electron Microscopy paper BB8
129. B.J. Spit, 5th International Congress for Electron Microscopy paper BB7
130. J. Dluogosz and A. Keller, J. Appl. Phys., 39, No 12 5778 (1968)

131. D.T. Grubb and G.W. Groves, *Phil. Mag.*, 24, No 190 815 (1971)
132. J. Mann and L. Roldan - Gonzalez, *J. Polym. Sci.*, 60, 1 (1962)
133. P.F. Dismore and W.O. Statton, *J. Polym. Sci.*, C13, 133 (1966)
134. G.A. Campbell, *J. Polym. Sci.*, B7, 629 (1969)
135. H.R. Jacobi, *Kunststoffe*, 47, No 5 234 (1957)
136. J.H. Dumbleton, D.R. Buchanan and B.B. Bowles, *J. Appl. Polym. Sci.*, 12, 2067 (1968)
137. C.V. Stephenson, B.C. Moses and W.S. Wilcox, *J. Polym. Sci.*, 55, 451 (1961)
138. C.V. Stephenson, B.C. Moses and R.E. Burhs, Jr., W.C. Coburn Jr., and W.S. Wilcox, *J. Polym. Sci.*, 55, 465 (1961)
139. C.V. Stephenson, J.C. Lacey, Jr. and W.S. Wilcox, *J. Polym. Sci.*, 55, 477 (1961)
140. C.V. Stephenson and W.S. Wilcox, *J. Polym. Sci.*, A1, 2741 (1963)
141. M.R. Kamal, *Polym. Engng. Sci.*, 10, No. 2 108 (1970)
142. H.J. Oswald and E. Turi, *Polym. Engng. Sci.*, 5, 152 (1965)
143. M.R. Kamal, *Polym. Engng. Sci.*, 6, 333 (1966)
144. P.P. Dagaev, *Soviet Plast.*, No. 6, 61 (1964)
145. B. Kamerbeck, G.H. Kroes and W. Grolle, *SCI Monograph No 13*, 357 (1961)
146. G.W. Harding and B.J. MacNulty, *SCI Monograph No 13*, 392 (1961)
147. S.N. Zhurkov and E.E. Thomashevskii, "Physical Basis of Yield and Fracture", Institute of Physics and Physical Society Conference Series No 1 Oxford, Sept, (1966) p 200.
148. D. Campbell and A. Peterlin, *J. Polym. Sci.*, B6, 481 (1968)
149. H.M. Heuvel and K.C.J.B. Lind, *J. Polym. Sci.*, A2 8, 401 (1970)
150. H.A. Taylor, W.C. Tincher and W.F. Hammer, *J. Appl. Polym. Sci.*, 14, 141 (1970).
151. S.B. Ratner and E.G. Lure, *Vys. Soed.*, 8, No 1 88 (1966)
152. J.P. Giltrow, *Wear*, 15, 71 (1970)
153. P.A. Small, *J. Appl. Chem. (London)*, 3, (2) 71 (1953)
154. J.K. Lancaster, *Wear*, 14, 223 (1969)
155. M. Watanabe, M. Karasawa and K. Matsubara, *Wear*, 12, 185 (1968)
156. R.B. Lewis, *Mech. Engng.*, 36, 32 (1964)

157. J.C. Benedyk, SPE J., 26, 78 (1970)
158. S.B. Ratner and I.I. Farberova, Soviet Plast., No 9, 51 (1960)
159. V.P. Mitrovich, Soviet Plast., No 8, 64 (1965)
160. S.B. Ratner and E.G. Lure DAN SSSR, 166, No 4 909 (1966)
161. I.I. Farberova, S.B. Ratner, E.G. Lure, I.M. Gurman, T.A. Ignatova and L.A. Nosova, Soviet Plast., No 9, 32 (1962)
162. I.P. Zemlyakov, in "Nylon 6 for machine parts" Mashgiz (1961)
163. K.G. MacLaren and D. Tabor, Lubrication and Wear Convention (1963) paper 18 (Inst. Mech. Engrs)
164. S.B. Ratner, I.I. Farberova, O.V. Radyakevich and E.G. Lure, Soviet Plast., No 7, 37 (1964)
165. V.A. Bely, V.G. Savkin and A.I. Sviridjonok, Wear, 18, 11 (1971)
166. V.G. Savkin, V.A. Bely, I.I. Sogolova and V.A. Kargin, Mekhanika polimerov, 5, 659 (1966)
167. G.V. Vinogradov, V.A. Mustafaev and Yu. Ya. Podolsky, Wear, 8, 358 (1965)
168. S.B. Ratner, in "Abrasion of Rubber", ed D.I. James MacLaren London 1967
169. J.K. Lancaster, 7th Tribology Group. Conv., Gothenburg, Sweden, 1969, Inst. Mech. Engrs., London, 1969, Paper 12.
170. K. Matsubara, J. Mech. Lab, 8, 8 (1954)
171. H.A. Stuart, "Die Physik der Hochpolymeren" Vol IV Springs-Verlag Berlin-Heidelberg-Gottingen, 1956 p 638
172. E. Takeuchi, J. Appl. Phys. (Japan), 28, 233 (1959)
173. T. Sata and M. Mizuno, Rept. Inst. Phys. Chem. Res (Tokyo), 33, 45 (1957)
174. H.W. Starkweather and R.E. Moynihan, J. Polym. Sci., 22, 363 (1956)
175. M.O.W. Richardson, Wear, 17, 89 (1971)
176. E.A. Fedorchuk. Soviet Plast., No 11, 23 (1961)
177. V.J.I. Zichy, private communication
178. Bacon Ke and A.W. Sisko, J. Polym. Sci., 50, 89 (1961)
179. T.R. White, Nature, 175, 895 (1955)
180. T. Arakawa, F. Nagatoshi and N. Arai, J. Polym. Sci., B6, 513 (1968)
181. S. Masuoka, J.H. Deane, H.E. Bair and T.K. Kwei, J. Polym. Sci., B6, 87 (1968)

182. F. Rybníkar, J. Polym. Sci., 28, 633 (1958)
183. G.A. Gordon, J. Polym. Sci., A2 9 1693 (1971)
184. J.P. Bell, P.E. Slade and J.H. Dumbleton, J. Polym. Sci., A2 6 1773 (1968)
185. J.P. Bell and J.H. Dumbleton, J. Polym. Sci., A2 7 1033 (1969)
186. R. Brill, J. Prakt. Chem., 161 49 (1942)
187. A. Blount, private communication
188. J.H. Magill, J. Polym. Sci., A2 4 243 (1966)
189. E.S. Clark, SPE J., 23, 46 (1967)
190. E.S. Clark, SPE, RTC., University of Tennessee, March 1972
191. D.C. Bassett, private communication
192. R.R. Smith, private communication
193. N.M. Gaunt, paper read at PI Symposium, "Education in Injection Moulding", Solihull, March 1973
194. D.G. Street, private communication
195. EM6 Electron Microscope Manual, AEI, Trafford Park, Manchester
196. E.B. Atkinson, P.R. Brooks, T.D. Lewis, R.R. Smith and K.A. White, Trans. Plastics Inst., 35, 549 (1967)
197. J. Maxwell, private communication
198. C.G. Cannon, F.P. Chappel and J.I. Tidmarsh, J. Text. Inst., 54, T210 (1963)
199. M. Bevis, private communication
200. B.G. Ackhammer, F.W. Reinhart and G.M. Kline, J. Appl. Chem., 1, 301 July (1951)

